Chemical Analyses of Non-Volatile Flower Oils and Related Bee Nest Cell linings

Dissertation

Zur Erlangung des akademischen Grades

doctor rerum naturalium (Dr. rer. nat.)

vorgelegt der

Naturwissenschaftlich Fakutät II — Chemie und Physik

der Martin-Luther-Universität Halle-Wittenberg

von Frau M.Sc. Kanchana Dumri

geboren am 15. October 1976 in Chiang Mai (Thailand)

ACKNOWLEDGEMENT

I owe my gratitude to loving family whose dynamically elaborative instructions, manifold suggestions and distilled wisdom always helped me to solve my problems. All that I have achieved so far is actually their achievement. I wish to give a very special thanks to Dau Hung Anh. He shared and tried to solve my problems. It would have been impossible for me to successfully finish this work without his moral support understanding and unlimited patience.

Kanchana Dumri

CONTENTS

ABBREVIATIONS

CID	collision induced dissociation
DABA	3-(dansylamino)phenylboronic acid
DAG	diacylglycerol
DMDS	dimethyldisulfide
e.e.	*enantiomeric excess*
EI	electron ionization
ESI	electrospray ionization
FAME	*Fatty Acid Methyl Ester*
FTICR-MS	Fourier-transform ion cyclotron resonance mass spectrometry
GC/MS	gas chromatography/mass spectrometry
rel. int.	relative intensity
LC/MS	liquid chromatography/mass spectrometry
LM	light microscopy
M^+	molecular ion
MAG	monoacylglycerol
MW	molecular weight
m/z	mass to charge ratio
MSTFA	2,2,2-trifluoro-*N*-methyl-*N*-(trimethylsilyl) acetamide
MTBE	*t*-butylmethylether
SEM	scanning electron microscopy
TAG	triacylglycerol
TEM	transmission electron microscopy
TIC	total ion chromatogram
TMS	trimethylsilyl
t_R	retention time

SUMMARY

- The thesis describes the investigation and identification of chemical constituents of non-volatile oils secreted by specialized flowers belonging to plants of the families Cucurbitaceae, Iridaceae, Malpighiaceae, Orchidaceae, Myrsinaceae and Scrophulariaceae.

- The predominant compounds of floral oils from *Diascia purpurea*, *D. vigilis*, *D. cordata*, *D. megathura*, and *D. integerrima* (Scrophulariaceae) investigated are partially acetylated acylglycerols of (3*R*)-acetoxy fatty acids (C_{14}, C_{16}, and C_{18}).

- The non-volatile floral oils of *Thladiantha dubia*, *Momordica anigosantha*, *Momordica foetida* (Cucurbitaceae)*, Angelonia integerrima* (Scrophulariaceae), *Lysimachia vulgaris* (Myrsinaceae), *Cypella herbertii* (Iridaceae), *Zygostates lunata, Pterygodium magnum, Pterygodium hastata, Corycium dracomontanum, Cyrtochilum serratum, Sigmatostalix putumayensis, Oncidium cheirophorum, Oncidium ornithorhynchum* (Orchidaceae), *Malpighia urens, Bunchosia argentea, Stigmaphyllon ellipticum, Byrsonima coriacea* and *Janusia guaranitica* (Malpighiaceae) were analyzed by both ESI-FTICR-MS and GC/EI-MS techniques. These oils are composed of fatty acids, (3*R*)-acetoxy fatty acids, partially acetylated dihydroxy fatty acids as well as mono-, di-, and triacylglycerols. These identified acylglycerols possess one or two acetyl residues and one long chain of fatty acid or a mono- or diacetoxy fatty acid (oxidation at C-3 and/or C-9).

- Calyx glands of oil-producing flowers of *Heteropterys chrysophylla* (Malpighiaceae) were investigated in different stages The lipid secretion from calyx glands in 3 stages of flowering development (initial, blooming and senescence stages) were observed by transmission electron microscopy (TEM). TEM micrographs reveal the presence of secretory cells with cytoplasm, vesicles, mitochondria, Golgi bodies, rough endoplasmic reticulum (RER) and the lipid droplets. The number of lipid droplets in the cell structure increased from initial to blooming stage. The large lipid droplets located around the mitochondria are especially found in blooming flowers (active stage), whereas, only some small lipid droplets are present in the cytoplasm of senescence stage. GC-MS

investigations of the oil secreted by the calyx glands show acylglycerols containing long-chain 3,9-diacetoxy fatty acid as predominant constituents.

- Finally, a chemical study dealing with the biotransformation of oil constituents from *Lysimachia punctata* (Myrsinaceae) by solitary oil-collecting female bee *Macropis fulvipes* (Melittidae) in the course of the nest cell lining is presented, based on GC-EIMS, ESI-FTICR-MS and LC-ESI-MS/MS. The newly formed compounds arise from esterification of the monoacylglycerols of the *Lysimachia* oil with a further 3-hydroxy fatty acid. Besides the formation of a 1,2 and/or 1,3-diglycerols, oligoester formation is coupling to the 3-hydroxy group of 3-hydroxy fatty acid moieties. The involvement of labial gland secretions in the formation of oligoesters proceeds via the free 3-hydroxy group of the oxidized fatty acid moiety. This could be evidenced for the first time: *in vitro* experiments of *L. punctata* oil treated with *M. fulvipes* labial gland secretions also revealed novel intermediate compounds. The results obtained show that the labial gland secretions of *M. fulvipes* play an important role in regard to the nest cell lining construction.

ZUSAMMENFASSUNG

- Gegenstand der vorliegenden Arbeit sind Untersuchungen zur chemischen Zusammensetzung von nichtflüchtigen Blütenölen, insbesonde von ölsekretierenden Pflanzen der Familien Cucurbitaceae, Iridaceae, Malpighiaceae, Orchidaceae, Myrsinaceae and Scrophulariaceae. In einem gesonderten Kapitel werden Ergebnisse zur biochemischen Transformation von Blütenölbestandteilen von *Lysimachia punctata* (Myrsinaceae) durch weibliche Tiere der solitären Biene *Macropis fulvipes* (Melittidae) vorgestellt und diskutiert.

- Als Hauptverbindungen der Blütenöle der *Diascia*-Arten *Diascia purpurea, D. vigilis, D. cordata, D. megathura* und *D. integerrima* (Scrophulariaceae) wurden partiell acetylierte Acylglycerole von (3R)-Acetoxyfettsäuren (C$_{14}$, C$_{16}$, and C$_{18}$) identifiziert.

- Die nichtflüchtigen Blütenöle von *Thladiantha dubia, Momordica anigosantha, Momordica foetida* (Cucurbitaceae)*, Angelonia integerrima* (Scrophulariaceae), *Lysimachia vulgaris* (Myrsinaceae), *Cypella herbertii* (Iridaceae), *Zygostates lunata, Pterygodium magnum, Pterygodium hastata, Corycium dracomontanum, Cyrtochilum serratum, Sigmatostalix putumayensis, Oncidium cheirophorum, Oncidium ornithorhynchum* (Orchidaceae), *Malpighia urens, Bunchosia argentea, Stigmaphyllon ellipticum, Byrsonima coriacea* und *Janusia guaranitica* (Malpighiaceae) wurden mittels ESI-FTICR-MS und GC/EI-MS analysiert. Diese Blütenöle bestehen aus freien Fettsäuren, (3R)-Acetoxyfettsäuren, partiell acetylierten Dihydroxyfettsäuren sowie Mono-, Di- und Triacylglycerolen. Die identifizierten Acylglycerole besitzen ein oder zwei Acetylreste und eine einfache langkettige Fettsäure oder eine Mono- oder. Diacetoxyfettsäure (oxidation C-3 und/oder C-9).

- Die in verschiedenen Stadien (knospig-, blühend- und abgeblüht) gesammelten ölproduzierenden Blüten von *Heteropterys chrysophylla* (Malpighiaceae) wurden mittels Transmissionselektronenmikroskopie (TEM) untersucht. Die TEM-Aufnahmen zeigen deutlich einen sowohl zahlenmäßig als auch größenmäßigen Anstieg der Lipidtröpfchen während der Blütenentwicklung. Die großen Lipidtröpfchen in der Umgebung der Mitochodrien finden sich vor allem in der

Blühphase, nur noch wenige konnten im abgeblühten Stadium angetroffen werden. Als Hauptverbindungen dieses Blütenöls wurden Acylglycerole mittels GC-MS nachgewiesen, die langkettige 3,9-Diacetoxyfettsäuren enthalten.

- Basierend auf Untersuchungen mittels GC-EIMS, ESI-FTICR-MS and LC-ESI-MS/MS wurden im Bienennest Biotransformationsprodukte von Verbindungen aus *Lysimachia punctata* (Myrsinaceae), die durch weibliche Bienen der ölsammelnden solitären Spezies *Macropis fulvipes* (Melittidae) gebildet werden, analysiert. Diese neu gebildeten Verbindungen entstehen durch Veresterung eines Monoacylglycerols des *Lysimachia* Blütenöls mit einer weiteren 3-Hydroxyfettsäure. Neben der möglichen Bildung von 1,2– und 1,3-Diglycerolen konnte erstmals auch eine Veresterung über die 3-Hydroxygruppe des Fettsäureteils (oligoester bildung) nachgewiesen werden. *In vitro* Experimente mit *L. punctata* Öl, das mit Labialdrüsensekret von *M. fulvipes* behandelt ist, weisen neue Intermediate auf, die bereits die relevanten Strukturmerkmale der neu gebildeten Bienennestbestandteile aufweisen. Damit konnte zum erstenmal die Einbeziehung der. Labialdrüsensekrete in diese Biotransformation bewiesen werden, was deren wichtige Rolle beim Nestbau von *M. fulvipes* zeigt.

LIST OF COMPOUNDS

Table 1. List of compounds

No.	Compound	Abbreviation	MW
1	myristic acid	FA 14:0	228
2	palmitoleic acid	FA 16:1	254
3	palmitic acid	FA 16:0	256
4	oleic acid	FA 18:1	282
5	stearic acid	FA 18:0	284
6	*cis*-11-eicosenoic acid	FA 20:1	310
7	eicosanoic acid	FA 20:0	312
8	*cis*-13-docosenoic acid	FA 22:1	338
9	(3*R*)-hydroxymyristic acid	3-OH 14:0	244
10	(3*R*)-hydroxypalmitic acid	3-OH 16:0	272
11	(3*R*)-hydroxyoleic acid	3-OH 18:1	298
12	(3*R*)-hydroxystearic acid	3-OH 18:0	300
13	(3*R*)-hydroxyeicosanoic acid	3-OH 20:0	328
14	(3*R*)-acetoxymyristic acid	3-OAc 14:0	286
15	(3*R*)-acetoxypalmitic acid	3-OAc 16:0	314
16	(3*R*)-acetoxyoleic acid	3-OAc 18:1	340
17	(3*R*)-acetoxystearic acid	3-OAc 18:0	342
18	(3*R*)-acetoxyeicosenoic acid	3-OAc 20:1	368
19	(3*R*)-acetoxyeicosanoic acid	3-OAc 20:0	370
20	2-[(3*R*)-acetoxymyristoyl]glycerol	2-MAG (3-OAc 14:0)	360
21	1-[(3*R*)-acetoxymyristoyl]glycerol	1-MAG (3-OAc 14:0)	360
22	2-[(3*R*)-acetoxymyristoyl]-1-acetylglycerol	1,2-DAG (3-OAc 14:0, OAc)	402
23	1-[(3*R*)-acetoxymyristoyl]-3-acetyl]glycerol	1,3-DAG (3-OAc 14:0, OAc)	402
24	2-[(3*R*)-acetoxymyristoyl]-1,3-diacetylglycerol	TAG(3-OAc 14:0, diOAc)	444
25	unknown	u_1	430
26	unknown	u_2	430
27	2-[(3*R*)-acetoxypalmitoyl]glycerol	2-MAG (3-OAc 16:0)	388
28	1-[(3*R*)-acetoxypalmitoyl]glycerol	1-MAG (3-OAc 16:0)	388
29	2-[(3*R*)-acetoxypalmitoleoyl]-1-acetylglycerol	1,2-DAG (3-OAc 16:1, OAc)	428
30	2-[(3*R*)-acetoxypalmitoyl]-1-acetylglycerol	1,2-DAG (3-OAc 16:0, OAc)	430

Table 1. (continued)

No.	Compound	Abbreviation	MW
31	1-[(*3R*)-acetoxypalmitoyl]-3-acetylglycerol	1,3-DAG (3-OAc 16:0, OAc)	430
32	2-[(*3R*)-acetoxypalmitoyl]-1,3-diacetylglycerol	TAG (3-OAc 16:0, diOAc)	472
33	unknown	u$_3$	458
34	2-[(*3R*)-acetoxyoleolyl]glycerol	2-MAG (3-OAc 18:1)	414
35	2-[(*3R*)-acetoxystearoyl]glycerol	2-MAG (3-OAc 18:0)	416
36	1-[(*3R*)-acetoxyoleolyl]glycerol	1-MAG (3-OAc 18:1)	414
37	1-[(*3R*)-acetoxystearoyl]glycerol	1-MAG (3-OAc 18:0)	416
38	2-[(*3R*)-acetoxyoleoyl]-1-acetylglycerol	1,2-DAG (3-OAc 18:1, OAc)	456
39	2-[(*3R*)-acetoxystearoyl]-1-acetylglycerol	1,2-DAG (3-OAc 18:0, OAc)	456
40	1-[(*3R*)-acetoxyoleoyl]-2-acetylglycerol	1,2-DAG (3-OAc 18:1, OAc)	458
41	1-[(*3R*)-acetoxystearoyl]-2-acetylglycerol	1,2-DAG (3-OAc 18:0, OAc)	458
42	1-[(*3R*)-acetoxyoleoyl]-3-acetylglycerol	1,3-DAG (3-OAc 18:1, OAc)	456
43	1-[(*3R*)-acetoxystearoyl]-3-acetylglycerol	1,3-DAG (3-OAc 18:0, OAc)	458
44	2-[(*3R*)-acetoxystearoyl]-1,3-diacetylglycerol	TAG (3-OAc 18:0, diOAc)	500
45	2-[(*3R*)-acetoxyeicosenoyl]glycerol	2-MAG (3-OAc 20:1)	442
46	2-[(*3R*)-acetoxyeicosanoyl]glycerol	2-MAG (3-OAc 20:0)	444
47	1-[(*3R*)-acetoxyeicosanoyl]glycerol	1-MAG (3-OAc 20:0)	444
48	2-[(*3R*)-acetoxyeicosanoyl]-1-acetylglycerol	1,2-DAG (3-OAc 20:0, OAc)	486
49	2-[(*3R*)-acetoxyeicosanoyl]-1,3-diacetylglycerol	TAG (3-OAc 20:0, diOAc)	528
50	1-[(*3R*)-acetoxydocosanoyl]glycerol	1-MAG (3-OAc 22:0)	472
51	2-[(*3R*)-acetoxydocosanoyl]-1,3-diacetylglycerol	TAG (3-OAc 22:0, diOAc)	556
52	3,7-diacetoxystearic acid	3,7-diOAc 18:0	400
53	3,7-diacetoxyeicosanoic acid	3,7-diOAc 20:0	428
54	3,9-diacetoxyeicosanoic acid	3,9-diOAc 20:0	428
55	7-acetoxy-3-hydroxyeicosanoic acid	7-OAc, 3-OH 20:0	386
56	9-acetoxy-3-hydroxyeicosanoic acid	9-OAc, 3-OH 20:0	386
57	3,7-diacetoxydocosanoic acid	3,7-diOAc 22:0	456
58	3,9-diacetoxydocosanoic acid	3,9-diOAc 22:0	456

Table 1. (continued)

No.	Compound	Abbreviation	MW
59	7-acetoxy-3-hydroxydocosanoic acid	7-OAc, 3-OH 22:0	414
60	9-acetoxy-3-hydroxydocosanoic acid	9-OAc, 3-OH 22:0	414
61	3,7-diacetoxytetracosanoic acid	3,9-diOAc 24:0	484
62	3,9-diacetoxytetracosanoic acid	3,7-diOAc 24:0	484
63	9-acetoxy-3-hydroxytetracosanoic acid	9-OAc, 3-OH 24:0	442
64	3,9-diacetoxyhexadocosanoic acid	3,9-diOAc 26:0	512
65	7-acetoxy-3-hydroxyhexacosanoic acid	7-OAc, 3-OH 26:0	470
66	9-acetoxy-3-hydroxyhexacosanoic acid	9-OAc, 3-OH 26:0	470
67	1-acetyl-2-myristoylglycerol	1,2-DAG (FA 14:0, OAc)	344
68	1-acetyl-3-myristoylglycerol	1,3-DAG (FA 14:0, OAc)	344
69	1,3-diacetyl-2-myristoylglycerol	TAG (FA 14:0, diOAc)	386
70	2-palmitoylglycerol	2-MAG (FA 16:0)	330
71	1-palmitoylglycerol	1-MAG (FA 16:0)	330
72	1-acetyl-2-palmitoylglycerol	1,2-DAG (FA 16:0, OAc)	372
73	1-acetyl-3-palmitoylglycerol	1,3-DAG (FA 16:0, OAc)	372
74	1,3-diacetyl-2-palmitoleoylglycerol	TAG (FA16:1, diOAc)	412
75	1,3-diacetyl-2-palmitoylglycerol	TAG (FA16:0, diOAc)	414
76	2-linoleoylglycerol	2-MAG (FA 18:2)	354
77	2-oleoylglycerol	2-MAG (FA 18:1)	356
78	2-stearoylglycerol	2-MAG (FA 18:0)	358
79	1-stearoylglycerol	1-MAG (FA 18:0)	358
80	1-acetyl-2-linoleoylglycerol	1,2-DAG (FA 18:2, OAc)	386
81	1-acetyl-2-oleoylglycerol	1,2-DAG (FA 18:1, OAc)	388
82	1-acetyl-2-stearoylglycerol	1,2-DAG (FA 18:0, OAc)	400
83	1,3-diacetyl-2-oleoylglycerol	TAG (FA18:1, diOAc)	440
84	1,3-diacetyl-2-stearoylglycerol	TAG (FA18:0, diOAc)	442
85	2-eisosenoylglycerol	2-MAG (FA 20:1)	384
86	1,3-diacetyl-2-eisonaoylglycerol	TAG (FA 20:0, diOAc)	470
87	1-acetyl-2-(3,9-diacetoxyeicosanoyl)glycerol	1,2-DAG (diOAc 20:0, OAc)	544
88	1-acetyl-3-(3,9-diacetoxyeicosanoyl)glycerol	1,3-DAG (diOAc 20:0,OAc)	544
89	1,3-diacetyl-2-(3,9-diacetoxyeicosanoyl)glycerol	TAG (diOAc 20:0, diOAc)	586
90	1-acetyl-2-(3,9-diacetoxydocosanoyl)glycerol	1,2-DAG (diOAc 22:0, OAc)	572

Table 1. (continued)

No.	Compound	Abbreviation	MW
91	1-acetyl-3-(3,9-diacetoxydocosanoyl)glycerol	1,3-DAG (diOAc 22:0, OAc)	572
92	1,3-diacetyl-2-(3,9-diacetoxydocosanoyl)glycerol	TAG (diOAc 22:0, diOAc)	614
93	1-[(3R)-hydroxyoleoyl]glycerol	1-MAG (3OH 18:1)	372
94	1-[(3R)-hydroxystearoyl]glycerol	1-MAG (3OH 18:0)	374
95	1-[(3R)-hydroxyoleoyl]-2-acetylglycerol	1,2-DAG (3OH 18:1, OAc)	414
96	1-[(3R)-hydroxystearoyl]-2-acetylglycerol	1,2-DAG (3OH 18:0, OAc)	416
97	1-[(3R)-hydroxyoleoyl]-3-acetylglycerol	1,2-DAG (3OH 18:1, OAc)	414
98	1-[(3R)-hydroxystearoyl]-3-acetylglycerol	1,2-DAG (3OH 18:0, OAc)	416
99[a]	di-[hydroxy fatty acid (C18:1)]monoacylglycerol	CL_1	652
100[a]	di-[hydroxy fatty acid (C18:0 and C18:1)]monoacylglycerol	CL_2	654
101[a]	di-[hydroxy fatty acid (C18:0)]monoacylglycerol	CL_3	656
102[a]	di-[hydroxy fatty acid (C18:1)]-acetyl-diacylglycerol	CL_1Ac	694
103[a]	di-[hydroxy fatty acid (C18:0 and C18:1)]-acetyl-diacylglycerol	CL_2Ac	696
104[a]	di-[hydroxy fatty acid (C18:0)]-acetyl-diacylglycerol	CL_3Ac	698
105[a]	di-[acetoxy fatty acid (C18:1) and hydroxyl fatty acid (C18:1)]-acetyl-diacylglycerol	CL_1diAc	736
106[a]	di-[acetoxy/or hydroxy fatty acid (C18:1/ or C18:0)]-acetyl-diacylglycerol	CL_2diAc	738
107[a]	di-[acetoxy fatty acid (C18:0) and hydroxyl fatty acid (C18:0)]-acetyl-diacylglycerol	CL_3diAc	740

[a]proposed structures and see in Chapter 5

AIMS OF STUDY

The main objectives are to investigate:

- Chemical compositions of non-volatile oils which are produced by oil-secreting flowers belonging to the plant families Cucurbitaceae, Iridaceae, Malpighiaceae, Orchidaceae, Myrsinaceae and Scrophulariaceae,

- Chemical compositions of cell lining and salivary glands of *Macropis fulvipes* (Melittidae) solitary bees,

- To prove the hypothesis that *M. fulvipes* bees collect oil from *Lysimachia punctata* for nest cell lining construction, based on the chemical investigations

The thesis consists of:

1. Investigations of the chemical compositions of floral oils from the oil-secreting flowers by different mass spectrometric methods (GC/EI-MS and ESI-FTICR-MS) (Chapters 2 and 3),

2. Study of the ontogeny, structural and ultrastructural morphology of the calyx glands in *Heteropterys chrysophylla* (Malpighiaceae) and identification of their chemical composition (Chapter 4),

3. Investigation of the chemistry of the nest cell lining and salivary glands of the oil-collecting bee *M. fulvipes* (Melittidae), and its association between to *Lysimachia punctata* (Myrsinaceae) oil-secreting flowers (Chapter 5).

CHAPTER 1
General Introduction

1.1. History of the flower oil syndrome

Prof. Dr. Stefan Vogel was the first to describe non-volatile flower oils, presented at the International Botanical Congress in 1969 with a subsequent publication in the congress abstracts (Vogel 1969). Vogel had discovered the phenomenon while studying a species of *Angelonia* (Scrophulariaceae) in 1964. Vogel listed examples of species having oil-secreting glands from three plant families: Scrophulariaceae, Malpighiaceae, and Orchidaceae. These families are widespread, but oil-secreting glands were only found in some species at that time and restricted to the neotropics. Field observation of the pollinators has revealed that *Centris* (Anthophoridae) bees were capable of floral oil collecting. In 1971 Vogel published further findings with oil secreting glands from the neotropical Krameriaceae, and the large cosmopolitan family Iridaceae. The representatives having oil glands were restricted to the neotropics. The total number of species with oil glands was estimated to about 500 species (Vogel 1971). Vogel also presented first data about chemical structures of the oil constituents, and suggested the use of oils as brood provision in the bee nest. He proposed a tight co-evolution between oil flowers and their pollinators. By now, oil-secreting flower also have been reported from Europe, Africa and Asia.

1.2. Oil secretion

There are two types of floral glands that secrete oil: epithelial and trichomal elaiophores (Vogel 1974). Positioning of the elaiophores varies between species. The group of Simpson found that the existence of elaiophores correlated with a lack of nectar (Simpson *et al*., 1977, Simpson and Neff 1981). However, Vogel revealed that in staminated flowers of the Cucurbitaceae family, nectar is produced as an additional floral reward and exploited by oil-collecting bees (Vogel 1981).

1.2.1. Epithelial elaiophores

Epithelial elaiophores are small areas of secretory epidermal cells. The oils are secreted in very small (μL) to more often large quantities of up to several mL under the thin and protective layer of cuticle (Figure 1.1). This elaiophore type is found in Krameriaceae, Malpighiaceae, and some Orchidaceae (Vogel 1974; Buchmann 1987).
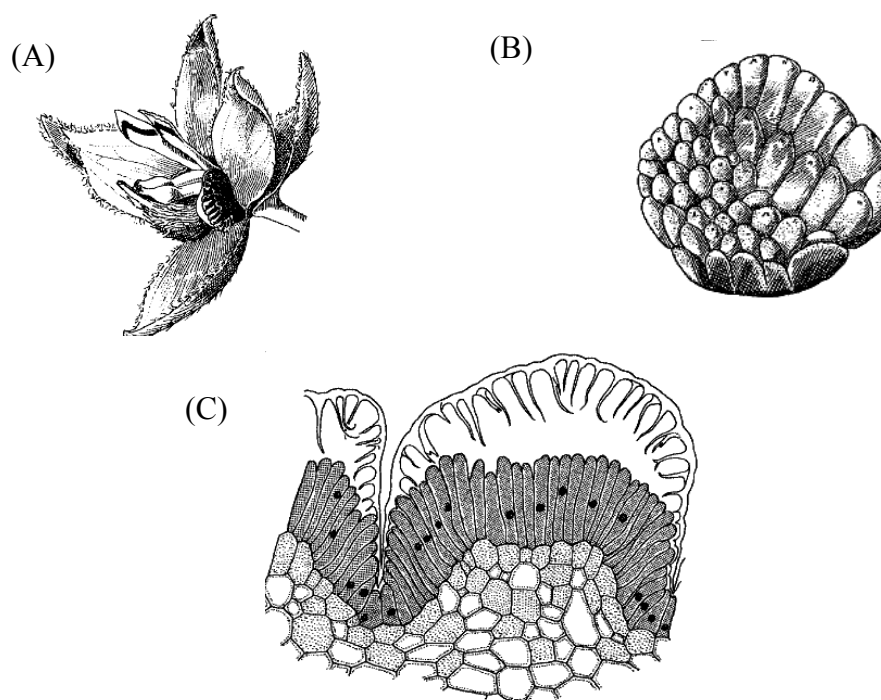
Figure 1.1. (A) The *Krameria triandra* flower with an epithelial elaiophore, (B) the illustration of elaiophores and (C) cross section with the protective cuticular, reproduced from Prof. Vogel 1974 with permission.

1.2.2. Trichomal elaiophores

The trichomal elaiophores consist of a few hundred up to even more than 50,000 glandular trichomes (Figure 1.2, Vogel 1974). The glandular area measures from 1.2 mm^2 (in *Calceolaria pinnata,* Scrophulariaceae) to 183 mm^2 (in *Bowkeria,* Scrophulariaceae). There is no protective layer, as in the above described epithelial cuticle. The only protection is a film of oil which covers the trichomal elaiophores. In some genera, elaiophores are protected inside the flower corolla such as in *Calceolaria* and *Diascia.* Oil production is always lower than in oil flowers with epithelial elaiophores. It is in the range of a few μL of oil (Vogel 1974). The oil production of

Angelonia begins when the flower opens and continues until the end of anthesis (Vogel and Machado 1991). Trichomal elaiophores are found in genera of the following families: Cucurbitaceae, Myrsinaceae, Scrophulariaceae, Solanaceae, Iridaceae, and some Orchidaceae (*e.g. Zygostates*) (Vogel 1974; Buchmann 1987).
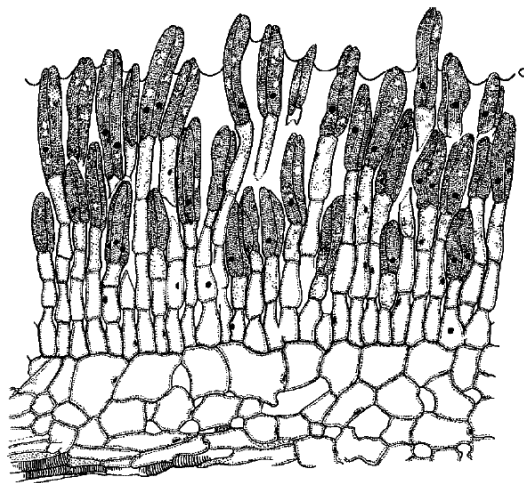
Figure 1.2. The cross section of trichomal elaiophores of *Calceolaria pavonii* (Scrophulariaceae), reproduced from Prof. Vogel 1974 with permission.

Trichomal elaiophores of *Calceolaria* have been studied more than other genera (e.g., Vogel studied 34 *Calceolaria* species, and Raman studied 3 *Calceolaria* species) (Vogel 1974; Raman 1989).

Calceolaria pavonii is found to some 2,290 trichome glands per mm^2, or a total of about 50,000 trichome glands in 22 mm^2 of entire elaiophores area. The trichome is club-shaped and measures about 100 μm (up to 250 μm) in length and 23 μm in width. Vogel (1974) revealed that trichome glands are produced when the floral bud reached a length of 2 mm. Oil production is initiated 1−2 days after the corolla is opened (Vogel 1974).

1.3. Characteristics of the floral oil

The oils are colourless or sometimes yellow, non-volatile and without odour (Vogel 1974; Buchmann 1987). Vogel was the first to report a chemical analysis of a floral oil, and found the following elements in the oil of *Calceolaria arachnoides*: 60% carbon, 31% oxygen, 9% hydrogen, and 1.4% phosphorus. Lipids of *Calceolaria* and *Krameria* are made up of β-acetoxy substituted fatty acids (C_{16}, C_{20}, C_{22}) and the rare 3-hydroxy

fatty acids (Seigler 1978; Buchmann 1987). The unique acylglycerols containing β-acetoxy fatty acids were also found as main lipid components of oil-secreting flowers (Vogel 1969, 1974, 1986, 1990a,b; Simpson *et al.*, 1977, Simpson and Neff 1981, 1983; Seigler 1978; Cane *et al.*, 1983; Buchmann 1987; Vinson *et al.*, 1997). Novel diacylglycerols of *Ornithophora radicans* (Orchidaceae) were reported by Reis *et al.* (2000, 2003, 2007). The partially acetylated dihydroxy fatty acids, as the new type of component in *Malpighia coccigera* (*Malpighiaceae*) oil flower were first reported by our group (Seipold *et al.*, 2004).

1.4. Oil collecting bees

To collect and transport floral oils, branched hairs of oil collecting bees have evolved to restrain the oil. These oil-collecting structures have evolved independently in four different families of oil collecting bees (Table 1.1, Roberts and Vallespir 1978, Figure 1.3, Vogel 1974). *Macropis* bees (Melittidae) collect floral oils from *Lysimachia* (Myrsinaceae) (Cane *et al.*, 1983; Vogel 1986). It has been suggested that *Macropis* bees are tightly associated with *Lysimachia* oil flowers (Myrsinaceae) (Cane *et al.*, 1983). From *Rediviva* bees (Melittidae), it is known that they have adapted elongated forelegs to exploit the floral oils from long spurs of the genus *Diascia* (Scrophulariacece) and some orchids (Orchidaceae) (Steiner and Whitehead 1988). *Ctenoplectrini* bees are known to collect floral oils from Cucurbitaceae (Steiner and Whitehead 1990). In the New World tropics, female *Centridini* and *Tapinotaspidini* bees collect floral oils from all neotropical plant families. The group of Simpson revealed that *Tetrapediini* bees collect oil, but are rarely found to pollinate the oil flowers. The two genera of stingless *Meliponini* bees collect floral oils, but are not equipped with any specialized tools for their collection (Simpson *et al.*, 1990).

(A) (B) (C)
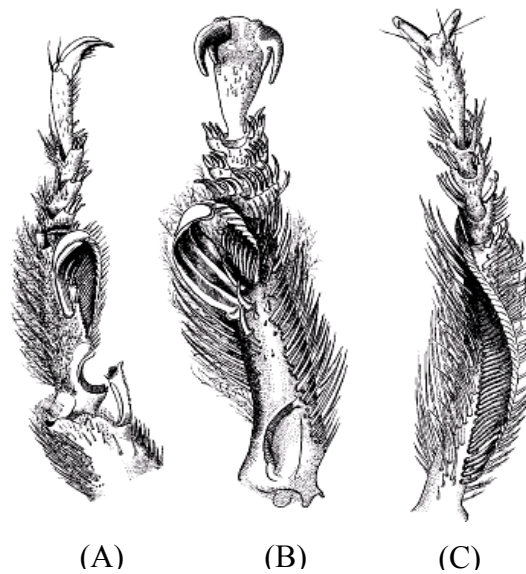
Figure 1.3. The oil-collecting tools on the right foreleg (A) *C. trigonoides,* (B) *C. autrani* and (C) the midleg of *C. trigonoides*, reproduced from Prof. Vogel 1974 with permission.

Table 1.1. Families and genera of known oil-collecting bees (from Buchmann 1987).

Family	Subfamily	Tribe	Genera
Melittidae	Melittinae		*Macropsis*
			Rediviva
Ctenoplectridae		Ctenoplectrini	*Ctenoplectra*
Anthophoridae	Anthophorinae	Centridini	*Centris*
			Epicharis
		Tapinotaspidini	*Arhysoceble*
			Caenonomada
			Chalepogenus
			Lanthanomelissa
			Monoeca
			Paratetrapedia
			Tapinotaspis
			Tapinotaspoides
			Trigonopedia
		Tetrapediini	*Tetrapedia*
Apidae	Meliponinae	Meliponini	*Trigona*
			Melipona

1.5. Lipid Biosynthesis

The fatty acid biosynthetic pathway as a primary metabolic pathway is found in every cell of the plant and is essential for developmental process. The major fatty acids of plants (and most other organisms) have a chain length of 16 or 18 carbons and contain from one to three *cis* double bonds. The fatty acids C16:0, C18:1, C18:2, C18:3 and in some species C16:3 make up over 90% of the acyl chains in the structural glycerolipids of almost all plant membranes. Glycerolipid membranes have fatty acids, attached to both the *sn*-1 and *sn*-2 positions of the glycerol backbone and a polar headgroup, which is attached to the *sn*-3 position. The combination of nonpolar fatty acyl chains and polar headgroups causes the amphiphelic physical properties of glycerolipids, being essential for the formation of membrane bilayers. If all three positions of glycerol are esterified with fatty acids, the triacylglycerol (TAG) formed is not suitable for membrane formation. However, TAGs represent the major form of lipids for storage in seeds. The cuticular lipids are found on the surface of all terrestrial plants. They are polymers of primarily 16- and 18-carbon hydroxy fatty acids cross-linked by esterification of their carboxy groups to hydroxyl groups on neighbouring acyl chains (Slabas and Fawcett 1992; Ohlrogge and Browse 1995).

1.6   The fatty acid biosynthesis

Plants are fundamentally different from other eukaryotes in the enzyme regulation of the fatty acid synthesis. At least 30 enzymatic reactions are required to produce a 16 or 18 carbon fatty acid from acetyl-CoA and malonyl-CoA. In animals, fungi, and some bacteria, all the reactions are catalyzed by a multifunctional polypeptide complex, located in the cytosol. In plants, the individual enzymes of the pathway are dissociable soluble components, located in the stroma of plastids. The central carbon donor for fatty acid synthesis is malonyl-CoA, produced by ACCase. However, before entering the fatty acid synthesis pathway, the malonyl group is transferred from CoA to a protein cofactor, acyl carrier protein (ACP) (Figure 1.4). ACP is a small acidic protein (9 kD) that contains a phosphopantetheine prosthetic group to which the growing acyl chain is attached as a thioester. After transfer into ACP, the malonyl-thioester enters into a series of condensation reactions with acyl-ACP (or acetyl CoA) acceptors. Release of CO_2 will direct this reaction to make it essentially irreversible. At least three separate condensing enzymes, also known as 3-ketoacyl-ACP synthases (*KAS*) are required to

produce an 18 carbon fatty acid. The first condensation of acetyl-CoA and malonyl-ACP to form a four-carbon product is catalyzed by *KAS III* (Jaworski *et al.*, 1989). A second condensing enzyme, *KAS* I, is assumed to catalyse the production of alkanoates with chain lengths from 6 to 16 carbons. Finally, elongation of the 16 carbon palmitoyl-ACP to stearoyl-ACP requires a separate condensing enzyme, *KAS II*. The initial product of each condensation reaction is a 3-ketoacyl-ACP. Three additional reactions occuring after each condensation will form a saturated fatty acid. The 3-ketoacyl-ACP is reduced at the carbonyl group by the enzyme 3-ketoacyl-ACP reductase, which uses NADPH as the electron donor. The next reaction is dehydration by hydroxyacyl ACP dehydratase. Each cycle of fatty acid synthesis is then completed by the enzyme enoyl-ACP reductase, which uses NADH or NADPH to reduce the *trans*-2 double bond to form a saturated fatty acid. The combined action of these four reactions leads to the lengthening of the precursor fatty acid by two carbons while it is still attached to ACP as a thioester (Harwood 1988; Slabas and Fawcett 1992; Ohlrogge *et al.*, 1993; Ohlrogge and Browse 1995).
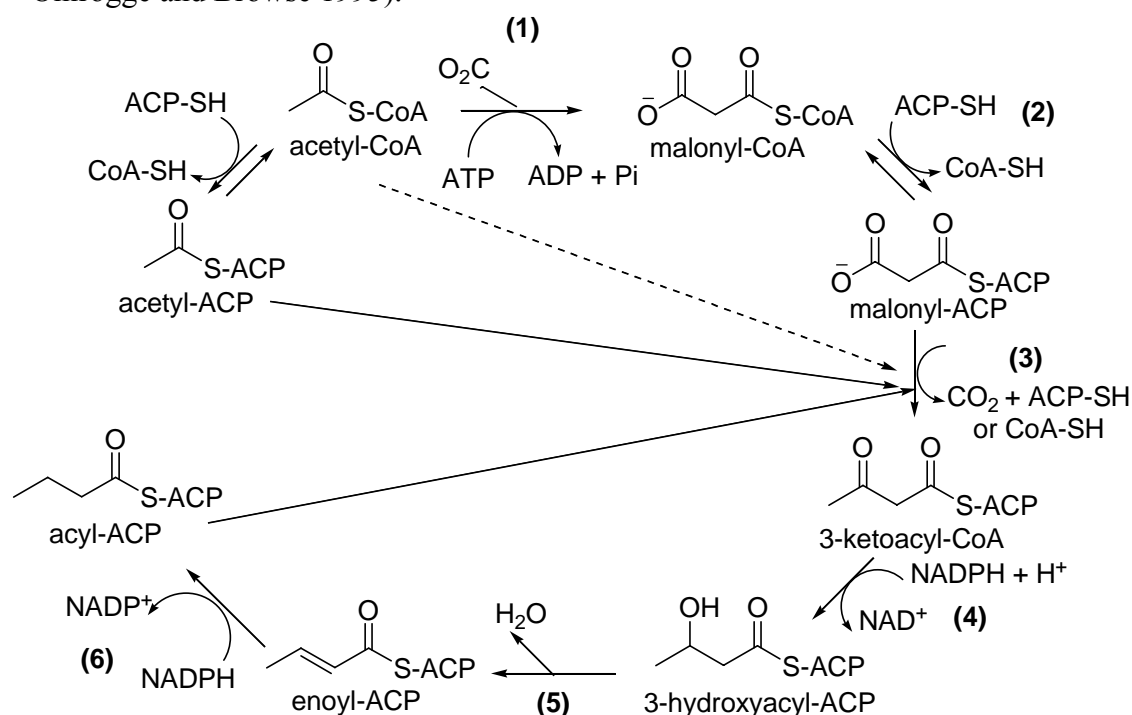
Figure 1.4. The reactions involved in saturated fatty acid biosynthesis (from Ohlrogge and Browse 1995). Acetyl-CoA is the basic building block of the fatty acid chain and enters the pathway both as a substrate for acetyl-CoA carboxylase (reaction **1**) and as a primer for the initial condensation reaction (reaction **3**). Reaction **2**, catalyzed by

malonyl-CoA: ACP transacylase, transfers malonyl from CoA to ACP. Malonyl-ACP is the carbon donor for all subsequent elongation reactions. After each condensation, the 3-ketoacyl-ACP product is reduced (reaction **4**), dehydrated (reaction **5**), and reduced again (reaction **6**), by 3-ketoacyl-ACP reductase, 3-hydroxyacyl-ACP dehydrase, and enoyl-ACP reductase, respectively.

The fatty acid biosynthetic pathway produces saturated fatty acids, but in most plant tissues, over 75% of the fatty acids are unsaturated. The first double bond is introduced by the soluble enzyme stearoyl-ACP desaturase. Structural studies have led to an elucidation of the fatty acid desaturation mechanism and recycled the nature of active site (Buist 2004). The enzyme is a homodimer in which each monomer has an independent active site consisting of a diironoxo cluster. The two iron atoms are coordinated within a central four helix bundle in which the motif (D/E)-E-X-R-H is represented in two of the four helices. The elongation of fatty acids in the plastids is terminated when the acyl group is removed from ACP. This can happen in two ways. In most cases, an acyl-ACP thioesterase hydrolyzes the acyl-ACP and releases free fatty acid. Alternatively, one of two known acyltransferases in the plastid transfers the fatty acid from ACP to glycerol-3-phosphate or to monoacylglycerol-3-phosphate. The first of these acyltransferases is a soluble enzyme that prefers oleoyl-ACP as a substrate. The second acyltransferase resides in the inner chloroplast envelope membrane and preferentially selects palmitoyl-ACP. If a thioesterase acts on acyl-ACP, the free fatty acid is able to leave the plastid. It is not known, how free fatty acids are transported out of the plastid. One option is simple diffusion across the envelope membrane. On the outer membrane of the chloroplast envelope, an acyl-CoA synthetase is thought to assemble an acyl-CoA thioester being then available for acyltransferase reactions to form glycerolipids in the endoplasmic reticulum (ER) (Ohlrogge *et al.*, 1993; Ohlrogge and Browse 1995).

Now acyl-CoA moves from the outer chloroplast envelope to the ER is unknown, but it may involve acyl-CoA binding proteins, small abundant proteins recently found to be present in plants (Hills *et al.*, 1994).

1.7. Gas chromatography-mass spectrometry (GC-MS)

Gas chromatography in combination with mass spectrometry has become one of the most powerful tools for the lipid analysis (Christie 1989). Chemical derivatization is also used to increase the intensity of the molecular ion peaks or specific fragment ions for a more reliable determination of the molecular weight of the compounds under study by electron impact (EI) mass spectrometry. In lipid studies, methyl ester derivatives are not always the most useful ones for identification purposes. Therefore, trimethysilyl (TMS) derivatives can be used to induce a characteristic fragmentation for structure elucidation. Such derivatives are common involved in lipid trace analysis. Recently, the application of TMS derivatives in routine GC/MS work was reviewed (Halket and Zaikin 2003).

1.8. Liquid chromatography-mass spectrometry (LC-MS)

LC-MS refers to the combination of liquid chromatographic separation with mass spectrometric detection. It offers possibilities for a better separation of a mixture and for easier identification. It also allows for an additional level of characterization of components based on their chromatographic behaviour as well as on the MS results. Pulfer and Murphy (2003) suggested that normal- and reversed-phase chromatography should be combined for a complete separation of lipids. MS is widely recognized as a superior detection method compared to the classic methods of ultraviolet or light scattering. In most LC/MS systems the interface configuration can be changed to produce ions for ionization with either positive or negative charge. The two common types of interface in the modern LC/MS systems are the electrospray ionization (ESI) and atmospheric-pressure chemical ionization (APCI) or ion spray (IS) interfaces. The ESI method is a very soft technique and recommended for use with highly polar and ionized materials. APCI is most commonly used to produce intact molecular ions for molecular weight determinations (McMaster 2005). There are a number of publications for both ESI and APCI, in the terms of lipid analysis (Byrdwell and Neff 1996; Byrdwell *et al.*, 1996; Byrdwell 2001; Sjövall *et al.*, 2001; Raith *et al.*, 2005,). In electrospray processes, the ions observed may be quasimolecular ions created by the addition of a proton (a hydrogen ion) and denoted $[M+H]^+$ or of another cation such as the sodium ion, $[M+Na]^+$ or the removal of a proton, $[M-H]^-$. Multiply-charged ions

such as $[M+2H]^{2+}$ are also observed (Fenn *et al.*, 1990; Byrdwell 2001). However, the chemical data are sometimes insufficient to identify the compounds, which present in the effluent from the liquid chromatograph. Therefore, the application of LC/MS-MS for the characterization and identification of compounds has proved enormously successful. Not only molecular weights but also fragments of other ions (precursor ions) help to develop a structural interpretation of the analyzed compound. The use of LC/MS-MS nowadays is the most common system for advanced lipid routine analyzes (Kuksis and Myher 1995).

1.9. Eletrospray ionization-Fourier transform ion cyclotron resonance mass spectrometry (ESI-FTICR-MS)

A method utilizing electrospray ionization (ESI) coupled with FT-ICR-MS is well known for its capabilities in the structural characterization of several classes of molecules (Feng and Siegel 2007), including lipid studies (Fard *et al.*, 2003; Ham *et al.*, 2004). The number of applications of ESI-FTICR-MS to lipid analysis is rapidly growing (Ham *et al.*, 2004; Wu *et al.*, 2004). FTICR detects the mass-to-charge ratio (*m/z*) of ions based on the cyclotron frequency of the ions in a fixed magnetic field (Marshall *et al.*, 1998). Fourier transform ion cyclotron resonance (FTICR) mass spectrometry is a very high resolution technique and the *m/z* values can be determined with high accuracy (10^5 to 10^6 range) (Hendrickson and Emmett 1999).

The ions are generated in the source and then pass through a series of pumping stages at increasing high vacuum (see Figure 1.5). When the ions enter the cyclotron cell (ion trap), pressures are in the range of 10^{-10} to 10^{-11} mBar with the temperature close to absolute zero. The cell is located inside a spatial uniform static superconducting high field magnet (typically 4.7 to 13 Tesla) cooled by liquid helium and liquid nitrogen (Comisarow and Marshall 1974). Excitation of each individual *m/z* is achieved by sweeping RF pulses across the excitation plates of the cell. The frequency of this current is the same as the cyclotron frequency of the ions. The intensity is proportional to the number of ions. The useful signal is extracted from these data by performing a Fourier transform procedure to give a mass spectrum (Figure 1.5).
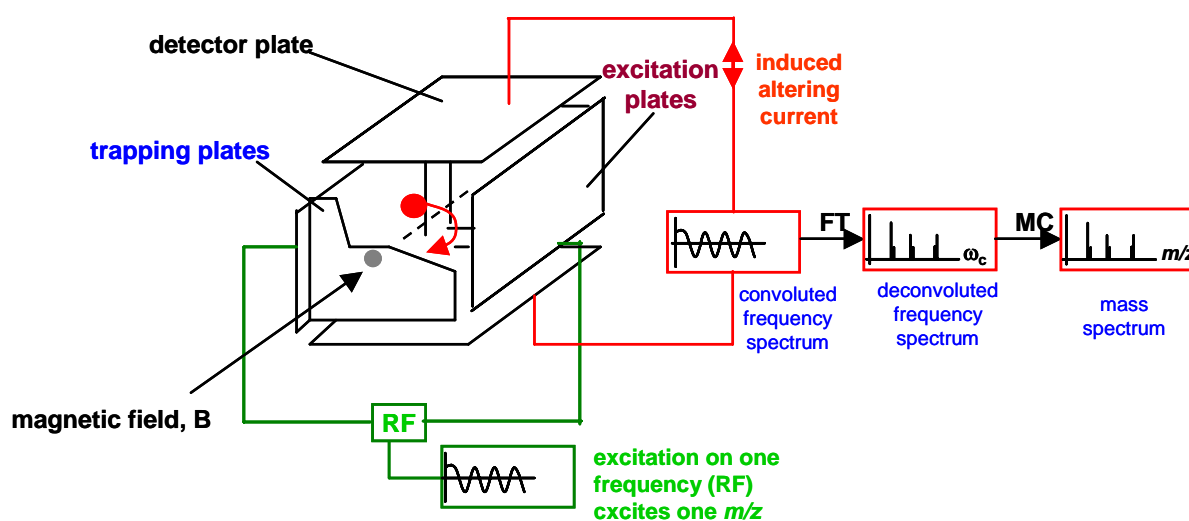
Figure 1.5. A schematic of FTICR-MS showing the ion trapping, detection and signal genation (ω_c = induced cyclotron frequency, *m/z* = mass to charge ratio and RF = radio frequency. **B** = magnetic field strength, **MC** = mast cells, **FT** = Fourier-transform) (modified from http://www.chm.bris.ac.uk/ms/theory/fticr-massspec.html).

CHAPTER 2

Non-Volatile Floral Oils of *Diascia* spp. (Scrophulariaceae)*

Summary

The floral oils of *Diascia purpurea*, *D. vigilis*, *D. cordata*, *D. megathura*, and *D. integerrima* (Scrophulariaceae) have been selectively collected from trichome elaiophores. The trimethylsilyl (TMS) derivatized floral oils were analyzed by electron impact (EI) gas chromatography-mass spectrometry (GC-MS), whilst the underivatized floral oil samples by electrospray Fourier-transform ion cyclotron resonance mass spectrometry (ESI-FTICR-MS). The predominant compounds of floral oils from five *Diascia* spp. investigated are partially acetylated acylglycerols of (3*R*)-acetoxy fatty acids (C_{14}, C_{16}, and C_{18}), as was proven with synthetic reference sample. The mass spectral interpretation of significant compounds is presented in detail. The importance of *Diascia* floral oils for *Rediviva* bees is also discussed in a co-evolutionary context.

Results and Discussion

2.1. *Fatty acid methyl ester* (FAME) Profiling of the *Diascia* spp.

Diascia oils from trichome elaiophores (Figure 2.1) are naturally yellowish.
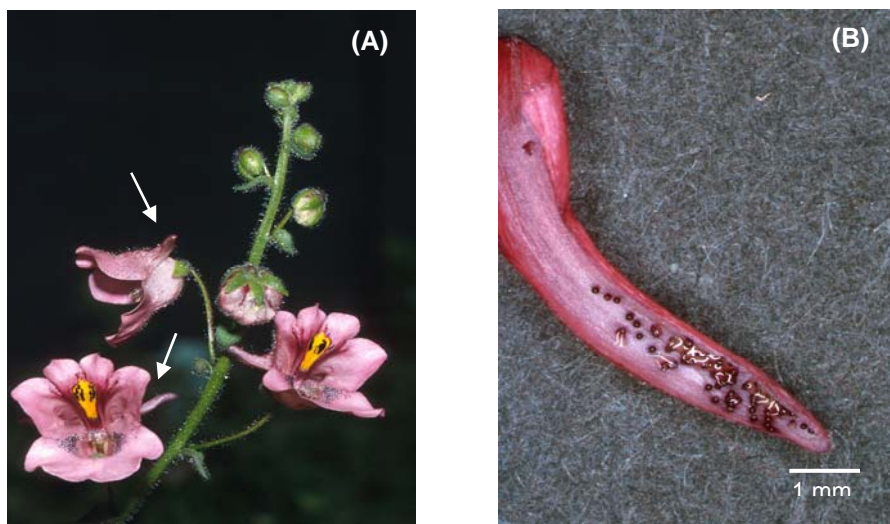
Figure 2.1. *Diascia megathura* (Scrophulariaceae): (A) inflorescence showing spurs (B) spur longitudinally split, showing the elaiophores with free oil. Arrows are showing the spurs (photos by G. Gerlach).

Figure 2.2 illustrates the total ion chromatogram (TIC) of the FAME profiling of *D. vigilis*. The FAME profiling results of *D. vigilis* are presented in Table 2.1. Fatty acids and (3*R*)-hydroxy fatty acids with even-numbered chain length ranging from C_{14} to C_{18} represent the main compounds of the lipid collection. In all cases, there were no traces of acylglycerols due to the complete trans-esterification reaction. The main compound of all derivatized *Diascia* oil samples was (3*R*)-hydroxypalmitic acid (**10**, *ca.* 55–75%) (Table 2.1). The EI mass spectra of TMS derivatives of 3-hydroxy fatty acid methyl ester show a poor molecular ion peak, but the molecular weight can be ascertained from a characteristic ion at *m/z* $[M-Me]^+$. Its formed by elimination of a methyl radical from the TMS group. The characteristic ions of oxygenated fatty acid TMS derivatives have common ions at *m/z* 73 ($[SiMe_3]^+$) and 89 ($[OSiMe_3]^+$) (Curstedt 1974). A predominant ion at *m/z* 175, $[MeO(CO)CH_2CH(OSiMe_3)]^+$ can be attributed to a cleavage between C_3 and C_4 of the carbon chain which is diagnostic of the hydroxyl group position of fatty acid chain (Mayberry 1980; Mielniczuk *et al*., 1992, 1993).
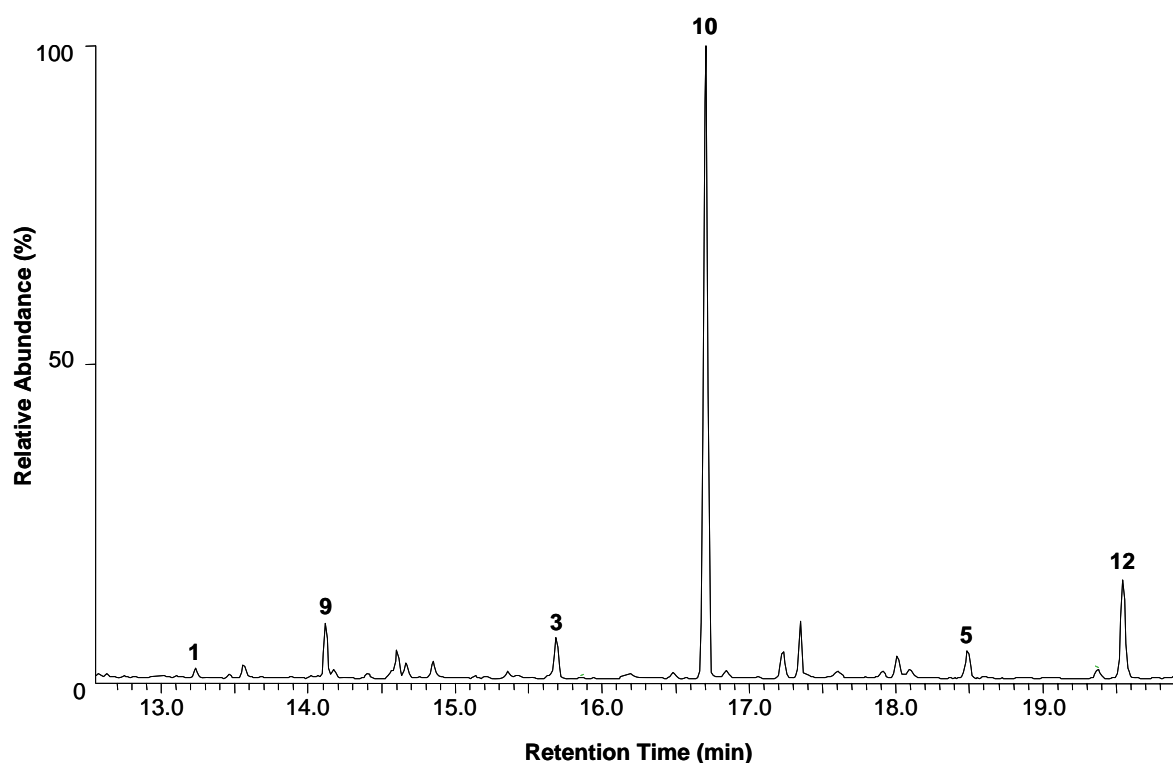
Figure 2.2. Total ion chromatogram (TIC) of the FAME profiling of *D. vigilis* floral oil (for the identification of compound members see Table 2.1, conditions **GC1**)

3-hydroxy fatty acids possess a chiral carbon. Due to the small amounts of samples available, only a chromatographic method is suitable to determine the absolute configuration. Thus diastereomeric derivatives were generated by esterification with optically pure (2*S*)-phenyl propionic acid from the acid chloride. The results were based on the GC-retention time comparison with a (2*S*)-phenylpropionyl derivative of a synthetic (see Appendix 1) (Hammarström 1975; Gradowska 1994; Weil *et al*., 2002; Seipold 2004). In most cases, the hydroxyl group at C-3 has (*R*)-configuration. The results were related to the fact of (*R*)-hydroxy family are intermediate during the fatty acid biosynthesis (Mayberry 1980).

Table 2.1. FAME profiling of *Diascia* spp. (as TMS derivatives[a]).

No.	Compound[b]	t_R (min)	Relative composition (%)				
			D. purpurea	*D. vigilis*	*D. cordata*	*D. megathura*	*D. integerrima*
1	myristic acid	13.24	1.3	1.1	0.3	1.7	0.9
3	palmitic acid	15.69	6.7	5.0	2.0	11.3	8.4
5	stearic acid	18.48	5.3	3.4	1.4	7.8	6.4
9	(3*R*)-hydroxymyristic acid	14.12	0.2	6.6	24.5	3.7	9.2
10	(3*R*)-hydroxypalmitic acid	16.71	56.5	72.1	65.0	55.8	61.1
12	(3*R*)-hydroxystearic acid	19.54	30.1	11.9	6.8	19.7	14

[a]The examplary data were obtained from *D. vigilis*. [b]see Appendix 2 for EI-mass spectral data (Table A 2.1 and A 2.2).

2.2   GC/EI-MS analysis of the acylglycerols of *Diascia* oils

A GC/EI-MS study of TMS derivatives of *Diascia* oils yielded both monoacylglycerols (MAGs) and diacylglycerols (DAGs) as main constituents along with small amounts of triacylglycerols (TAGs) (Table 2.2). According to the results obtained from the TMS derivatives, the detected acylglycerols of *Diascia* spp. contain one or two acetyl groups and (3*R*)-acetoxy fatty acid attached to the glycerol backbone. Furthermore, the ESI-FTICR-MS profiling analysis of underivatized *Diascia* oils confirmed the (3*R*)-acetoxy fatty acids, as long-chain moieties of the acylglycerols (see 2.3). The acetylation of the 3-hydroxy acids may be related to the export of the floral oils out of the cells. It has been reported that a hydroxyl group in fatty acids reduces the lipid transporter affinity compared to unfunctionalized fatty acids (Zachowski *et al*., 1998). Therefore, the acetylation could be crucial for an improved transport property (Seipold *et al*., 2004).

Figure 2.3 shows the total ion chromatogram of the TMS derivative of *D. vigilis* floral oil. The identified compounds and relative composition of acylglycerols of the *Diascia* flower oils are summarized in Table 2.2. The key ions of the EI mass spectral data of the identified compounds are presented in Appendix 2. The two main components of *D. vigilis* floral oil are 2-[(3*R*)-acetoxypalmitoyl]glycerol (**27**) and 2-[(3*R*)-acetoxypalmitoyl]-1-acetylglycerol (**30**, Table 2.2).
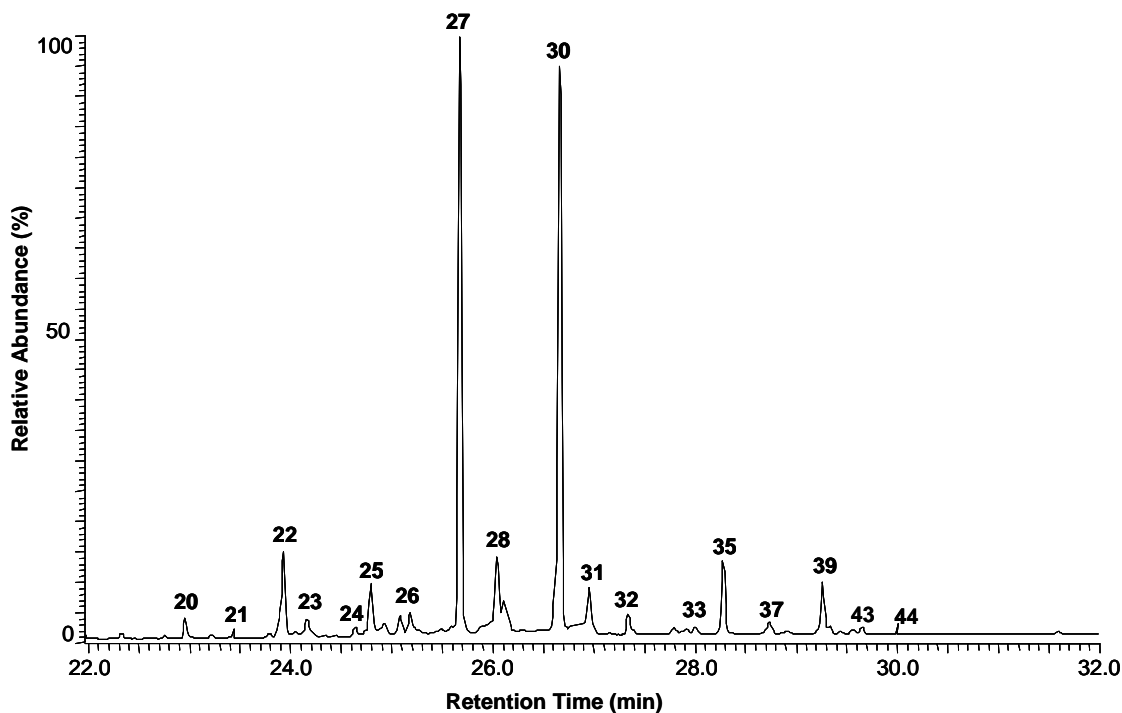
Figure 2.3. Total ion chromatogram (TIC) of TMS derivatives of *D. vigilis* floral oil (for the identification of compound members see Table 2.2, conditions **GC1**).

Table 2.2. Acylglycerols of the *Diascia* spp. identified as TMS derivatives by GC/EI-MS.

No.	t_R (min)[a]	Compound[b]	Relative composition (%)				
			D. purpurea	*D. vigilis*	*D. cordata*	*D. megathura*	*D. integerrima*
20	22.96	2-[(3R)-acetoxymyristoyl]glycerol	1.2	1.3	1.7	-	1.7
21	23.41	1-[(3R)-acetoxymyristoyl]glycerol	0.3	0.2	9.5	0.8	-
22	23.93	2-[(3R)-acetoxymyristoyl]-1-acetylglycerol	0.3	5.8	1.2	1.6	3.1
23	24.22	1-[(3R)-acetoxymyristoyl]-3-acetylglycerol	0.1	0.2	-	4.7	-
24	24.64	2-](3R)-acetoxymyristoyl]-1,3-diacetylglycerol	0.9	0.6	-	0.2	6.6
25	24.79	unknown	17.4	2.5	-	-	-
26	25.18	unknown	6.5	1.1	39.8	-	-
27	25.67	2-[(3R)-acetoxypalmitoyl]glycerol	16.2	35.6	8.7	13.6	40.2
28	26.14	1-[(3R)-acetoxypalmitoyl]glycerol	9.2	3.6	4.2	12.5	5.6
30	26.66	2-[(3R)-acetoxypalmitoyl]-1-acetylglycerol	17.6	35.7	25.8	24.9	17.9
31	26.96	1-[(3R)-acetoxypalmitoyl]-3-acetylglycerol	6.8	2.0	1.5	19.6	1.7
32	27.39	2-[(3R)-acetoxypalmitoyl]-1,3-diacetylglycerol	3.2	0.1	-	5.5	9.2
33	27.92	unknown	2.0	0.3	-	-	-
35	28.28	2-[(3R)-acetoxystearoyl]glycerol	8.2	4.8	0.3	2.1	8.9
37	28.73	1-[(3R)-acetoxystearoyl]glycerol	5.8	1.2	9.1	4.0	2.8
39	29.27	2-[(3R)-acetoxystearoyl]-1-acetylglycerol	2.5	4.4	-	5.0	2.4
43	29.56	1-[(3R)-acetoxystearoyl]-3-acetylglycerol	1.8	0.4	-	5.0	0.1
44	30.00	2-[(3R)-acetoxystearoyl]-1,3-diacetylglycerol	-	0.1	-	0.6	0.4

[a]obtained from *D. vigilis*, [b]see Appendix 2 for EI-mass spectral data (Table A 2.5, A 2.6, A 2.7 and A 2.15), (-) = not detected.

Our results indicated that the 1-monoacyl and 2-monoacyl isomer of (3*R*)-acetoxy fatty acids can be distinguished by their EI-MS data of the TMS derivatives. Figure 2.4 shows a comparison of the EI mass spectra of the 1-monoacyl and 2-monoacyl isomers of (3*R*)-acetoxypalmitoylglycerol. The mass spectra of the acylglycerol TMS derivatives show the characteristic ions at *m/z* 73, 89 and 103 corresponding to the fragments $[SiMe_3]^+$, $[OSiMe_3]^+$, and $[CH_2OSiMe_3]^+$, respectively (Curstedt 1974). Furthermore, the prominent ions at *m/z* 117 $[OCOSiMe_3]^+$ and 129 $[CH_2CHCHOSiMe_3]^+$ are commonly detected in the spectra of TMS derivatives of acylglycerols (Curstedt 1974; Wood 1980). The molecular weight of MAGs of (3*R*)-acetoxy fatty acids in *Diascia* spp. was deduced from the appearance of a significant ion type **a**, ($[M-Me-HOAc]^+$, Seipold 2004). In case of the MAGs of fatty acid, $[M-Me]^+$ ion, formed by loss of methyl radical from the trimethylsilyl group represents the peak of highest mass (Curstedt 1974; Wood 1980). The ion at *m/z* 147 $[Me_2SiOSiMe_3]^+$ was due to the rearrangement ions, frequently detected in TMS derivative of monoacylglycerols. Scheme 2.1 shows the characteristic fragmentation of 2-[(3*R*)-acetoxypalmitoyl]glycerol (**27**) and 1-[(3*R*)-acetoxypalmitoyl]glycerol (**28**). An important key fragment of the 2-MAG isomer is the ion of type **e** at *m/z* 218 (**20**, **27**, **35**), while the ion of type (**b**−HOAc) is a typical fragment of 1-MAG (**21**, **28**, **37**). As previously suggested the 2-MAG displays a significant ion at *m/z* 218 which is formed by loss of the oxygenated fatty acid from the $[M]^+$ (Johnson and Holman 1966). Rearrangement of a TMS group from the acylglycerol backbone to the carboxyl group of the fatty acids leads to a **c**-type ion at *m/z* 311 (after loss of a HOAc unit). The ion of type (**d**−HOAc) corresponds to the acylium ion after loss of 3-acetoxy group. Ion at *m/z* 203 (**e**−Me) appears in both 1- and 2-monoacyl isomers. The most significant evidence of the 1-MAGs of (3*R*)-acetoxy fatty acid is the formation of an ion at *m/z* 369 (**b**−HOAc) as an unique peak, including the **f**-type ion at *m/z* 205. In most of the 1-MAGs, the ion of type **b** ($[M-103]^+$) corresponding to the loss of $CH_2OSi(CH_3)_3$, represents the base peak (Figure 2.4, see Appendix 2: Table A 2.5) (Johnson and Holman 1966; Curstedt 1974; Myher *et al.*, 1974; Wood 1980).
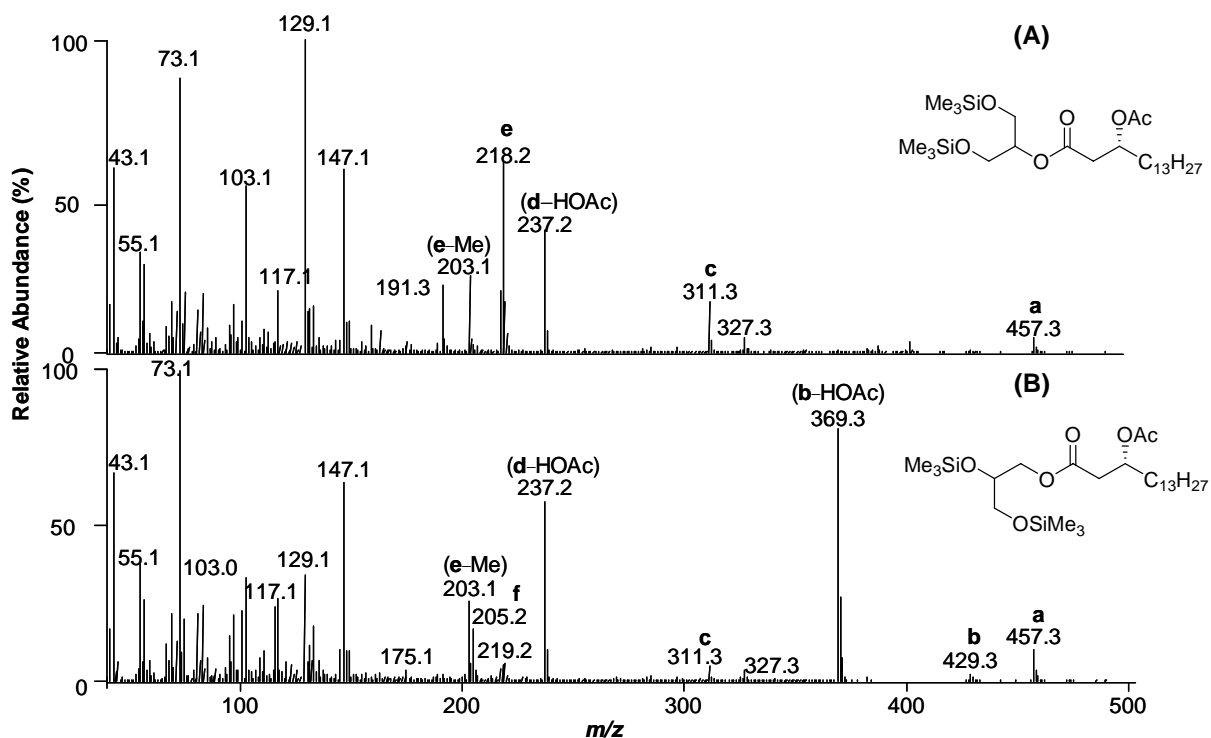
Figure 2.4. 70 eV-EI mass spectra of the TMS derivatives of monoacylglycerols (MAGs): (A) 2-[(3*R*)-acetoxypalmitoyl]glycerol (**27**) and (B) 1-[(3*R*)-acetoxypalmitoyl]glycerol (**28**). The significant fragment ions are described in Scheme 2.1.
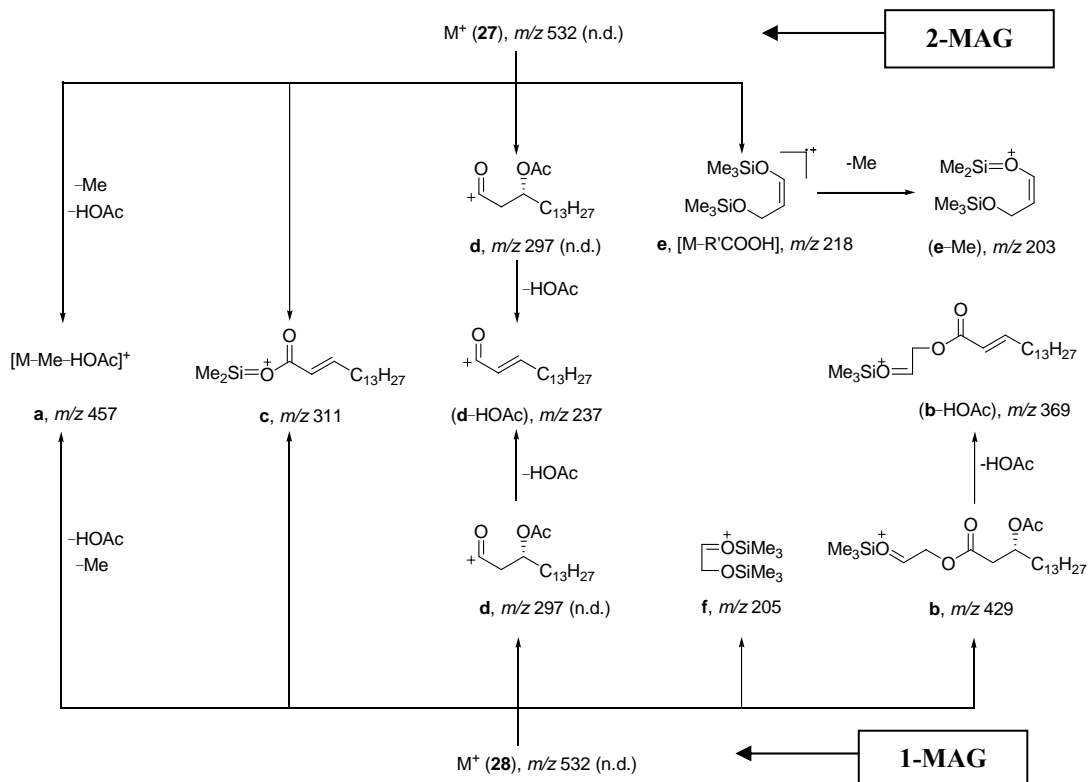
Scheme 2.1. Mass spectral fragmentation of the monoacylglycerols 2-[(3*R*)-acetoxypalmitoyl]glycerol (**27**) and 1-[(3*R*)-acetoxypalmitoyl]glycerol (**28**) (n.d. = not detected).

Figure 2.5 illustrates the EI mass spectra of the TMS derivatives of 2-[(3*R*)-acetoxypalmitoyl]-1-acetylglycerol (**30**) and 1-[(3*R*)-acetoxypalmitoyl]-3-acetylglycerol (**31**). Generally, the mass spectral behavior of DAGs containing (3*R*)-acetoxy fatty acids and an acetyl moiety is similar to that of the MAGs. An ion at *m/z* 189 (**g**) appearing both in 1,2- and 1,3-DAGs can be explained as a cyclic structure (Curstedt 1974) as shown in Scheme 2.2. The TMS derivatives of 1,2-diacylglycerols (**22**, **30**, **39**) showed an analogous fragment at *m/z* 188 (type **e**) with moderate intensity (see Appendix 2: Table A 2.6). On the other hand, the e_1-type ion (*m/z* 188, e_1) in 1,3-DAGs was of low abundance. This ion can be a first hint that the (3*R*)-acetoxy fatty acid was attached to the secondary hydroxyl group of the glycerol backbone. The ion **k** at *m/z* 145 confirming a 1,2-DAG was not observed in the TMS derivatives of 1,3-diacylglycerols (**23**, **31**, **43**) (Curstedt 1974). It should be pointed out that the ions at *m/z* 175 (type **h**) and *m/z* 146 (e_1–CH_2CO) only appear in the mass spectra of 1,3-diacylglycerols (Scheme 2.2, Table 2.2) (Seipold 2004).
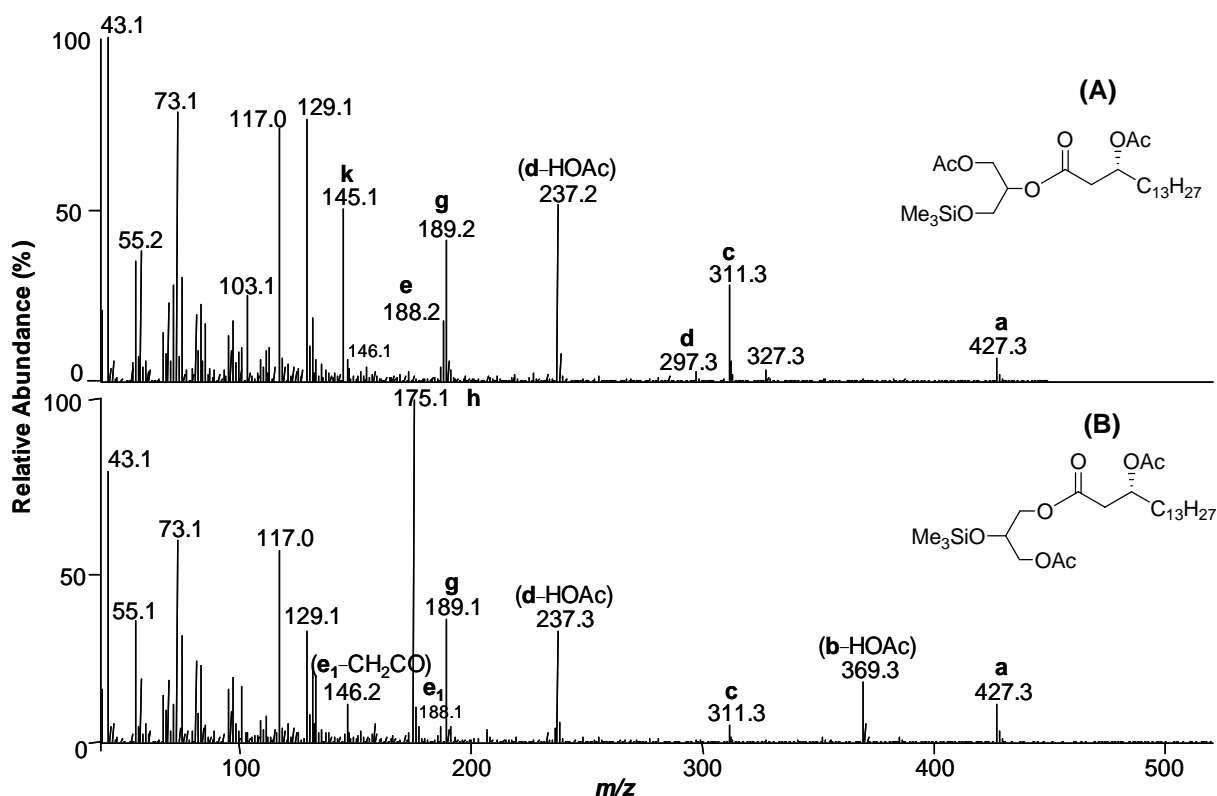
Figure 2.5. 70 eV-mass spectra of TMS derivatives of diacylglycerols (DAGs): (A) 2-[(3*R*)-acetoxypalmitoyl]-1-acetylglycerol (**30**) and (B) 1-[(3*R*)-acetoxypalmitoyl]-3-acetylglycerol (**31**). The significant fragment ions are described in Scheme 2.1 and 2.2.

M$^+$ (**30**), *m/z* 502 (n.d.) ◄── | **1,2-DAG** |

−Me
−HOAc

AcO⌐·$^+$
Me$_3$SiO
e, [M−R'COOH]$^+$, *m/z* 188

$\overset{+}{O}$
OSiMe$_3$
k, *m/z* 145

[M−Me−HOAc]$^+$
a, *m/z* 427

O
$\overset{+}{O}$
OSiMe$_3$
g, *m/z* 189

Me$_3$SiO⌐·$^+$
OH
(**e$_1$**−CH$_2$CO), *m/z* 146

−CH$_2$CO

−HOAc
−Me

Me$_3$SiO⌐·$^+$
OAc
e$_1$, *m/z* 188 (n.s.)

Me$_3$SiO=$\overset{+}{}$
OAc
h, *m/z* 175

M$^+$ (**31**), *m/z* 502 (n.d.) ◄── | **1,3-DAG** |
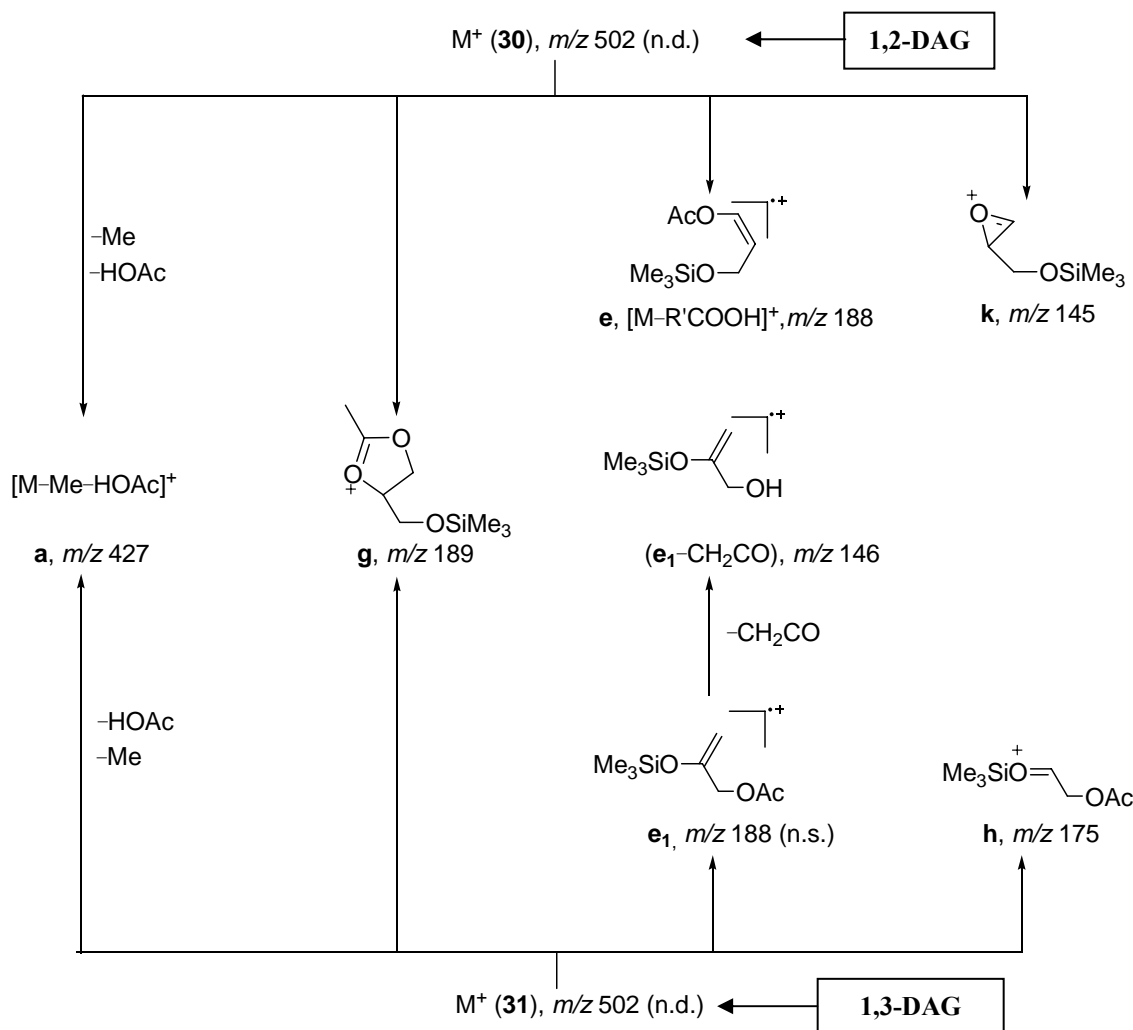
Scheme 2.2. Mass spectral fragmentation of the diacylglycerols 2-[(3*R*)-acetoxypalmitoyl]-1-acetylglycerol (**30**) and 1-[(3*R*)-acetoxypalmitoyl]-3-acetylglycerol (**31**) (n.d. = not detected; n.s. = not significant).

The TAGs in floral oil of *D. vigilis* (**24**, **32**, **44,** Table 2.2) consist of one (3*R*)-acetoxy fatty acids (C$_{14,}$ C$_{16}$ and C$_{18}$) at C-2 and two acetyl moieties at C-1 and C-3 of the glycerol backbone. Figure 2.6 illustrates the EI mass spectrum of 2-[(3*R*)-acetoxypalmitoyl]-1,3-diacetylglycerol (**32**). Mass spectra of these compounds show no molecular ion, but an ion at *m/z* [M−2HOAc]$^+$ (**a$_1$**) as a peak of highest mass. Ion of type **d** was observed in very low abundance, whereas ion type (**d**−HOAc) was dominantly detected. The fragment at *m/z* 159 (**e$_2$**) was formed by loss of oxygenated fatty acid from the molecule which indicate the evidence of 1,3-diacetylglycerol (Vogel 1974). To confirm the diagnostic of fragments ion, the acetylation of [^{2}H]-labelled was

further performed (Scheme 2.3). The EI mass spectrum of [²H]-labelled 2-[(3*R*)-acetoxypalmitoyl]-1,3-diacetylglycerol (**32**) is figured in Appendix 3 (Figure A 3.1). EI mass spectrum of [²H]-labelled acetylated derivatives can certainly explain the potential sequence of the loss of acetoxy groups to form an ion at *m/z* [M–2HOAc]$^+$ (**a₁**, *m/z* 355) which occur by [²H₃] incorporation into the structure. Such an experiment gave evidence that the two acetoxy groups originate from the oxygenated fatty acid long chain and the second from glycerol backbone. The ion of type **e₂** (*m/z* 159) is shifted by 6 mass units toward high masses in the [²H₆]-labelled (2 × COCD₃) derivative (Scheme 2.3, see also Figure A 3-1 in Appendix 3). This fragment confirmed a 1,3-diacetylglycerol which correspond to loss of the oxygenated fatty acid. EI mass spectra of 1-acyl-2,3-diacetyl-glycerols were also previously described (Reis *et al.,* 2003).
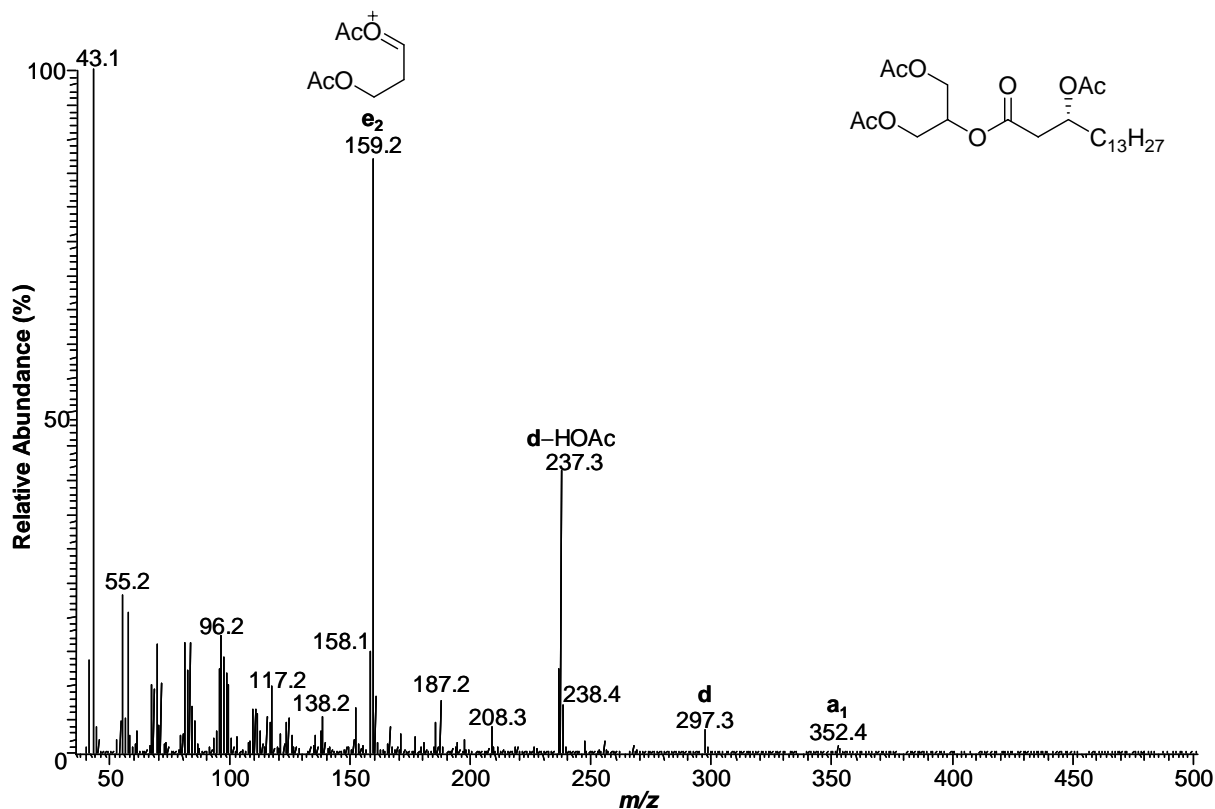
Figure 2.6. 70 eV EI-mass spectrum of TMS derivative of triacylglycerol: 2-[(3*R*)-acetoxypalmitoyl]-1,3-diacetylglycerol (**32**). The significant fragment ions are described in Scheme 2.1 and 2.2.

(32)   [²H]-labelled of **32**
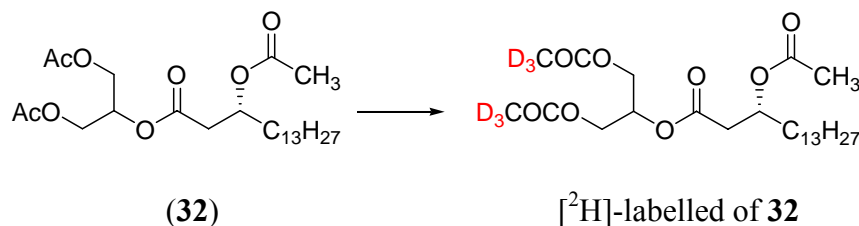
Scheme 2.3. [²H]-acetylation of 2-[(3*R*)-acetoxypalmitoyl]-1,3-diacetylglycerol (**32**) (see EI-mass spectrum in Figure A 3.1, Appendix 3).

The unidentified compounds **25**, **26** and **33** are assumed to be isomers of 2-[(3*R*)-acetoxypalmitoyl]-1-acetylglycerol (**30**), 1-[(3*R*)-acetoxypalmitoyl]-3-acetylglycerol (**31**) and 1-[(3*R*)-acetoxystearoyl]-3-acetylglycerol (**43**), respectively (Table 2.2), but no unequivocal assignment is possible. An isomerization via an acyl-migration probably can occur during storage or measurement (Lyubachevskaya and Boyle-Roden 2000; Seipold 2004; Christie 2006). Therefore, the compounds **25, 26** and **33** might be also artefacts.

In most cases, the floral oils of the five *Diascia* spp. exhibit a similar pattern with respect to their MAGs, DAGs and TAGs distribution, respectively. Exceptionally, in floral oil of *D. cordata*, TAGs could not be detected. Fatty acids were not detected by TMS derivatization of the floral oils of *Diascia* spp. DAGs represent the most abundant class (*ca.* 60−80%) compared to MAGs (*ca.* 20−30%) and TAGs (<15%) (Table 2.2). MAGs and DAGs as well as a small amount of TAGs were also described as the main oil components in *Byrsonima crassifolia* (Malpighiaceae) elaiophores (Vinson *et al*., 1997). The dominance of MAGs and DAGs is probably related to the insect digestive system. It has been shown that both MAGs and DAGs are better digestible than TAGs (Vinson *et al*., 1997).

2.3   Analysis of acylglycerols of underivatized *Diascia* oils

The underivatized floral oils of the *Diascia* spp. are also investigated by ESI-FTICR-MS to obtain high resolution mass data of the lipid compounds. This will allow a rapid profiling of different oils in the future. All measurements were performed in the positive ion mode. In these cases, the electrospray mass spectra of the investigated oils show the sodium adducts ($[M+Na]^+$) of the corresponding compounds (Table 2.3). The positive ESI-FTICR mass spectrum of *D. integerrima* displays a DAG signal (base peak) that comprises the compounds **25**, **26**, **30** and **31** (*m/z* 453.28256) and contains even-number oxygenated fatty acid(s). The homology of investigated DAGs result in the compounds **22**, **23** (*m/z* 425.25130) and compounds **33**, **39**, **43** (*m/z* 481.31404) (Figure 2.7). The MAGs signals represent the loss of an acetyl group (CH_2CO) from the DAGs, whereas TAGs show further an additional of acetyl moiety in their structures. Both of ESI-FTICR and GC/EI-MS results of *Diascia* floral oils represent the acetylated acylglycerols as the main compounds. In some case studied, such as ESI-FTICR-MS results of *D. cordata* floral oil noticeably indicated that TAGs consist long chain of (3*R*)-acetoxy fatty acids with chain lengths of C_{14} and C_{16} and two acetyl moieties, whereas the EI-MS data shows no hint of those TAGs. Likewise, fatty acids were not generally observed, when positive mode-ESI was applied. However, fatty acids were easily detected and characterized by GC/EI-MS methods (see Table 2.1). The high resolution ESI-FTICR-MS results provide the high mass accuracy and elemental compositions of acetylated acylglycerols which usefully help the structural elucidation. However, the absolute abundance or even relative abundance of peaks in the ESI-FTICR does not certainly reflect the real proportions (Pulfer and Murphy 2003; Han and Gross 2005). Thus, in most cases, GC/EI-MS data were taken for an indication of the relative abundance of indicative compounds. Nonetheless, the most significant acylglycerols were detected in both methods.
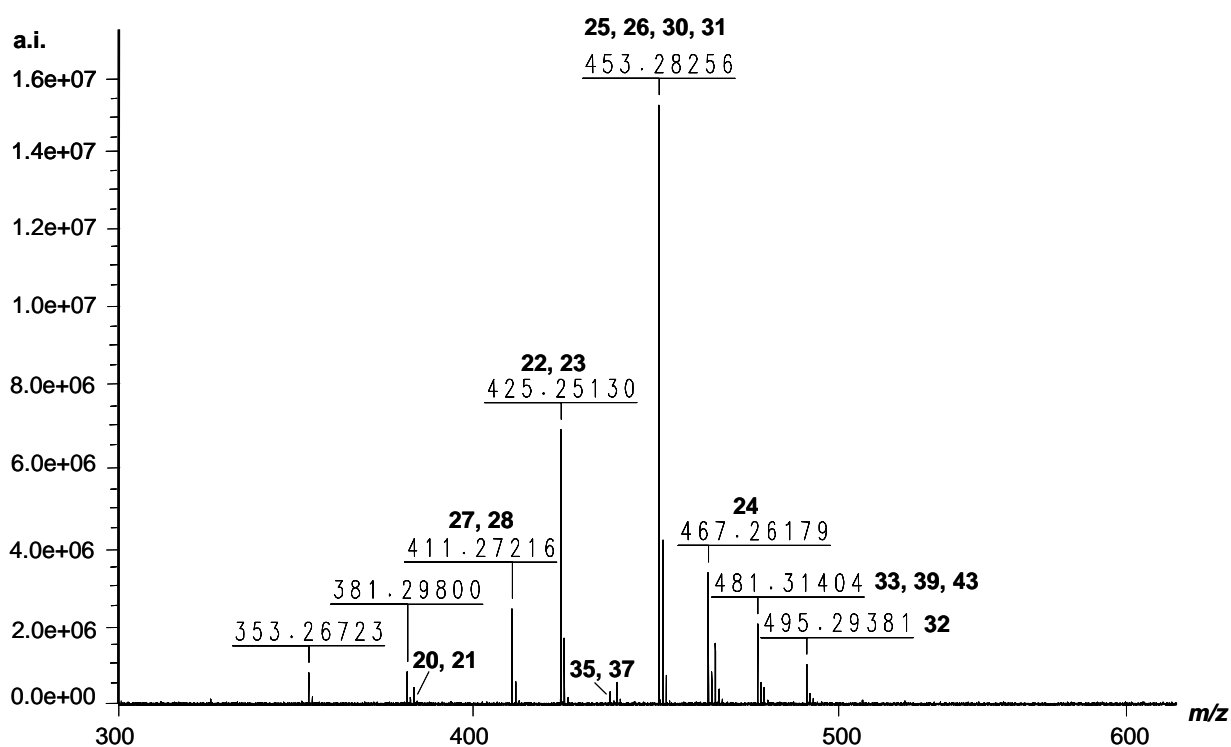
Figure 2.7. Positive-ion ESI-FTICR mass spectrum of the acylglycerol profile of *D. integerrima.* Peak heights are scaled relative to the highest magnitude peak (for the identified compounds see Table 2.3).

Table 2.3. Positive ion ESI-FTICR mass spectral data of the floral oils of the *Diascia* spp.[a]

No.	Compound type[b]	Elemental composition	*m/z* ([M+Na]$^+$)	Error (ppm)	MW	Relative abundance (%)				
						Diascia purpurea	*Diascia vigilis*	*Diascia cordata*	*Diascia megathura*	*Diascia integerrima*
20, 21	MAG (3-OAc 14:0)	$C_{19}H_{36}O_6\,Na^+$	383.29800	+0.2	360	1.3	0.3	2.5	1.8	2.9
22, 23	DAG (3-OAc 14:0, OAc)	$C_{21}H_{38}O_7\,Na^+$	425.25130	+0.8	402	4.8	10.5	38.3	38.9	45.9
24	TAG (3-OAc 14:0, diOAc)	$C_{23}H_{40}O_8\,Na^+$	467.26179	+0.8	444	7.0	4.0	22.7	25.4	22.1
25, 26, 30, 31	DAG (3-OAc 16:0, OAc)	$C_{23}H_{42}O_7\,Na^+$	453.28256	+0.8	430	100	100	100	100	100
27, 28	MAG (3-OAc 16:0)	$C_{21}H_{40}O_6\,Na^+$	411.27216	+1.1	388	28.2	8.4	16.0	12.0	16.1
32	TAG (3-OAc 16:0, diOAc)	$C_{25}H_{44}O_8\,Na^+$	495.29318	+0.7	472	38.9	3.5	8.6	10.1	6.8
33, 39, 43	DAG (3-OAc 18:0, OAc)	$C_{25}H_{46}O_7\,Na^+$	481.31404	+1.4	458	62.7	28.0	15.6	16.5	13.5
35, 37	MAG (3-OAc 18:0)	$C_{23}H_{44}O_6\,Na^+$	439.30342	+1.0	416	17.9	2.6	2.2	2.2	2.2
44	TAG (3-OAc 18:0, diOAc)	$C_{27}H_{48}O_8\,Na^+$	523.32383	-0.6	500	13.8	-	-	1.4	-

[a]The examplary data were obtained from *D. integerrima* (exception: compound **44** from *D. purpurea*),[b]see full name of compounds in Table 2.2, MW= molecular weight,
(-) = not detected.

In conclusion, positive ion ESI-FTICR mass spectra of the non-derivatized floral oils of *Diascia* spp. provided important results with respect to the acyglycerol profile. The determination of the elemental composition can provide a quick look at the lipid pattern of the oil-secreting *Diascia* flowers. With respect to the most prominent components were revealed in both the ESI-FTICR-MS and the GC/EI-MS experiments (Table 2.2 and 2.3).

Based on these results, the related compositions of *Diascia* species indicate that they originate from the same evolutionary background as it is to be expected within a genus. It has been known that *Diascia* species are tightly associated with *Rediviva* oil collecting bees. The field observation revealed that variation in foreleg lengths of *Rediviva* bees can be explained as an evolutionary response to or rather a co-evolutionary development with *Diascia* floral spur lengths (Steiner and Whitehead 1990, 1991). The floral oils play an important role in larval provision and have also been suggested to be used in nest construction (Cane *et al.*, 1983; Buchmann 1987). Some hydroxylated fatty acids were reported to possess antibiotic properties (Valcavi *et al.*, 1989; Weil *et al.*, 2002). The prevalence of such chemical species in the *Diascia* flower oils instead of simple fatty acid oils may be necessary to keep the larval foods from microbial decomposition. The additional acetylation may either be required by the plant for excretion (Seipold *et al.,* 2004) or reduced the water content of oil, or for the nest cell lining. Also, there is no detailed report on the chemistry of *Rediviva* bee nest cell lining. Therefore, some further investigations have to be carried out to verify the chemical nature of the association between *Diascia* flower oil and *Rediviva* bee cell lining. Further question concern the natural variation of flower oil compositions within a species or with flower age, the absolute configuration of acylglycerols with a chiral center at the *sn*-1 or *sn*-2 position, and if stereochemistry has any relevance in the biological context.

CHAPTER 3

Chemical and Ecological Aspects of Floral Oil Secondary Metabolites

Summary

The non-volatile oils of *Thladiantha dubia, Momordica anigosantha, Momordica foetida* (Cucurbitaceae)*, Angelonia integerrima* (Scrophulariaceae), *Lysimachia vulgaris* (Myrsinaceae), *Cypella herbertii* (Iridaceae), *Zygostates lunata, Pterygodium magnum, Pterygodium hastata, Corycium dracomontanum, Cyrtochilum serratum, Sigmatostalix putumayensis, Oncidium cheirophorum, Oncidium ornithorhynchum* (Orchidaceae), *Malpighia urens, Bunchosia argentea, Stigmaphyllon ellipticum, Byrsonima coriacea* and *Janusia guaranitica* (Malpighiaceae) floral species are investigated. The derivatized and non-derivatized floral oils were analyzed by gas chromatography electron ionization (EI)-mass spectrometry (GC/EI-MS) and electrospray ionization (ESI)-Fourier-transform ion cyclotron resonance mass spectrometry (FTICR-MS). Positive ion-ESI-FTICR mass spectra of the non-derivatized floral oils exposed considerable results and rapidly yielded the lipid pattern of the oil-secreting flowers. With respect to the relative composition of the floral oils, the most prominent components were detected by both ESI-FTICR-MS and GC/EI-MS techniques. The analyses revealed that the investigated floral oils are composed of fatty acids, (3*R*)-acetoxy fatty acids, partially acetylated dihydroxy fatty acids as well as mono-, di-, and triacylglycerols. These acylglycerols possess one or two acetyl residues, one long chain of fatty acid or a mono-/diacetoxy fatty acid. The specialized lipids secreted by the various flower species might be the result of a co-evolution with their highly specialized pollinating bees. This fact may explain the mutualistic interactions between pollination vectors (oil bees) and the plant flowers (oil-secreting flowers).

3.1. Cucurbitaceae (*Thladiantha dubia*, *Momordica anigosantha* and *Momordica foetida*)

Cucurbitaceae family is predominately distributed in the tropical areas. The oils are released from trichomal elaiophores located on the flowers specially area of the flower which has elaiophores (Figure 3.1) (Simpson and Neff 1981; 1983; Buchmann 1987).
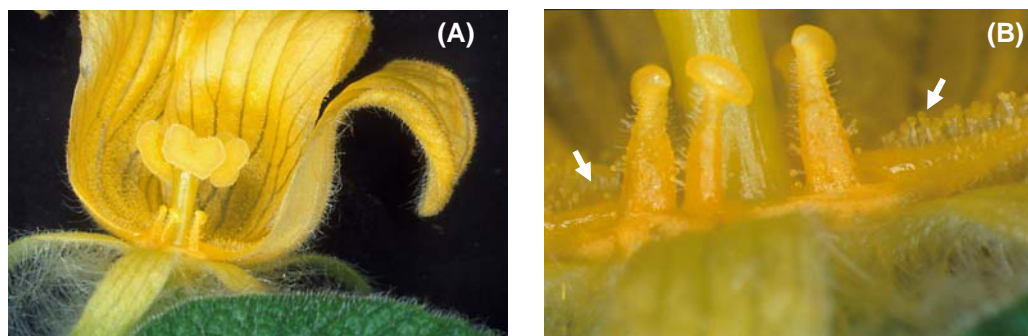
Figure 3.1. (A) The cross section of *Thladiantha dubia* (Cucurbitaceae) oil flower and (B) Frontal view of trichome elaiophore glands of *T. dubia*. Arrows indicate the trichomal elaiophores which look like hairs (photo by G. Gerlach).

Some *Momordica* species produce floral oils and are visited by specialized pollinators in the Ctenoplectridae family. The Ctenoplectrini are on aberrant group of Apidae bees (*ca.* 30 species) with short tongues and an unusual form of abdominal wagging to harvest oils (from trichomal petal elaiophores) without using modified leg appendages as found in all other oil bees (Buchmann 1987). They occur in Africa, Eastern Asia, Australia and various Pacific islands. They build their nests in small holes of various kinds, which they provide with floral oils, primarily gathered from plants of the family Cucurbitaceae. The thorax is somewhat cylindrical, presumably correlated to their nesting habits. *Thladiantha* species are tuber plant (Figure 3.1). Furthermore, these species are used in local medicine to cure stomach illness of the lower intestines and gastric ulcer.

Results

Oil rewards of *Momordica anigosantha*, *M. foetida* and *Thladiantha dubia* floral oils are considerably investigated. TIC of TMS derivatives of *Momordica anigosantha* and *M. foetida* species is shown in Figure 3.2. *M. anigosantha* and *M. foetida* floral oils consist of saturated (3*R*)-acetoxy fatty acids as major compounds along with unsaturated non-

oxygenated fatty acids (Table 3.1). EI-MS results of *Thladiantha dubia* floral oils showed both unsaturated and saturated (3*R*)-acetoxy fatty acids as main compounds and trace mount of unsaturated fatty acids (Figure 3.3, Table 3.1). (*R*)-Configuration results were based on the GC-retention time comparison with a (2*S*)-phenylpropionyl derivatives of a synthetic standard (see Appendix 1). Most of the mass spectra of fatty acids were evaluated by comparison with data from the National Institute of Standards and Technology (NIST) library version 1.6d.

The underivatized floral oils of *M. anigosantha, M. foetida* and *T.dubia* (Curcubitaceae) were also analyzed by positive ion mode of ESI-FTICR-MS. The results allowed the fast characterization of the compounds. The mass accuracy of the $[M+Na]^{+}$ions and the deduced elemental compositions revealed acetoxy fatty acids as the most significant lipid class of *M. anigosantha, M. foetida* and *T. dubia* (Table 3.2). Fatty acids were not observed by positive ion ESI-FT-ICR though they were easily charaterized by GC/EI-MS methods. However, all significant components were observed in both GC/EI-MS and ESI-FT-ICR.
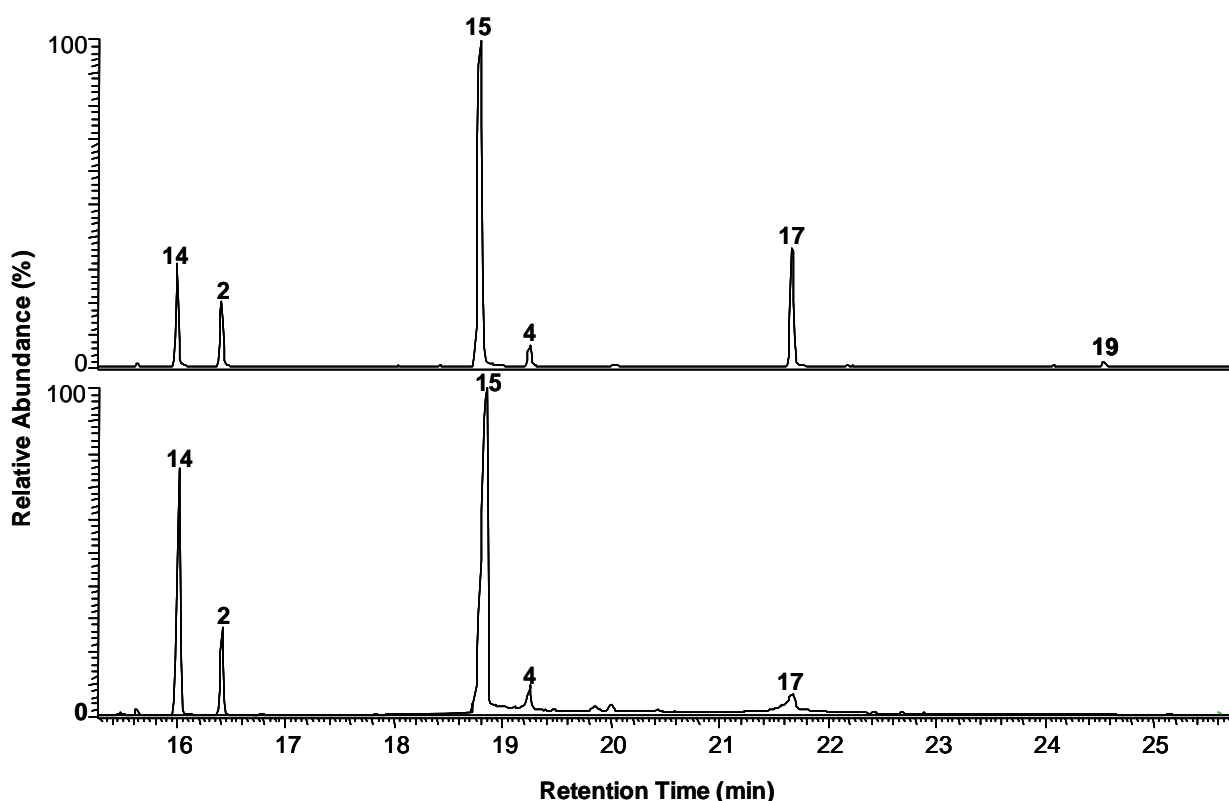
Figure 3.2. TIC of TMS derivatives of floral oils of (A) *M. foetida* and (B) *M. anigosantha* (for the identification compound members see Table 3.1, conditions **GC2**).

Figure 3.3. TIC of TMS derivative of *T. dubia* floral oil (for the identification compound members see Table 3.1, conditions **GC2**).

Table 3.1. TMS derivatives of compounds of *M. foetida*, *M. anigosantha* and *T. dubia* floral oils identified by GC/EI-MS.

No.	t_R(min)[a]	Compound[c]	Relative composition (%)		
			M. foetida	*M. anigosantha*	*T. dubia*
2	16.41	palmitoleic acid	9.4	8.0	-
4	19.26	oleic acid	3.2	3.8	0.8
14	16.00	(3*R*)-acetoxymyristic acid	13.4	28.4	-
15	18.79	(3*R*)-acetoxypalmitic acid	53.9	53.3	8.9
16	20.66[b]	(3*R*)-acetoxyoleic acid	-	-	10.7
17	21.67	(3*R*)-acetoxystearic acid	19.0	6.5	32.4
18	23.45[b]	(3*R*)-acetoxyeicosenoic acid	-	-	39.8
19	24.53	(3*R*)-acetoxyeicosanoic acid	1.1	-	7.4

[a]obtained from *M. foetida,* [b]obtained from *T. dubia* (Cucurbitaceae), [c]see Appendix 2 for EI-mass spectral data (Table A 2.1 and A 2.4), (-) = not detected.

Table 3.2. Positive ion ESI-FTICR mass spectral data of the floral oils of *M. foetida*, *M. anigosantha* and *T. dubia*.

No.	Compound type[a]	Elemental composition	*m/z* ([M+Na]+)	Error[b] (ppm)	MW	Relative abundance (%)		
						M. foetida	*M. anigosantha*	*T. dubia*
14	3-OAc 14:0	$[C_{16}H_{30}O_4Na]^+$	309.20371	+0.3	286	12.8	20	-
15	3-OAc 16:0	$[C_{18}H_{34}O_4Na]^+$	337.23534	+1.2	314	100	100	55.5
16	3-OAc 18:1	$[C_{20}H_{36}O_4Na]^+$	363.30097	-0.5	340	-	-	25
17	3-OAc 18:0	$[C_{20}H_{38}O_4Na]^+$	365.26674	-0.7	342	39.5	85	100
18	3-OAc 20:1	$[C_{22}H_{40}O_4Na]^+$	391.25563	+0.2	368	-	-	50
19	3-OAc 20:0	$[C_{22}H_{42}O_4Na]^+$	393.29828	+1.9	370	13.9	10	15

[a]see full name of compounds in Table 3.1, [b]taken from the examplary data of *M. anigosantha* (exception: compounds **18** and **19** from *T. dubia*), MW = molecular weight, (-) = not detected.

3.2. Scrophulariaceae (*Angelonia integerrima*)

The genus *Angelonia* comprises *ca.* 25 species from tropical South America reaching to Mexico and the West Indies; many species are cultivated as ornamental plants (von Poser *et al.*, 1997). The floral morphology and biology of *Angelonia* species have been previously observed by Vogel (1974) and Steiner and Whitehead (1988, 1990). *Angelonia* oils are secreted by trichomatous, oil-producing gland fields. They are located at the outer edge of pocket (Vogel and Machado 1991, Machado *et al.*, 2002). Figure 3.5 shows the inflorescence of *Angelonia integerrima* (Scrophulariaceae).

Figure 3.4. The florescence of *A. integerrima* (Scrophulariaceae) (photo by G. Gerlach).

Results

GC/EI-MS of TMS derivatives allows to evaluate the composition of lipids of *A. integerrima* non-volatile floral oil (Figure 3.5). (3*R*)-Acetoxy fatty acids with the even-numbered chains C_{14} (**14**), C_{16} (**15**) and C_{18} (**17**) represent the dominant compounds with up to 90% of the TIC, whereas acetylated acylglycerols have only 10% share (Table 3.3). The key ions of EI-mass spectra of (3*R*)-acetoxy fatty acids are described in Appendix 2 (Table A 2.4). The mass spectra interpretation of acylglycerols is discussed in detail in Chapter 2 (see Appendix 2: Table A 2.5 and A 2.6). (*R*)-configuration results were based on the GC-comparison between the (2*S*)-phenylpropionyl derivatives of a synthetic standard and the samples (see Appendix 1). The underivatized oil of *A. integerrima* is further investigated by positive ion ESI-FTICR-MS (Table 3.4). The most abundant acetoxy fatty acid (C_{16}) is indicated by the ions $[C_{18}H_{34}O_4Na]^+$ at *m/z* 337.23507 (**15**) along with acetoxy fatty acids (C_{14} and C_{18}) by the ion $[C_{16}H_{34}O_4Na]^+$ at *m/z* 309.20399 (**14**) and $[C_{20}H_{38}O_4Na]^+$ at *m/z* 365.26653 (**17**), respectively. The C_{20}-acetoxy fatty acid (**19**) could only detected by the ESI-FTICR method. Otherwise, the FTICR-MS results confirm and amend the GC/EI-MS results.

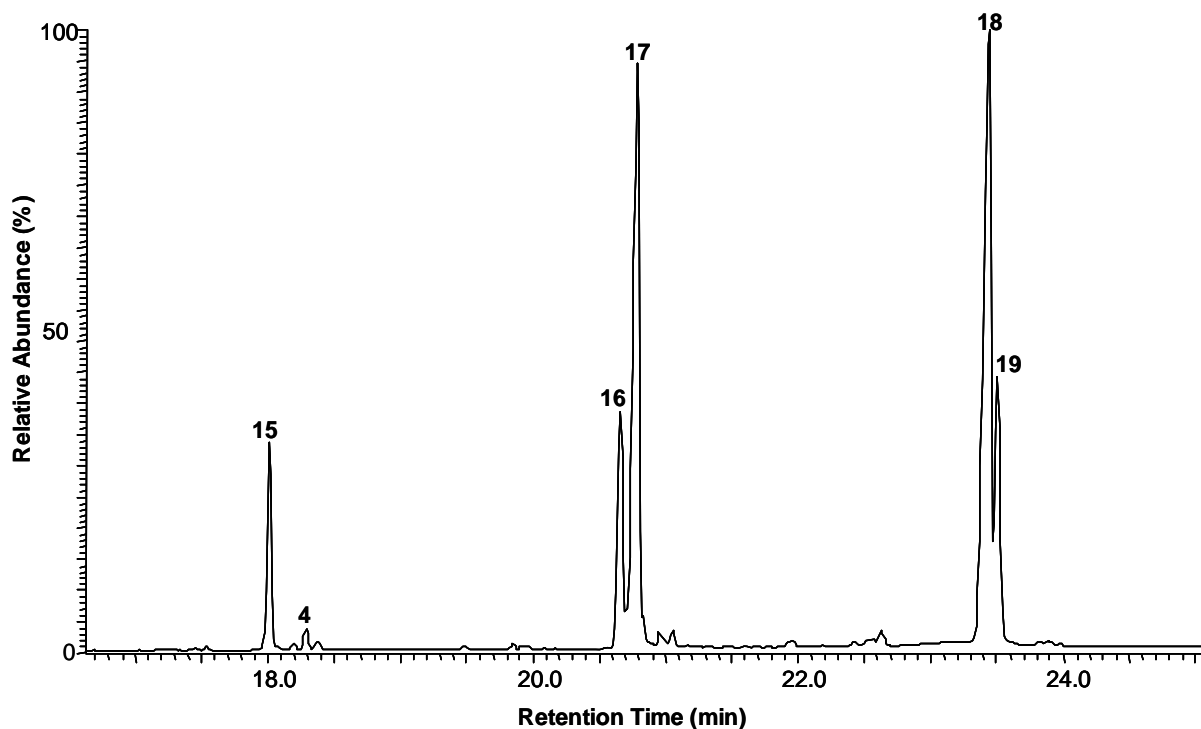**Figure 3.5.** TIC of TMS derivatives of *A. integerrima* floral oil (for the identification compound members see Table 3.3, conditions **GC1**).

Table 3.3. TMS derivatives of compounds of *A. integerrima* floral oil identified by GC/EI-MS.

No.	t_R (min)	Compound[a]	Relative composition (%)
14	16.45	(3*R*)-acetoxymyristic acid	15.2
15	19.33	(3*R*)-acetoxypalmitic acid	61.1
17	22.20	(3*R*)-acetoxystearic acid	15.5
20	23.38	2-[(3*R*)-acetoxymyristoyl]glycerol	1.4
21	23.84	1-[(3*R*)-acetoxymyristoyl]glycerol	0.3
22	24.36	2-[(3*R*)-acetoxymyristoyl]-1-acetylglycerol	0.1
27	26.09	2-[(3*R*)-acetoxypalmitoyl]glycerol	4.4
28	26.55	1-[(3*R*)-acetoxypalmitoyl]glycerol	1.2
30	27.01	2-[(3*R*)-acetoxypalmitoyl]-1-acetylglycerol	0.5
35	28.68	2-[(3*R*)-acetoxystearoyl]glycerol	0.4

[a]see Appendix 2 for EI-mass spectral data (Table A 2.4, A 2.5 and A 2.6).

Table 3.4. Positive ion ESI-FTICR mass spectral data of the *A. integerrima* floral oil.

No.	Compound type[a]	Elemental composition	*m/z* ([M+Na]$^+$)	Error (ppm)	MW	Relative abundance (%)
14	3-OAc 14:0	$C_{16}H_{30}O_4\,Na^+$	309.20399	+1.0	286	6.2
15	3-OAc 16:0	$C_{18}H_{34}O_4\,Na^+$	337.23507	+0.4	314	100
17	3-OAc 18:0	$C_{20}H_{38}O_4\,Na^+$	365.26653	+0.8	342	4.2
19	3-OAc 20:0	$C_{22}H_{42}O_4\,Na^+$	393.29807	+1.4	370	30.3
20, 21	MAG (3-OAc 14:0)	$C_{19}H_{36}O_6\,Na^+$	383.24050	+0.1	360	15
22	DAG (3-OAc 14:0, OAc)	$C_{21}H_{38}O_7\,Na^+$	425.25154	+1.3	402	25.7
27, 28	MAG (3-OAc 16:0)	$C_{21}H_{40}O_6\,Na^+$	411.27215	+1.1	388	57.0
30	DAG (3-OAc 16:0, OAc)	$C_{23}H_{42}O_7\,Na^+$	453.28263	+0.8	430	26.7
35	MAG (3-OAc 18:0)	$C_{23}H_{44}O_6\,Na^+$	439.30339	-0.9	416	10

[a]see full name of compounds in Table 3.3, MW = molecular weight

3.3. Iridaceae *(Cypella herbertii)*

Cypella is a genus in the Iridaceae with about 15 species found from Mexico to Argentina. The trichomal elaiophores are located in the yellow sword-shaped leaves (Figure 3.6). The amount of non-valatile oils are varied from 2–5 µL/ flower. Up to date, there is no chemical investigation of *Cypella herbertii* oil.

Figure 3.6. (A) *Cypella herbertii* (Iridaceae) and (B) trichomal elaiophores of *C. herbertii*. The arrow points the elaiophore area (photos by G. Gerlach).

Results

(3*R*)-Acetoxypalmitic acid (**15**) represents the main component (70%) together with fatty acids (*ca.* 16%, **2**–**4**) and acetylated acylglycerols (**27**, **29**–**30**, **35**) (Figure 3.7, Table 3.5). The double bond position of unsaturated fatty acids was established by dimethyldisulfide derivatization (Christie 1987) and evaluated by comparison with data from the National Institute of Standards and Technology (NIST) library version 1.6d. The characteristic EI-MS ions of the acetylated compounds are exhaustively described in Appendix 2 (Table A 2.4). (*R*)-Configurations were accomplished by GC-comparison between (2*S*)-phenylpropionyl derivatives of a synthetic standard and the samples (see Appendix 1).
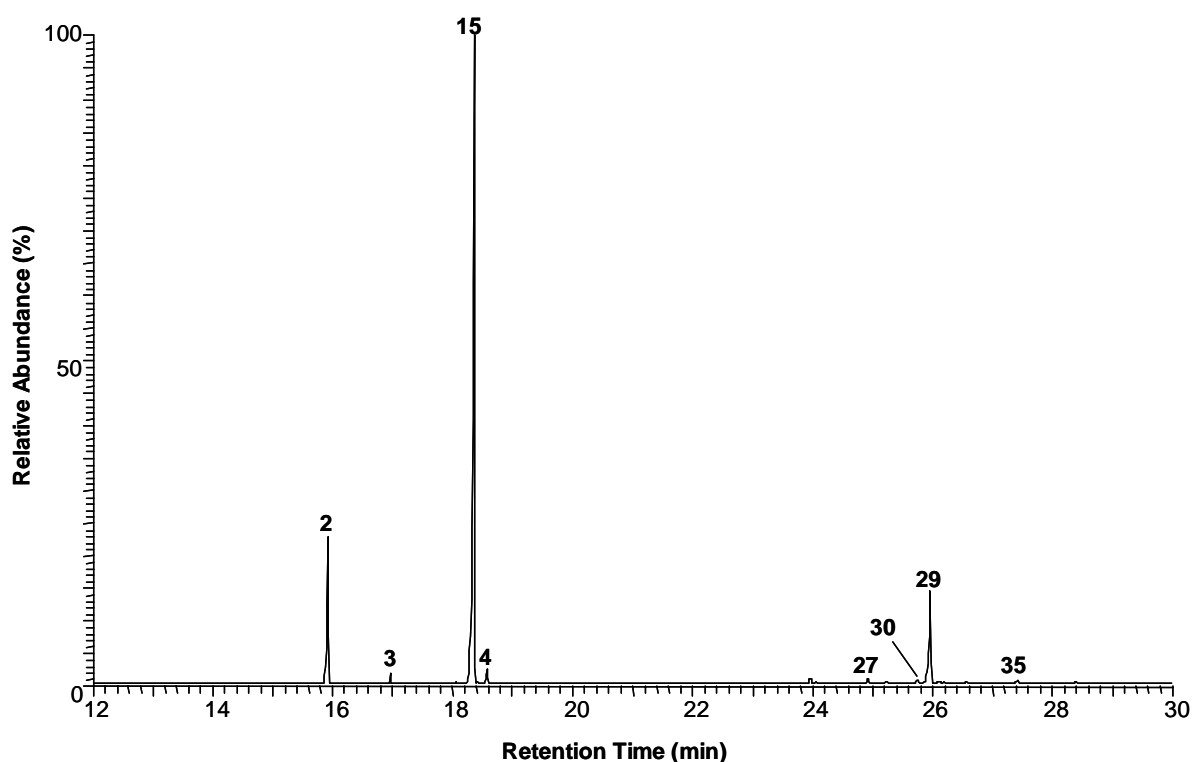
Figure 3.7. TIC of TMS derivatives of *C. herbertii* floral oil (for the identification compound members see Table 3.5, conditions **GC1**).

Table 3.5. TMS derivatives of compounds of *C. herbertii* floral oils identified by GC/EI-MS.

No.	t_R (min)	Compound[a]	Relative composition (%)
2	15.92	*cis*-9-palmitoleic acid	14
3	17.01	palmitic acid	0.7
4	18.58	*cis*-9-oleic acid	1.1
15	18.36	(3*R*)-acetoxypalmitic acid	70.4
27	24.93	2-[(3*R*)-acetoxypalmitoyl]glycerol	0.6
29	25.75	2-[(3*R*)-acetoxypalmitoleoyl]-1-acetylglycerol	0.4
30	25.97	2-[(3*R*)-acetoxypalmitoyl]-1-acetylglycerol	12.4
35	27.41	2-[(3*R*)-acetoxystearoyl]glycerol	0.3

[a]see Appendix 2 for EI-mass spectral data (Table A 2.1, A 2.4, A 2.5, and A 2.6).

Positive ion ESI-FTICR-MS data of underivatized *C. herbertii* oil are given in Table 3.6. The highest abundance ion $[C_{23}H_{42}O_7Na]^+$ at *m/z* 453.28349 is indicative of the DAG of a saturated C_{16}-acetoxy fatty acid and an acetyl moiety (**30**, 100%). Also, the ion $[C_{21}H_{40}O_7Na]^+$ at *m/z* 451.28720 represents DAG (**29**) containing an unsaturated acetoxy fatty acid ($C_{16:1}$) and an acetyl moiety. The C_{16}-acetoxy fatty acid (**15**) was detected in *ca.* 4%. None of the common non-oxidized fatty acids was detected by positive ion ESI-FTICR-MS.

Table 3.6. Positive ion ESI-FTICR mass spectral data of the floral oil of *C. herbertii*.

No.	Compound type[a]	Elemental composition	*m/z* ([M+Na]$^+$)	Error (ppm)	MW	Relative abundance (%)
15	3-OAc 16:0	$C_{18}H_{34}O_4\,Na^+$	337.23517	+0.5	314	4.1
27	MAG (3-OAc 16:0)	$C_{21}H_{40}O_6\,Na^+$	411.27205	+1.2	388	10.6
29	DAG (3-OAc 16:1)	$C_{21}H_{40}O_7\,Na^+$	451.28720	+1.4	428	15.3
30	DAG (3-OAc 16:0)	$C_{23}H_{42}O_7\,Na^+$	453.28349	+1.8	430	100
35	MAG (3-OAc 18:0)	$C_{23}H_{44}O_6\,Na^+$	439.30329	-1.0	416	3.3

[a]see full name of compounds in Table 3.5, MW = molecular weight

3.4. Myrsinaceae (*Lysimachia vulgaris*)

Lysimachia vulgaris (garden or yellow loosestrife) is one of the few plants with floral oil that are home in the holarctic area. *Macropis europaea* (Melittidae), a solitary bee rather smaller than a honeybee, can easily be spotted visiting *L. vulgaris* (Vogel 1986, Michez and Patiny 2005).

Results

EI-MS results of *L. vulgaris* oil derivatives reveal the MAG of saturated (3*R*)-acetoxysteric acid (**37**) as a main compound *ca.* 38% along with MAG of (3*R*)-acetoxyoleic acid ($C_{18:1}$, **36**) *ca.* 17% (Figure 3.8, Table 3.7). The double bond position of (3*R*)-acetoxy fatty acid obtained by FAME profiling method and identified by comparison to dada from NIST database library version 1.6d. (*R*)-Configurations were accomplished by GC-comparison between (2*S*)-phenylpropionyl derivatives of a

synthetic standard and the samples (see Appendix 1). DAGs and TAGs of (3*R*)-acetoxy fatty acid are also detected in *ca.* 29% (**38**, **39**, **42, 43**) and 10% (**44**), respectively. Mass spectra interpretation of these acylglycerols is previously described in Chapter 2.
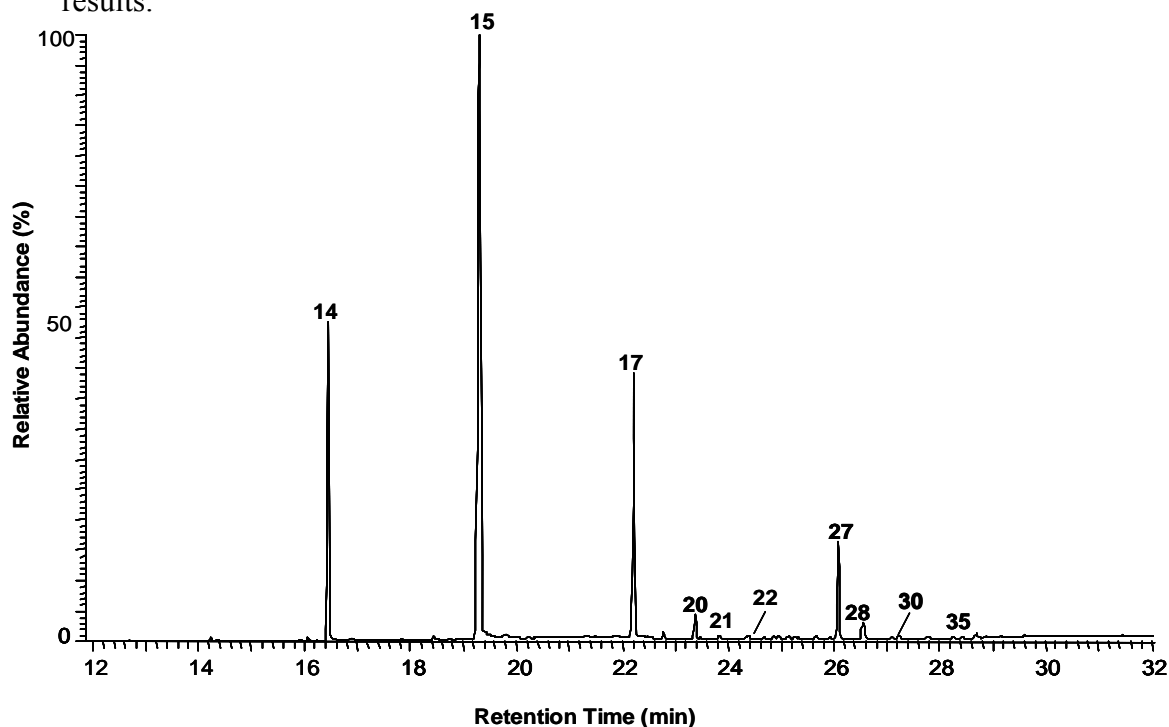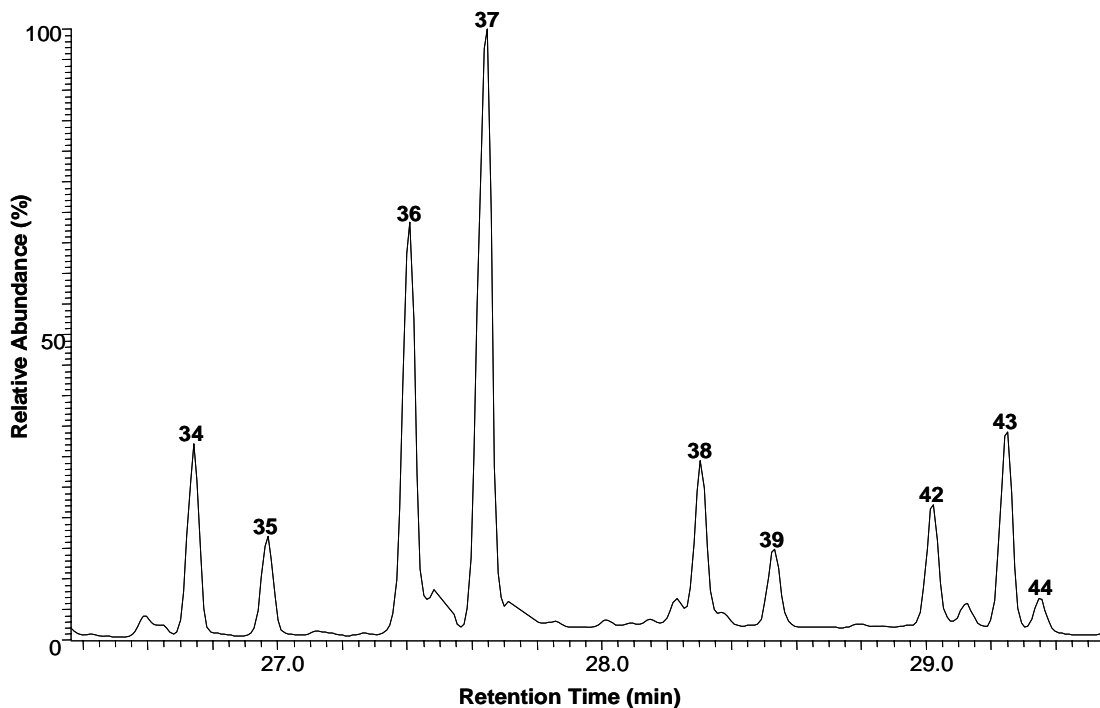

Figure 3.8. Partial TIC of TMS derivatives of *L. vulgaris* floral oil (for the identification compound members see Table 3.7, conditions **GC1**).

Table 3.7. TMS derivatives of compounds of *L. vulgaris* floral identified by GC/EI-MS.

No.	t_R(min)	Compound[a]	Relative composition (%)
34	26.73	2-[(3*R*)-acetoxyoleoyl]glycerol	13.6
35	26.96	2-[(3*R*)-acetoxystearoyl]glycerol	6.1
36	27.39	1-[(3*R*)-acetoxyoleoyl]glycerol	17.1
37	27.62	1-[(3*R*)-acetoxystearoyl]glycerol	35.8
38	28.29	2-[(3*R*)-acetoxyoleoyl]-1-acetylglycerol	9.5
39	29.01	2-[(3*R*)-acetoxystearoyl]-1-acetylglycerol	4.7
42	28.52	1-[(3*R*)-acetoxyoleoyl]-3-acetylglycerol	6.6
43	29.25	1-[(3*R*)-acetoxystearoyl]-3-acetylglycerol	13.0
44	29.35	2-[(3*R*)-acetoxystearoyl]-1,3-diacetylglycerol	3.9

[a]see Appendix 2 for EI-mass spectral data (Table A 2.4, A 2.5, and A 2.6).

The underivatized *L. vulgaris* oil was subsequently investigated by positive ion ESI-FTICR-MS. The electrospary mass spectrum demonstrates sodium adducts $[M+Na]^+$ of the corresponding compound (Table 3.8). The most abundant ion $[C_{25}H_{46}O_7Na]^+$ at *m/z* 481.31411 belongs to the DAGs **39** and **43** (100%). The acetylated MAGs (**34**, **35**, **36**, **37**) were detected *ca.* 4% abundance. The relative intensity of both GC/EI-MS and ESI-FTICR-MS revealed likely not related results. In generally aspect, the ESI-FTICR technique is powerful tool to confirm the structural identification of underivatized lipids but the absolute abundance or even relative abundance of peaks in the ESI-FTICR is often doubtful and does not certainly indicate to the actual proportions (Pulfer and Murphy 2003; Han and Gross 2005). Consequence, in most cases, GC/EI-MS data were preferably taken for an indication of the relative abundance of compounds. Nonetheless, the most significant compounds were detected in both methods.

Table 3.8. Positive ion ESI-FTICR mass spectral data of the floral oil of *L. vulgaris.*

No.	Compound type[a]	Elemental composition	*m/z* ($[M+Na]^+$)	Error[a] (ppm)	MW	Relative abundance (%)
34, 36	MAG (3-OAc 18:1)	$C_{23}H_{42}O_6\,Na^+$	437.28795	+1.3	414	2.9
35, 37	MAG (3-OAc 18:0)	$C_{23}H_{44}O_6\,Na^+$	439.30369	+1.6	416	1.2
39, 43	DAG (3-OAc 18:0, OAc)	$C_{25}H_{46}O_7\,Na^+$	481.31411	+1.0	458	100
38, 42	DAG (3-OAc 18:1, OAc)	$C_{25}H_{44}O_7\,Na^+$	479.29815	+0.5	456	60.2
44	TAG (3-OAc 18:0, diOAc)	$C_{27}H_{48}O_8\,Na^+$	523.32528	+2.0	500	15.3

[a]see full name of compounds in Table 3.7, MW = molecular weight

3.5. Malpighiaceae (*Malpighia urens, Bunchosia argentea*, *Stigmaphyllon ellipticum*, *Byrsonima coriacea* and *Janusia guaranitica)*

Non-volatile oils of oil-secreting flower species from Malpighiaceae are investigated. The floral oils being secreted by epithelial elaiophores are located at the calyx. The secretion accumulates directly under the cuticle, forming small blisters. Several authors have investigated the floral morphology and ecological aspects of the pollination (Taylor and Crepet 1987; Vogel 1990). Figure 3.9 shows (A) the inflorescence of *Malpighia urens* in front view and (B) their epithelial elaiophores located at the calyx.
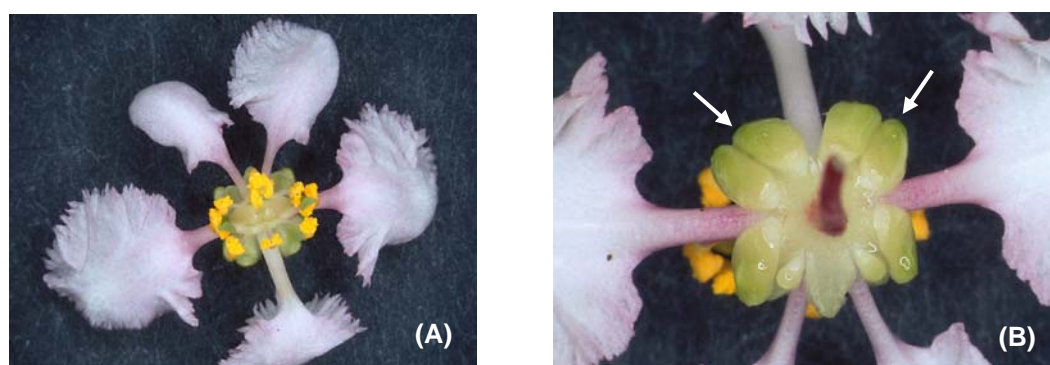
Figure 3.9. (A) Flower of *Malpighia urens* (Malpighiaceae) and (B) epithelial elaiophores indicated by arrows (photos by G. Gerlach).

Results

The floral oils of five different Malpighiaceae contain partially acetylated free dihydroxy fatty acids of even carbon number ranging from $C_{20}-C_{26}$ (**53−66**). Furthermore, trace amounts of common fatty acids (**2**, **4**, **6**) as well as acylglycerols (**37**, **39**, **47**, **50**) were detected (Figure 3.10, Table 3.9). The partially acetylated dihydroxy fatty acids represent the most dominant compounds with up to 90% of the TIC.
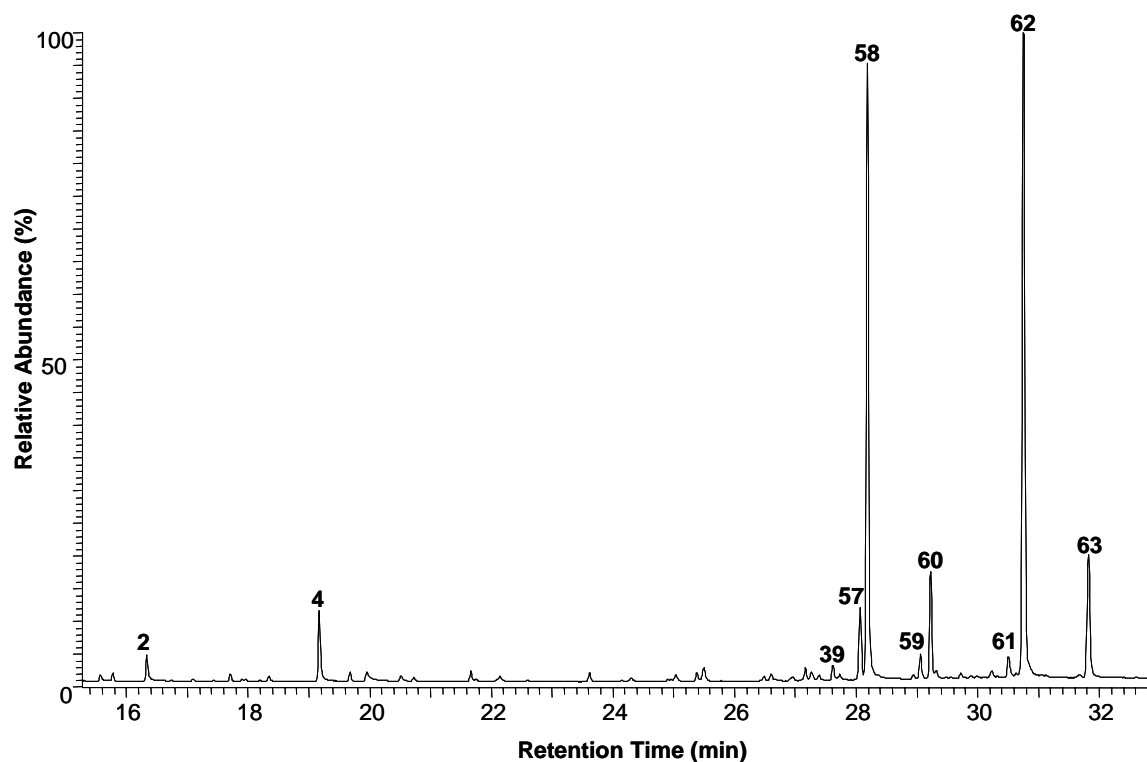
Figure 3.10. TIC of TMS derivatives of *Stigmaphyllon ellipticum* floral oil as an example (for the identification compound members see Table 3.9, conditions **GC1**).

The mass spectrum of TMS derivatives of 9-acetoxy-3-hydroxydocosanoic acid (**60**) is shown in Figure 3.11. The significant fragments are discussed in Scheme 3.1. The molecular weight was deduced from the ion type **a** ([M–Me–HOAc]$^+$). The position and type of functional groups at C-3 and C-9 can be determined by the α-cleavages leading to key ions of type α_1 and type α_3. While ion at *m/z* 233 (α_1) indicated the hydroxyl group to be at C-3, the acetoxy function must be located at C-9. This is caused by key ions at *m/z* 333 (α_3–CH$_2$CO) and *m/z* 367 (α_2–HOSiMe$_3$) which comprises the fatty acid chain from C-3 to C-20 (Scheme 3.1, Seipold *et al.*, 2004).
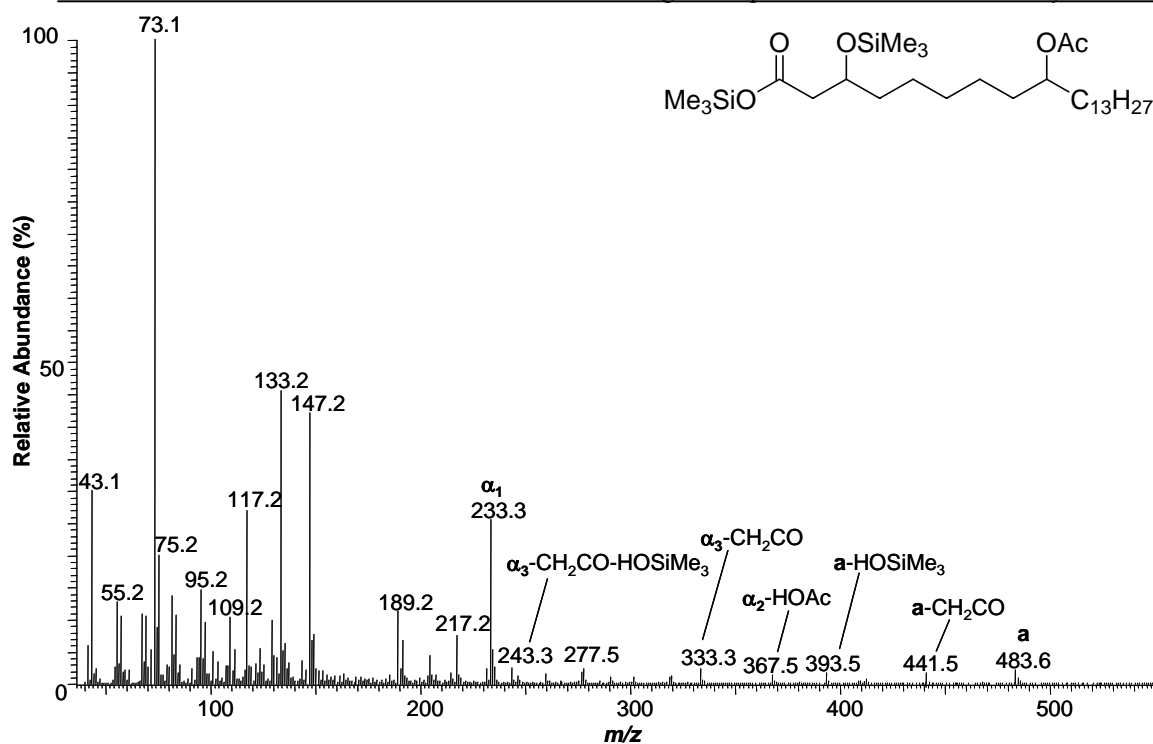
Figure 3.11. 70 eV-EI mass spectrum of the TMS derivatives of 9-acetoxy-3-hydroxydocosanoic acid (**60**).
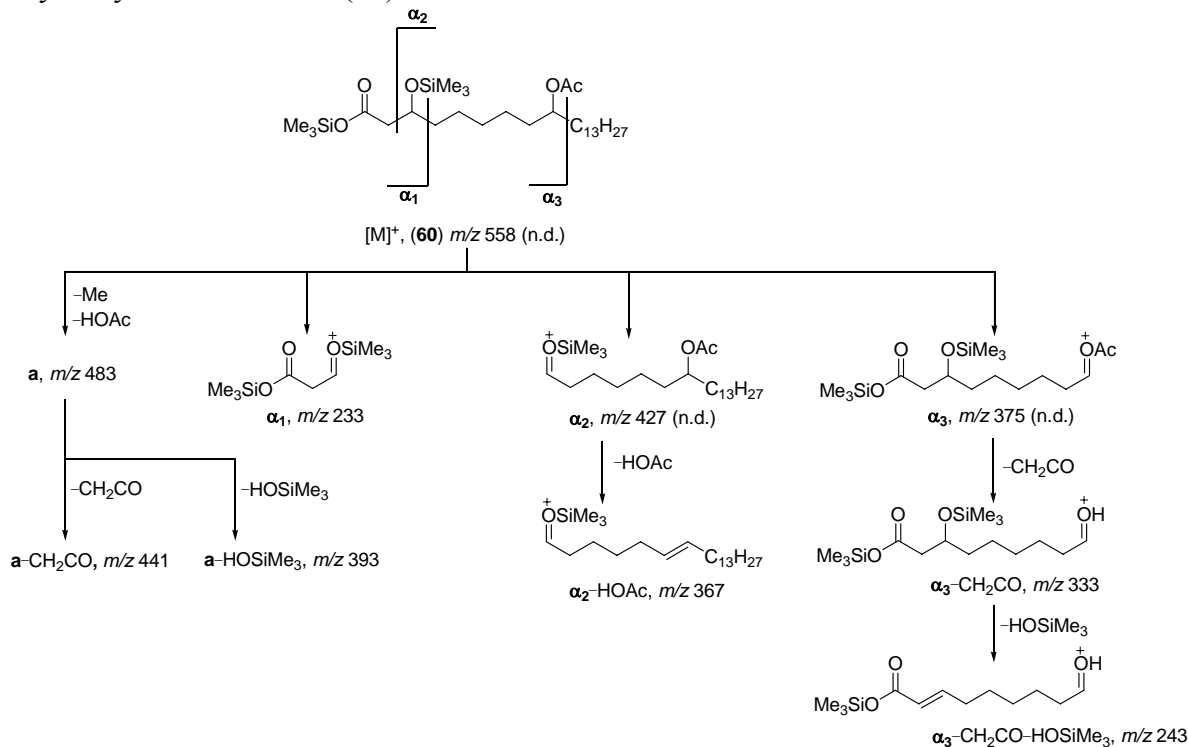
Scheme 3.1. Significant fragments of TMS derivative of 9-acetoxy-3-hydroxydocosanoic acid (**60**) (n.d. = not detected).

The mass spectrum of the TMS derivative of 3,9-diacetoxydocosanoic acid (**58**) is shown in Figure 3.12. The characteristic fragments are represented in Scheme 3.2. The mass spectrum of 3,9-diacetoxydocosanoic acid (**58**) shows no molecular ion. The molecular weight is deduced from ion type **a** ([M–HOAc–Me]$^+$) at *m/z* 453. The ion type **a$_1$** at *m/z* 408 indicates the evidence of two acetoxy groups in the fatty acid chain. The EI-MS spectrum showed the ion at *m/z* 303 (type **α$_3$**–CH$_2$CO) and *m/z* 243 (type **α$_3$**–CH$_2$CO–HOAc) which is indicative for an acetoxy function at the C-9 position. In this case, the ion which indicates the position of the other acetoxy function could not be detected. However, based on biosynthetic considerations, the further acetoxy group is likely to be attached at position C-3 or C-5. Based on the results, there was also no observervation of the fragment [SiMe$_3$O(CO)(CH$_2$)$_3$CH(OH)]$^+$ at *m/z* 189 which could correspond to the attachment C-5 (Seipold *et al.*, 2004). Therefore, an additional acetoxy function most likely is located at position C-3 of the fatty acid chain.

In case of 3,7-diacetoxydocosanoic acid (**57**), the corresponding fragments were observed at *m/z* 275 (type **α$_3$**-CH$_2$CO) and 215 (type **α$_3$**-CH$_2$CO) which indicative for an acetoxy group at C-7 position.
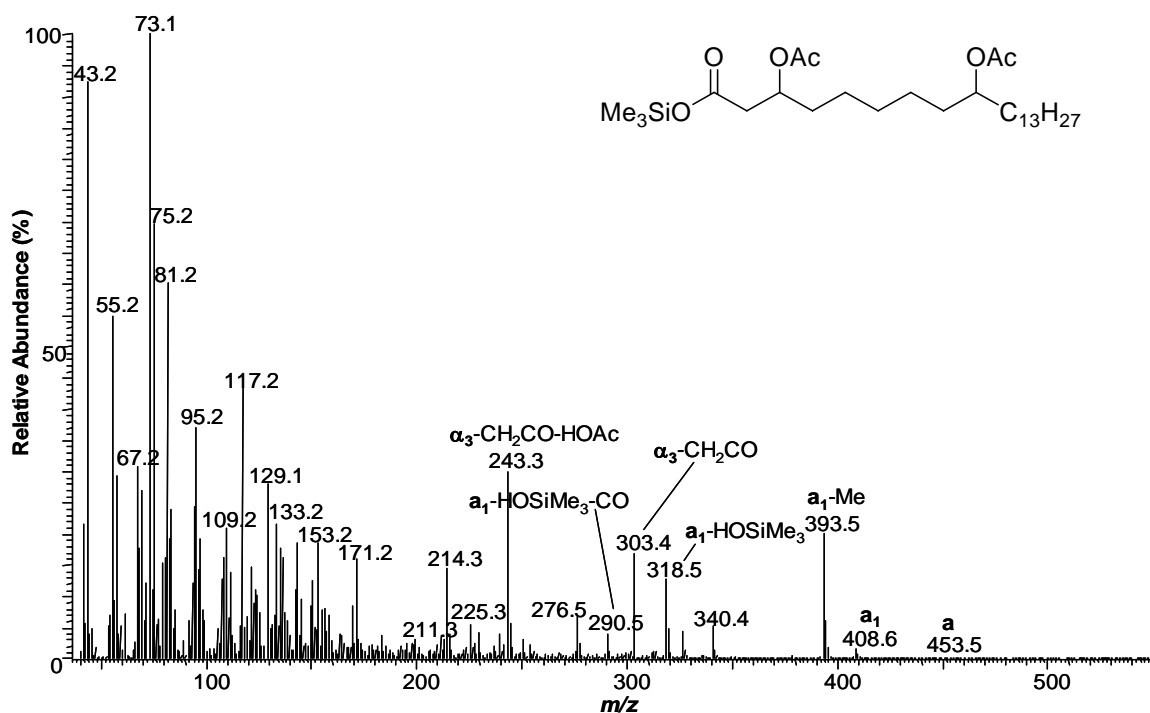
Figure 3.12. 70 eV EI mass spectrum of the TMS derivative of 3,9-diacetoxydocosanoic acid (**58**).
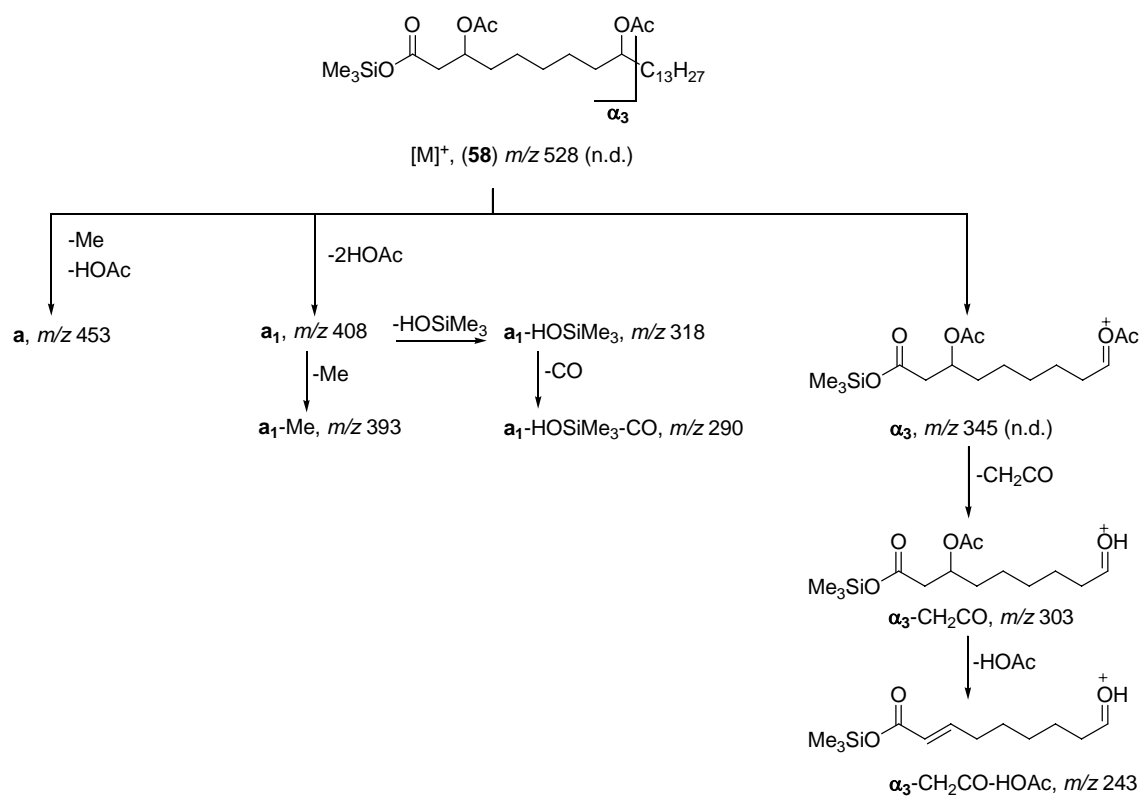
Scheme 3.2. Significant and expected fragments of the TMS derivative of 3,9-diacetoxydocosanoic acid (**58**) (n.d = not detected).

The positive ion mode ESI-FTICR mass spectra are obtained from oil-secreting flowers of Malpighiaceae. The accurate molecular weights and elemental compositions of lipid compounds are listed in Table 3.10. Both fatty acids and partially acetylated dihydroxy fatty acids are not detected in the positive ion ESI-FTICR-MS. However, in most cases, the significant compositions are detected in both of ESI-FTICR and GC/EI-MS methods.

Table 3.9. TMS derivatives of compounds of *Stigmaphyllon ellipticum*, *Malpighia urens*, *Janusia guaranitica*, *Byrsonima coriacea* and *Bunchosia argentea* (Malpighiaceae) identified by GC/EI-MS.

No.	Compound[a]	t_R (min)	Relative composition (%)				
			S. ellipticum	*M. urens*	*J. guaranitica*	*B. coriacea*	*B. argentea*
2	*cis*-9-palmitoleic	16.33[b]	1.7	-	-	-	-
4	oleic acid	19.17[b]	4.2	-	-	-	-
6	*cis*-11-eicosenoic acid	21.35[c]	-	-	-	-	0.5
37	1-[(3*R*)-acetoxystearoyl]glycerol	26.96[d]	-	-	3.8	-	-
39	2-[(3*R*)-acetoxystearoyl]-1-acetylglycerol	27.61[b]	1.3	-	-	-	-
47	1-[(3*R*)-acetoxyeicosanoyl]glycerol	29.25[d]	-	-	1.8	-	-
50	1-[(3*R*)-acetoxydocosanoyl]glycerol	32.25[d]	-	-	1.0	-	-
53	3,7-diacetoxyeicosanoic acid	25.39[e]	-	-	-	5.9	-
54	3,9-diacetoxyeicosanoic acid	25.84[c]	-	-	-	-	56.9
55	7-acetoxy-3-hydroxyeicosanoic acid	26.49[e]	-	-	-	5.8	20.0
56	9-acetoxy-3-hydroxyeisosanoic acid	27.39[e]	-	-	-	11.9	-
57	3,7-diacetoxydocosanoic acid	28.07[b]	3.7	-	73.3	32.0	-
58	3,9- diacetoxydocosanoic acid	28.19[b]	31.8	-	-	-	-
59	7-acetoxy-3-hydroxydocosanoic acid	29.06[b]	1.4	-	-	19.6	-

Table 3.9. (continued).

No.	Compound[a]	t_R (min)	Relative composition (%)				
			S. ellipticum	*M. urens*	*J. guaranitica*	*B. coriacea*	*B. argentea*
60	9-acetoxy-3-hydroxydocosanoic acid	29.23[b]	6.6	-	2.0	11.0	-
61	3,7-diacetoxytetracosanoic acid	30.51[b]	1.4	10.2	-	-	-
62	3,9-diacetoxytetracosanoic acid	30.75[b]	39.4	10.2	18.0	-	23.1
63	9-acetoxy-3-hydroxytetracosanoic acid	31.82[b]	8.5	-	-	-	-
64	3,9-diacetoxyhexacosanoic acid	36.47[f]	-	17.2	-	-	-
66	9-acetoxy-3-hydroxyhexacosanoic acid	37.44[f]	-	62.4	-	-	-

[a]see EI-mass spectral data compounds in Appendix 2 (Table A 2.1, A 2.5, A 2.6, A 2.8 and A 2.9), [b]obtained from *S. ellipticum*, [c]obtained from *B. argentea*, [d]obtained from *J. guaranitica*, [e]obtained from *B. coriacea,* [f]obtained from *M. urens*, (-) = not detected, conditions **GC1**.

Table 3.10. Positive ion ESI-FTICR mass spectral data of the floral oils of Malpighiaceae (*Stigmaphyllon ellipticum*, *Malpighia urens*, *Janusia guaranitica*, *Byrsonima coriacea* and *Bunchosia argentea*).

No.	Compound type[a]	Elemental composition	m/z ([M+Na]$^+$)	Error (ppm)	MW	Relative abundance (%)				
						S. ellipticum	*M. urens*	*J. guaranitica*	*B. coriacea*	*B. argentea*
37	MAG (3-OAc 18:0)	$C_{23}H_{44}O_6 Na^+$	439.30308	-1.0[b]	416	-	-	4.4	-	-
53, 54	diOAc 20:0	$C_{24}H_{44}O_6 Na^+$	451.30301	-1.0[c]	428	-	-	-	19.2	100
57, 58	diOAc 22:0	$C_{26}H_{48}O_6 Na^+$	479.33470	+0.7[d]	456	100	100.0	100	100	16.4
61, 62	diOAc 24:0	$C_{28}H_{52}O_6 Na^+$	507.36572	-0.6[d]	484	48.0	-	36.4	42.4	5.2
64	diOAc 26:0	$C_{30}H_{56}O_6 Na^+$	535.39693	+0.9[d]	512	13.2	20.4	-	-	-

[a]see full name of compounds in Table 3.7, [b]obtained from *J. guaranitica,* [c]obtained from *B. coriacea,* [d]obtained from *S. ellipticum*, MW = molecular weightc, (-) = not detected.

3.6   Orchidaceae (*Oncidium ornithorhynchum*, *Pterygodium hastata*, *Pterygodium magnum*, *Corycium dracomontanum*, *Oncidium cheirophorum*, *Zygostates lunata*, *Sigmatostalix putumayensis* and *Cyrtochilim serratum*)

Vogel (1974) has been the first to describe floral oils from Orchidaceae. Pollination of many orchids is mediated by oil collecting bees. *Tetrapedia diversipes* has been observed as a pollinator of *Oncidium* species (Alves dos Santos *et al.,* 2002).   The chemistry of *Oncidium* (Orchidaceae) was described for the first time by Reis *et al.,* 2000. The chemical investigations of orchid oil flowers (Orchidaceae) are reported. Figure 3.13 shows the flowers of (A) *Oncidium ornithorhynchum* and (B) *Zygostates lunata* (Orchidaceae).
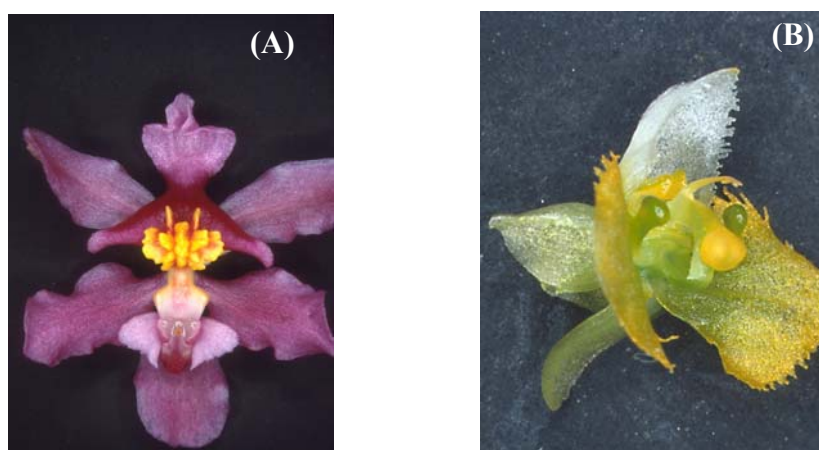
Figure 3.13. (A) *Oncidium ornithorhynchum* and (B) *Zygostates lunata* (Orchidaceae) (photos by G. Gerlach).

Results

The non-volatile flower oils of eight different Orchids consist of several lipid classes: fatty acids (**1**, **3**, **4**, **5**, **6**, **8**), (3*R*)-acetoxyfatty acids (**15**, **17**, **19**), partially acetylated dihydroxy fatty acids (**52**−**55**) as well as acylglycerols of one long chain monoacetoxy fatty acid as together with one or two acetyl groups on the glycerol backbone (**30**−**32**, **35**, **37**, **39**, **43**−**51**) (Table 3.11). Figure 3.14 shows the TIC of the TMS derivatives of *Pterygodium hastata* oil flower (Orchidaceae) as an example. Data of fatty acids were identified by comparison to data from the NIST database library version 1.6d. Mass spectra interpretation of partially acetylated dihydroxy fatty acids are described in the context of Malpighiaceae floral oil analyses (see Chapter 3.5) and characterization of

acetylated acylglycerols in previous Chapter 2. The acylglycerols that contain long chain diacetoxy fatty acid (**87**–**88**) are discussed in more detail in Chapter 4 (Ontogeny of *Heteropterys chrysophylla* (Malpighiaceae) calyx gland).

Furthermore, TMS derivatives of common acylglycerol of fatty acids were detected. Interpretations of these compound data were carried out based on a comparison to the data from the NIST-database library version 1.6d. It is possible to distinguish mass spectra of TMS derivatives between 1,2-DAGs and 1,3-DAGs isomers by GC/EI-MS. The ion $[M-Me]^+$ represents the highest *m/z* value. All the characteristic key ions in the EI mass spectra are presented in Appendix 2. In most cases, the double bond position of compounds was derived from FAME profiling results and compared to the data from NIST-library database version 1.6d.
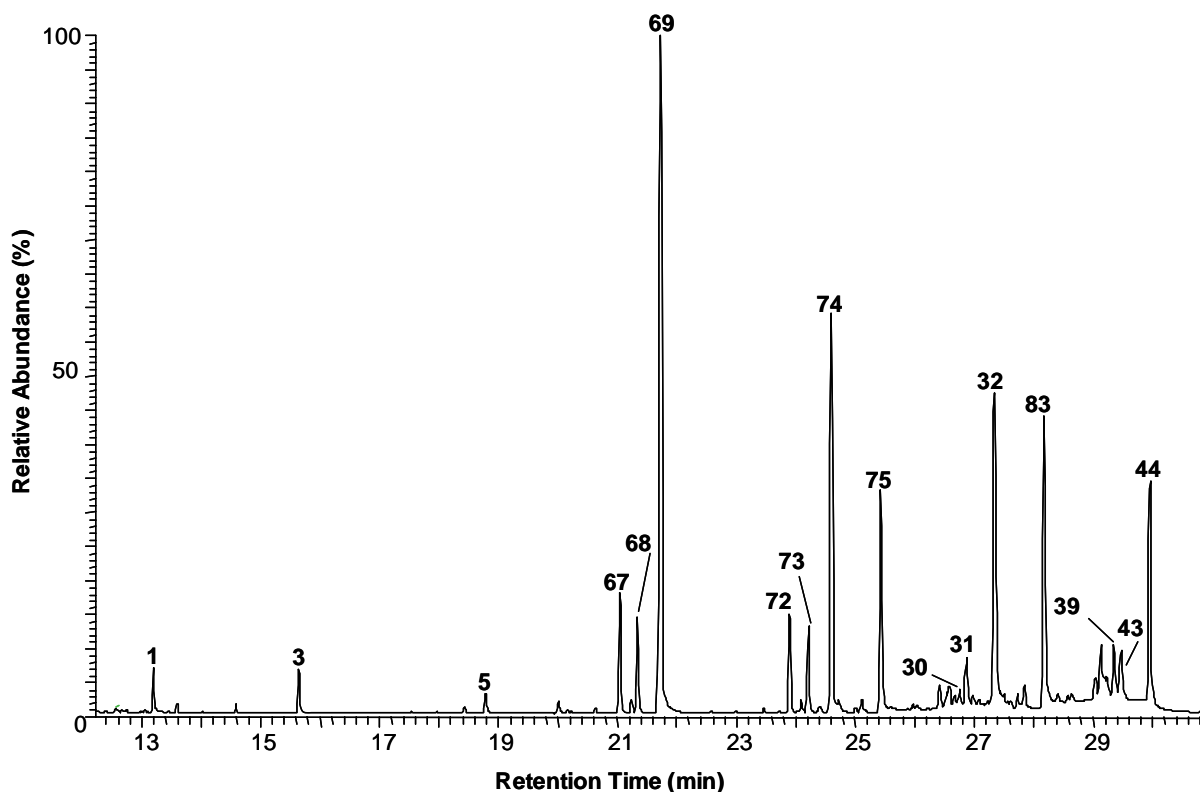
Figure 3.14. TIC of TMS derivatives of *Pterygodium hastata* oil flower constituents as an example for the Orchidaceae (for the identification compound members see Table 3.11, conditions **GC1**).

The crude oils of Orchidaceae flowers are also investigated by positive ion ESI-FTICR-MS. The ESI-FTICR mass spectra allowed a rapid identification of the lipid type. The corresponding sodium ion adducts ($[M+Na]^+$) and elemental compositions are shown in Table 3.12. The floral oil compounds of *Oncidium ornithorhynchum*, *Pterygodium hastata*, *Pterygodium magnum*, *Corycium dracomontanum*, *Oncidium cheirophorum*, *Zygostates lunata*, *Sigmatostalix putumayensis* and *Cyrtochilim serratum* are classified in several types: non-oxygenated free fatty acids, saturated or unsaturated acetoxy fatty acids, partially acetylated dihydroxy fatty acids, acylglycerols of mono- or diacetoxy fatty acids together with simple acylglycerol of fatty acids.

Table 3.11. TMS derivatives of compounds of *Pterygodium hastata, Pterygodium magnum, Corycium dracomontanum, Sigmatostalix putumayensis, Oncidium ornithorhynchum, Oncidium cheirophorum, Zygostates lunata* and *Cyrtochilim serratum* (Orchidaceae) identified by GC/EI-MS.

No.	Compound[a]	t_R (min)	Relative composition (%)							
			C. serratum	*O. ornithorhynchum*	*P. hastata*	*P. magnum*	*C. dracomontanum*	*S. putumayensis*	*Z. lunata*	*O. cheirophorum*
1	myristic acid	13.20[b]	-	-	1.2	-	-	-	-	-
3	palmitic acid	15.64[b]	-	-	1.3	-	1.1	-	-	-
4	*cis*-9-oleic acid	18.78[c]	-	-	-	1.8	3.0	-	-	2.5
5	stearic acid	19.26[b]	-	-	0.8	-	-	-	-	-
6	*cis*-11-eicosenoic acid	22.07[d]	-	-	-	-	-	-	-	2.1
8	*cis*-13-docosenoic acid	24.93[d]	-	-	-	-	-	-	-	0.5
15	(3*R*)-acetoxypalmitic acid	18.79[c]	-	-	-	4.4	3.2	-	-	-
17	(3*R*)-acetoxystearic acid	21.73[c]	-	-	-	19.4	23.9	-	-	-
19	(3*R*)-acetoxyeicosanoic acid	24.53[c]	-	-	-	1.2	0.3	-	-	-
30	2-[(3*R*)-acetoxypalmitoyl]-1-acetylglycerol	26.75[c]	-	-	0.4	8.5	18.4	-	-	-
31	1-[(3*R*)-acetoxypalmitoyl]-3-acetylglycerol	26.88[c]	-	-	2.2	2.5	2.8	-	-	-
32	2-[(3*R*)-acetoxypalmitoyl]-1,3-diacetylglycerol	27.35[c]	-	-	12.5	23.3	3.0	-	-	-

Table 3.11. (continued)

No.	Compound[a]	t_R (min)	Relative composition (%)							
			C. serratum	*O. ornithorhynchum*	*P. hastata*	*P. magnum*	*C. dracomontanum*	*S. putumayensis*	*Z. lunata*	*O. cheirophorum*
35	2-[(3R)-acetoxystearoyl]glycerol	26.67[e]	12.6	2.7	-	-	-	-	9.2	-
37	1-[(3R)-acetoxystearoyl]glycerol	27.22[e]	6.7	-	-	-	-	-	55.7	-
39	2-[(3R)-acetoxystearoyl]-1-acetyl]glycerol	29.36[c]	-	38.6	1.5	3.4	17.3	-	11.6	-
43	1-[(3R)-acetoxystearoyl]-3-acetylglycerol	29.49[c]	-	4.3	2.0	1.3	0.8	-	8.3	-
44	2-[(3R)-acetoxystearoyl]-1,3-diacetylglycerol	29.96[c]	-	25.1	7.8	12.9	1.1	-	4.8	15.1
45	2-[(3R)-acetoxyeicosenoyl]glycerol	28.20[f]	-	1.3	-	-	-	-	-	-
46	2-[(3R)-acetoxyeicosanoyl]glycerol	29.59[g]	-	-	-	-	-	5.7	-	-
47	1-[(3R)-acetoxyeicosanoyl]glycerol	30.60[g]	-	-	-	-	-	5.7	-	-
48	2-[(3R)-acetoxyeicosanoyl]-1-acetylglycerol	31.65[g]	-	4.7	-	-	-	5.3	-	-

Table 3.11. (continued)

No.	Compound[a]	t_R (min)	Relative composition (%)							
			C. serratum	*O. ornithorhynchum*	*P. hastata*	*P. magnum*	*C. dracomontanum*	*S. putumayensis*	*Z. lunata*	*O. cheirophorum*
49	2-[(3*R*)-acetoxyeicosanoyl]-1,3-diacetylglycerol	32.65[g]	-	-	-	-	-	19.6	-	3.6
51	2-[(3*R*)-acetoxydocosanoyl]-1,3-diacetylglycerol	33.85[g]	-	-	-	-	-	21.1	-	-
52	3,7-diacetoxystearic acid	22.57[d]	-	-	-	-	-	-	-	20.7
53	3,7-diacetoxyeicosanoic acid	25.40[d]	-	3.7	-	-	-	-	-	57.4
55	7-acetoxy-3-hydroxydocosanoic acid	26.48[d]	-	-	-	-	-	-	-	2.4
67	1-acetyl-2-myristoylglycerol	21.04[b]	-	-	3.5	-	-	-	-	-
68	1-acetyl-3-myristoyl glycerol	21.34[b]	-	-	3.4	-	-	-	-	-
69	1,3-diacetyl-2-myristoylglycerol	21.73[b]	-	-	26.6	-	-	-	-	-
70	2-palmitoylglycerol	22.50[c]	-	-	-	2.2	-	-	-	-
72	1-acetyl-2-palmitoyl glycerol	23.90[b]	-	-	2.6	-	-	-	-	-

Table 3.11. (continued)

No.	Compound[a]	t_R (min)	Relative composition (%)							
			C. serratum	*O. ornithorhynchum*	*P. hastata*	*P. magnum*	*C. dracomontanum*	*S. putumayensis*	*Z. lunata*	*O. cheirophorum*
73	1-acetyl-3-palmitoylglycerol	24.21[b]	-	-	2.7	-	-	-	-	-
74	1,3-diacetyl-2-palmitoleoylglycerol	24.61[b]	-	-	12.9	8.4	-	-	-	-
75	1,3-diacetyl-2-palmitoylglycerol	25.43[b]	-	-	8.8	-	0.8	-	-	-
76	2-(*cis*-9,11-octadecadienoyl)glycerol	25.22[f]	5.1	-	-	-	-	-	-	-
77	2-oleoylglycerol	25.41[f]	58.7	-	-	-	-	-	-	-
79	2-stearoylglycerol	25.64[f]	11.7	4.8	-	-	-	-	10.4	-
79	1-stearoylglycerol	25.88[f]	5.2	-	-	-	-			
83	1,3-diacetyl-2-oleoyl glycerol	27.33[b]	-	-	9.8	9.1	2.0	-	-	-
84	1,3-diacetyl-2-stearoyl glycerol	28.17[h]	-	-	-	-	22.3	-	-	-
85	2-eicosenoylglycerol	28.25[c]	-	-	-	1.6	-	-	-	-
86	1,3-diacetyl-2-eicosanoylglycerol	31.91[g]	-	14.8	-	-	-	6.7	-	-

Table 3.11. (continued)

No.	Compound[a]	t_R (min)	Relative composition (%)							
			C. serratum	*O. ornithorhynchum*	*P. hastata*	*P. magnum*	*C. dracomontanum*	*S. putumayensis*	*Z. lunata*	*O. cheirophorum*
87	1-acetyl-2-(3,9-diacetoxyeicosanoylglycerol	33.12[g]	-	-	-	-	-	22.7	-	0.8
88	1-acetyl-3-(3,9-diacetoxyeicosanoyl)glycerol	33.62[g]	-	-	-	-	-	13.2	-	-

[a]see key ions of mass spectral data in Appendix 2, [b]obtained from *P. hastata*, [c]obtained from *P. magnum*, [d] obtained from *O. cheirophorum*, [e] obtained from *Z. lunata*, [f]obtained from *C. serratum*, [g]obtained from *S. putumayensi*s, [h]obtained from *C. dracomontanum*, (-) = not detected, conditions **GC1**.

Table 3.12. Positive ion ESI-FTICR mass spectral data of the floral oils of Orchidaceae investigated.

No.	Compound type	Elemental composition	m/z ([M+Na]$^+$)	Error (ppm)	MW	Relative abundance (%)							
						C. serratum	*O. ornithorhynchum*	*P. hastata*	*P. magnum*	*C. dracomontanum*	*S. putumayensis*	*Z. lunata*	*O. cheirophorum*
15	3-OAc 16:0	$C_{18}H_{34}O_4$ Na$^+$	337.23534	+0.4[a]	314	-	-	-	4.5	1.7	-	-	-
17	3-OAc 18:0	$C_{20}H_{38}O_4$ Na$^+$	365.26674	-0.7[a]	342	-	-	-	2.2	2.8	-	-	-
19	3-OAc 20:0	$C_{22}H_{42}O_4$ Na$^+$	393.29828	+1.9[a]	370	-	-	-	8.1	4.5	-	-	-
30, 31	DAG (3-OAc 16:0, OAc)	$C_{23}H_{42}O_7$ Na$^+$	453.28359	+1.7[a]	430	-	-	13.0	5.0	54.2	-	-	-
32	TAG (3-OAc 16:0, diOAc)	$C_{25}H_{44}O_8$ Na$^+$	495.29403	+1.3[a]	472	-	-	88.7	100	100	-	-	3.3
37	MAG (3-OAc 18:0)	$C_{23}H_{44}O_6$ Na$^+$	439.30342	-0.3[b]	416	10.5	8.0	-	-	-	-	100	4.2
39, 43	DAG (3-OAc 18:0, OAc)	$C_{25}H_{46}O_7$ Na$^+$	481.31357	-1.1[a]	458	-	30.9	15.3	4.0	5.4	-	20.5	-
44	TAG (3-OAc 18:0, diOAc)	$C_{27}H_{48}O_8$ Na$^+$	523.32414	-1.1[a]	500	-	100	100	96.3	18.7	-	41.6	20.3
46, 47	MAG (3-OAc 20:0)	$C_{25}H_{48}O_6$ Na$^+$	467.27733	+1.2[c]	444	-	-	-	-	-	1.5	-	18.45
48	DAG (3-OAc 20:0, OAc)	$C_{27}H_{50}O_7$ Na$^+$	509.34500	-0.1[c]	486	-	1.0	-	-	-	3.2	3.0	-
49	TAG (3-OAc 20:0, diOAc)	$C_{29}H_{52}O_8$ Na$^+$	551.35543	-0.1[c]	528	-	-	7.4	1.7	-	2.7	-	-
51	TAG (3-OAc 22:0, diOAc)	$C_{31}H_{56}O_8$ Na$^+$	579.38670	+0.6[c]	556	-	-	-	-	-	28.4	-	-
53, 54	diOAc 20:0	$C_{24}H_{44}O_6$ Na$^+$	451.30266	-1.0[d]	428	-	4.5	-	-	-	-	-	100
67, 68	DAG (FA 14:0, OAc)	$C_{21}H_{40}O_5$Na$^+$	367.24637	-0.5[e]	344	-	-	1.1	-	-	-	-	-
72, 73	DAG (FA 16:0, OAc)	$C_{23}H_{44}O_5$Na$^+$	395.27822	-1.8[e]	372	-	-	1.5	-	-	-	-	-
75	TAG (FA 16:0, diOAc)	$C_{23}H_{42}O_6$Na$^+$	437.28814	+0.6[b]	414	10.5	-	12.7	-	-	-	-	-

Table 3.12. (continued).

No.	Compound type	Elemental composition	m/z ([M+Na]⁺)	Error (ppm)	MW	Relative abundance (%)							
						C. serratum	*O. ornithorhynchum*	*P. hastata*	*P. magnum*	*C. dracomontanum*	*S. putumayensis*	*Z. lunata*	*O. cheirophorum*
77	MAG (FA18:1)	$C_{21}H_{40}O_4 \, Na^+$	379.28209	-1.0^b	356	100	-	-	-	-	-	-	-
78	MAG (FA18:0)	$C_{21}H_{42}O_4 \, Na^+$	381.29795	$+1.2^b$	358	68.8	1.3	13.3	1.2	-	10.8	2.3	-
84	TAG (FA 18:0, diOAc)	$C_{25}H_{46}O_6 \, Na^+$	465.32039	-0.5^f	442	-	-	-	-	5.4	-	-	-
87, 88	DAG (diOAc 20:0, OAc)	$C_{29}H_{52}O_9 \, Na^+$	567.32309	$+0.2^c$	544	-	16.6	-	-	-	100	-	32.8

[a]obatined from *P. magnum* , [b]obatined from *C. serratum,* [c]obatined from *S. putumayensis,* [d]obatined from *O. cheirophorum,* [e]obatined from *P. hastata,* [f]obatined from *C. dracomontanum*, MW= molecular weight.

Discussion

The chemical investigations of non-volatile floral oils of the following species are described in detail:

- *Thladiantha dubia, Momordica anigosantha, Momordica fetida* (Cucurbitaceae),
- *Angelonia integerrima* (Scrophulariaceae),
- *Lysimachia vulgaris* (Myrsinaceae),
- *Cypella herbertii* (Iridaceae),
- *Zygostates lunata, Sigmatostalix putumayensis, Pterygodium magnum Pterygodium hastata, Corycium dracomontanum, Cyrtochilum serratum, Oncidium cheirophorum, Oncidium ornithorhynchum* (Orchidaceae),
- *Malpighia urens, Bunchosia argentea, Stigmaphyllon ellipticum, Byrsonima coriacea* and *Janusia guaranitica* (Malpighiaceae).

The positive ion ESI-FTICR-MS resulte in the high accuracy masses and elemental compositions and from a basis to interpret oil compound structures. GC/EI-MS is then capable to identify the floral oils compounds (secondary metabolites) as TMS derivatives with more hints for structure elements. Mass spectra are extensively described.

The lipid metabolites could be classified into twelve classes including non-oxygenated free fatty acids (**I**), oxygenated free fatty acids (**II**), acylglycerol of monoacetoxy fatty acids (**III–V**), acylglycerol of diacetoxy fatty acids (**VI–VII**), common acylglycerol of fatty acids (**VIII–X**), partially acetylated dihydroxy fatty acids (**XI**) and dicaetoxy fatty acids (**XII**) (see lipid structures in Table 3.13). Table 3.14 shows the comparison of EI-mass spectra results of detected lipids from studying floral oils. The results indicated that oxygenated fatty acid and mono- and diacylglycerols of monoacetoxy fatty acids were favorably detected among the six oil-secreting flower of the Scrophulariaceae family together with the Iridaceae family. In particular, mass spectra of *Diascia* spp. (see Chapter 2) are represented by four lipid types: non-oxygenanted free fatty acids (**I**), oxygenated free fatty acids (**II**) as well as mono- and diacylglycerols of acetoxy fatty acid (**III–IV**). Also, in *Lysimachia* floral oils (Myrsinaceae) were also significantly detected mono- and diacylglycerols of acetoxy fatty acid (**III–IV**). Interestingly, EI-MS results of floral oil compounds of Scrophulariaceae Iridaceae and Myrsinaceae families reveal related types of detected lipids classes' **I–IV**. In the frame of this work, the most

prevalent lipid category in Scrophulariaceae, Iridaceae and Myrsinaceae families are acyglycerols of monoacetoxy fatty acids (**III**). So far, in the case of Cucurbitaceae family no acylglycerols were observed. The main compounds detected are non-oxygenated free fatty acids (**I**) and oxygenated free (3*R*)-acetoxy fatty acid (**II**).

Interestingly, only Malpighiaceae oil flowers contain diacetoxy fatty acids (**XII**) as major components, while the individual floral oil of *Heteropterys chrysophylla* from that family contained acylglycerols of diacetoxy fatty acids (**VI**–**VII**) in abundance (see also Chapter 4). EI-MS results of orchid flower oils reveal variable lipid types, and thus these cannot be categorized.

The positive ion ESI-FTICR data usually correlate well with the GC/EI-MS data (Table 3.15). In most of the cases, non-oxygenated free fatty acids (**I**) were not detected by positive ion ESI-FTICR-MS experiments because they lack of the ionization efficiency in the positive ion mode (Han and Gross 2005). Nonetheless, fatty acids were easily detected and characterized by GC/EI-MS methods. The advantages of using ESI-FTICR-MS for lipid analyses are widely described (Kuksis and Myher 1995; Fard *et al.*, 2003; Kalo *et al.*, 2003; Pulfer and Murphy 2003; Ham *et al.*, 2004; Ishida *et al.*, 2004; Wu *et al.*, 2004).

However, the absolute intensity or even relative abundance of peaks in the ESI-FTICR results unlikely reflect to the real proportions (Pulfer and Murphy 2003; Han and Gross 2005). Therefore, in respect of the relative intensity, GC/EI-MS data were taken for an indication of the relative abundance of indicative compounds.

Thus, both GC/EI-MS and ESI-FTICR methods are required to characterize and identify the various significant secondary lipid metabolites in floral oils in general. Currently, there is only limited research in this area. Further studies will expand our knowledge and can eventually lead to an understanding of the natural interdependence of oil flowers and oil bees.

Table 3.13. Conclusion of lipid types of studying floral oils.
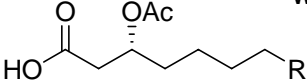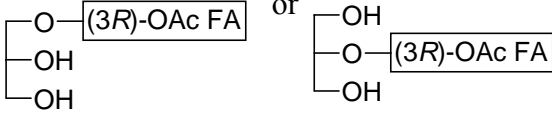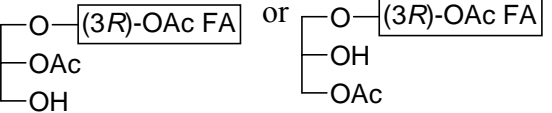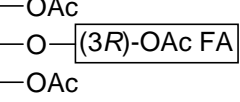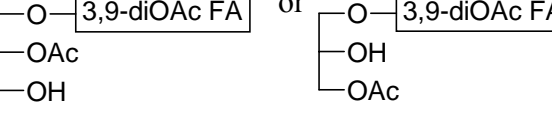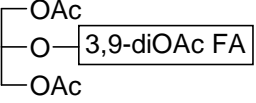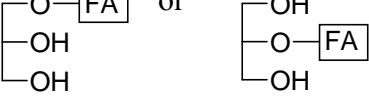
Type	Name	Structure
I	Non-oxygenated free fatty acid (FA) (unsaturated and saturated free fatty acid)	$CH_3(CH_2)_nCOOH$ or $n = 12, 14, 16,$ and 20 $CH_3(CH_2)_nCH{=}CH(CH_2)_mCOOH$ $n = 5, m = 7$ $n = 7, m = 7, 9$ and 11
II	Oxygenated fatty acid (unsaturated and saturated even-carbon numbered C_{14}, C_{16}, $C_{18:1}$, C_{18}, $C_{20:1}$ and C_{20})	when: R = alkyl
III	Monoacylglycerol of monoacetoxy fatty acid [(3R)-OAc FA = C_{14}, C_{16}, $C_{18:1}$, C_{18}, $C_{20:1}$ and C_{20}]	
IV	Diacylglycerol of monoacetoxy fatty acid [(3R)-OAc FA = C_{14}, $C_{16:1}$, C_{16}, $C_{18:1}$, C_{18} and C_{20}]	
V	Triacylglycerol of monoacetoxy fatty acid [(3R)-OAc FA =C_{14}, C_{16}, C_{18}, C_{22} and C_{22}]	
VI	Diacylglycerol of diacetoxy fatty acid (3,9-diOAc FA = C_{20} and C_{22})	
VII	Triacylglycerol of diacetoxy fatty acid (3,9-diOAc FA =C_{20} and C_{22})	
VIII	Monoacylglycerol of fatty acid (FA = C_{16}, $C_{18:2}$, $C_{18:1}$, C_{18} and $C_{20:1}$)	

Table 3.13. (continued).
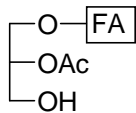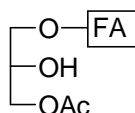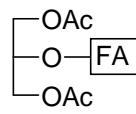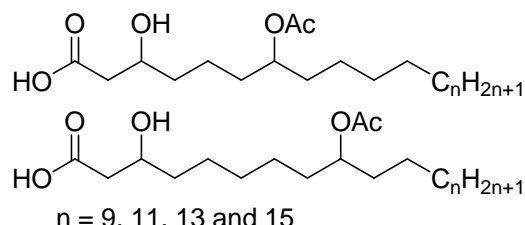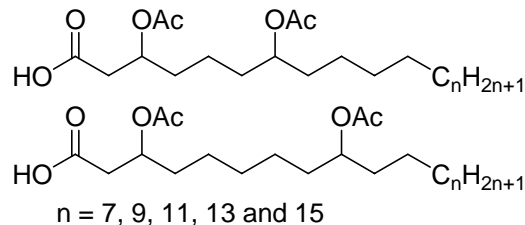
Type	Name	Structure
IX	Diacylglycerol of fatty acid (FA = C_{14}, C_{16}, $C_{18:2}$, $C_{18:1}$ and C_{18})	
X	Triacylglycerol of fatty acid (FA = C_{14}, $C_{16:1}$, C_{16}, $C_{18:1}$, C_{18} and C_{20})	
XI	Partically acetylated dihydroxy fatty acid	n = 9, 11, 13 and 15
XII	Diacetoxy fatty acid	n = 7, 9, 11, 13 and 15

Table 3.14. Conclusion of lipid types of floral oils investigated by GC/EI-MS (as TMS derivatives).

Oil flowers

Type[a]	Scrophulariaceae						Myrsinaceae		Iridaceae	Cucurbitaceae			Malpighiaceae						Orchidaceae							
	Diascia purpurea[a]	Diascia vigilis[a]	Diascia cordata[a]	Diascia megathura[a]	Diascia integerrima[a]	Angelonia integerrima	Lysimachia punctata[b]	Lysimachia vulgaris	Cypella herbertii	Momordica foetida	Momordica angosantha	Thladiantha dubia	Malpighia urens	Bunchosia argentea	Heteropterys chrysophylla[d]	Stigmaphyllon ellipticum	Byrsonima coriacea	Janusia guaranitica	Pterygodium magnum	Pterygodium hastata	Corycium dracomontanum	Zygostates lunata	Cyrtochilum serratum	Sigmatostalix putumayensis	Oncidium cheirophorum	Oncidium ornithorhynchum
I	+	+	+	+	+		+		+	+	+	+				+			+	+	+				+	
II	+	+	+	+	+	+	+	+	+	+	+	+							+		+					
III	+	+	+	+	+	+	+	+	+						+	+		+				+	+	+		+
IV	+	+	+	+	+	+	+	+	+										+	+	+	+		+		+
V	+	+	+	+	+			+											+	+	+			+	+	+
VI															+									+	+	
VII															+											
VIII							+												+				+	+		+
IX																				+						
X																			+	+	+			+		+
XI														+		+	+	+							+	
XII													+	+		+	+	+							+	+

[a]see lipid structures in Table 3.13, [b]*Diascia* spp. obtained from Chapter 2, [c]*Lysimachia punctata* data obtained from Chapter 5, [d]*Heteropterys chrysophylla* data obtained from Chapter 4, (+) = detected.

Table 3.15. Conclusion of lipid types of floral oils investigated by positive ion ESI-FTICR-MS.

Type[a]	Scrophulariaceae						Myrsinaceae		Iridaceae	Cucurbitaceae			Malpighiaceae						Orchidaceae							
	Diascia purpurea[b]	*Diascia vigilis*[b]	*Diascia cordata*[b]	*Diascia megathura*[b]	*Diascia integerrind*[b]	*Angelonia integerrima*	*Lysimachia punctata*[c]	*Lysimachia vulgaris*	*Cypella herbertii*	*Momordica foetida*	*Momordica anigosantha*	*Thladiantha dubia*	*Malpighia urens*	*Bunchosia argentea*	*Heteropterys chrysophylla*[d]	*Stigmaphyllon ellipticum*	*Byrsonima coriacea*	*Janusia guaranitica*	*Pterygodium magnum*	*Pterygodium hastata*	*Corycium dracomontanum*	*Zygostates lunata*	*Cyrtochilum serratum*	*Sigmatostalix putumayensis*	*Oncidium cheirophorum*	*Oncidium ornithorhynchum*
II						+			+	+	+	+							+			+				
III	+	+	+	+	+	+	+	+	+									+		+			+	+		+
IV	+	+	+	+	+	+	+	+	+										+	+	+	+				+
V	+	+	+	+	+				+										+	+		+			+	+
VI															+										+	
VII															+											
VIII																			+	+		+	+			+
IX																				+						
X																							+			
XI																+										
XII													+	+		+	+	+							+	+

[a]see lipid structures in Table 3.13, [b]*Diascia* spp. obtained from Chapter 2, [c]*Lysimachia punctata* data obtained from Chapter 5, [d] *Heteropterys chrysophylla* data obtained from Chapter 4,

(+) = detected.

CHAPTER 4

Ontogeny of *Heteropterys chrysophylla* (Malpighiaceae) Calyx Glands

Summary

The flowering process is one of the most intensely studied ones in plant development. Calyx glands of oil-producing flowers of *Heteropterys chrysophylla* (Malpighiaceae) were selectively collected in different stages. Morphology and lipid secretion of *H. chrysophylla* calyx glands are also described. Transmission Electron Microscopy (TEM) of the calyx glands during flower development revealed that the lipid droplets located around the mitochondria appear successively. The predominant constituents of the secreted calyx gland oil are acylglycerols with a long-chain diacetoxy fatty acid. The EI mass spectra of these acylglycerols are discussed in detail.

Results and Discussion

4.1. Morphology of ontogeny calyx glands

H. chrysophylla flowers consist of five yellow petals and eight greenish calyx glands, which inserted on the sepal abaxial side, being visible with the naked eyes. Glands are 2–3 mm high, and in average 3–4 mm broad, sessile and oval-shaped (Figure 4.1).

Figure 4.1. The developmental process of *H. chrysophylla* calyx glands from the initial stage (ϕ 2 mm; bud flower, left) to the active stage (ϕ 6 mm; blooming flower, right).

Light microscopy (LM) of longitudinal sections of the glands shows these features, from the outside to inside: thin cuticle, secretory tissue, a central core of sub-glandular parenchyma cells, and vascular supply bundles (Figure 4.2). The cuticle is smooth and thin. The uni-stratified secretory tissue is composed of a tightly layer packed cells which form a palisade layer involved in the synthesis and the secretion of the exudates. The sub-glandular parenchyma consisted of layers of isodiametric cells with the small intercellular spaces, including xylem and phloem.
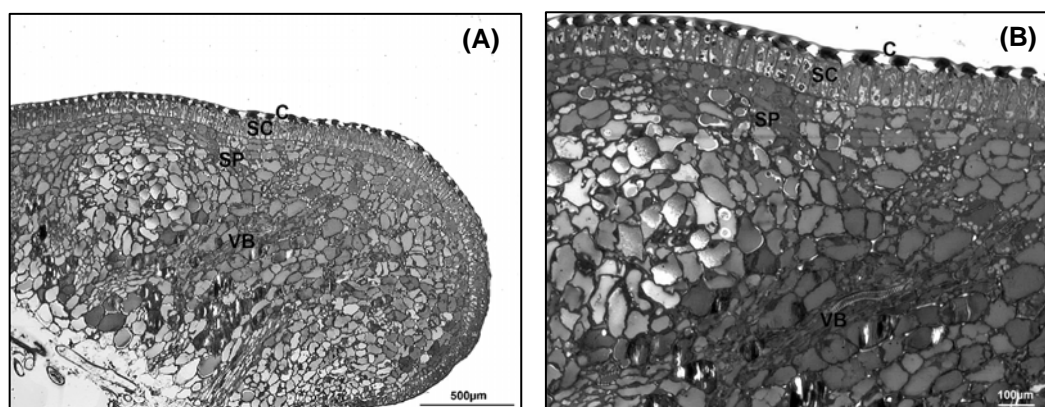
Figure 4.2. LM micrographs of active calyx gland in the initial stage: smooth cuticle, secretory cells, subglandular paremchyma. (A) Bar= 500 μm, (B) Bar= 100 μm. (C, cuticle; SC, secretory cell; SP, subglandular parenchyma) (photo by M. Birschwilks).

Figure 4.3 shows the TEM micrographs of secretory cells of *H. chrysophylla* flower in their initial stage (A, B), active (or blooming) stage (C, D) and senescence stage (E, F). The TEM observations of the initial stage reveal that the compact appearance of the cytoplasm results from an abundance of ribosomes, rough endoplasmic reticulum (RER), mitochondria, Golgi, numerous small and translucent vesicles, plastids, and a large vacuole (Figure 4.3 A, B). The RER is composed of narrow cisternae dispersed in cytoplasm or closely stacked near the plasma membrane (Figure 4.3B). Mitochondria are elliptic or globular, occur in great numbers and possess many well-developed cristae. They are dispersed or aggregated in the cytoplasm (Figure 4.3D). Golgi bodies are particularly present in active secretory cells and are abundant in the pre-secretory stage (Figure 4.3B).

Large vacuoles containing dense ergastic substances mixed with other more translucent products are observed. These are especially enlarged in the senescence stage (Figure 4.3E-F). Some lipid droplets are present in the cytoplasm. The inner side of the outer periclinal secretory cell wall presents slight ingrowths associated with plasma membrane. In the active stage (Figure 4.3C) and with the onset of secretion, the exudates released into the apoplastic space flow toward the wall and begin to accumulate beneath the cuticle. Some authors reported on the ultrastructure of calyx gland of *Banisteriopis variabilis* (Attala and Machado 2003) and *Galphimia brasiliensis* (Malpighiaceae) (Castro *et al*., 2001). They detected the lipid droplets during the active stage of calyx glands being in good agreement with our TEM observations.
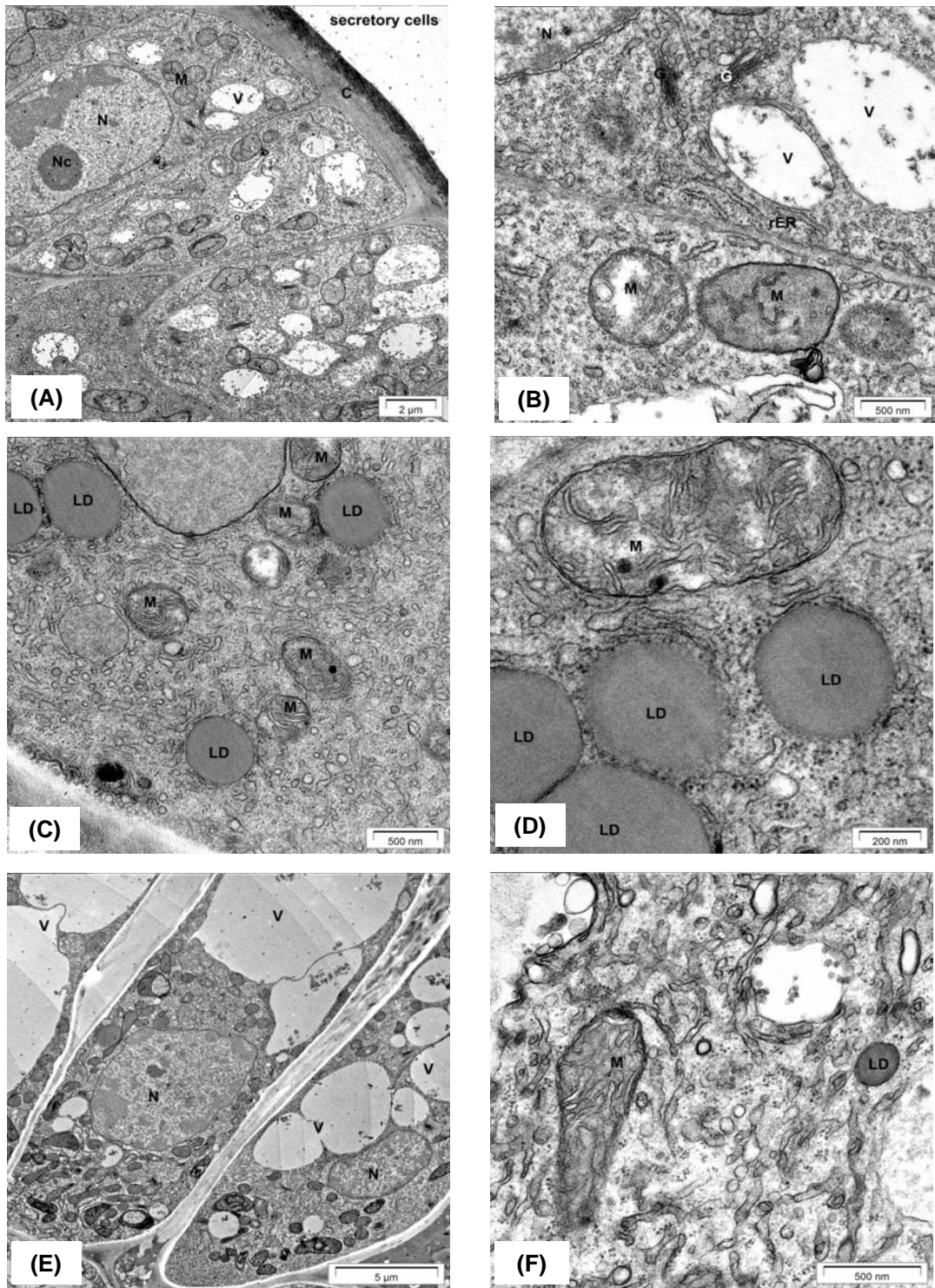
Figure 4.3. Secretory cells in developmental process of calyx glands of *H. chrysophylla*, TEM micrographs of the initial stage (A-B), active stage or blooming stage (C-D) and senescence stage (E-F) (**V**, vacuole; **N**, nucleus; **NC**, nucleolus; **G**, golgi bodies; **M**, mitochondria; **LD**, lipid droplet) (photo by M. Birschwilks).

4.2. Chemical composition of *H. chrysophylla* oil of calyx gland in differential stage

4.2.1 GC/EI-MS analysis

DAGs and TAGs containing a long chain diacetoxy fatty acid and one or two acetyl moieties respectively, represent the major constituents of *H. chrysophylla* oil. Figure 4.4 shows the TIC of TMS derivatives of *H. chrysophylla* floral oil resulting from a GC-MS analysis.
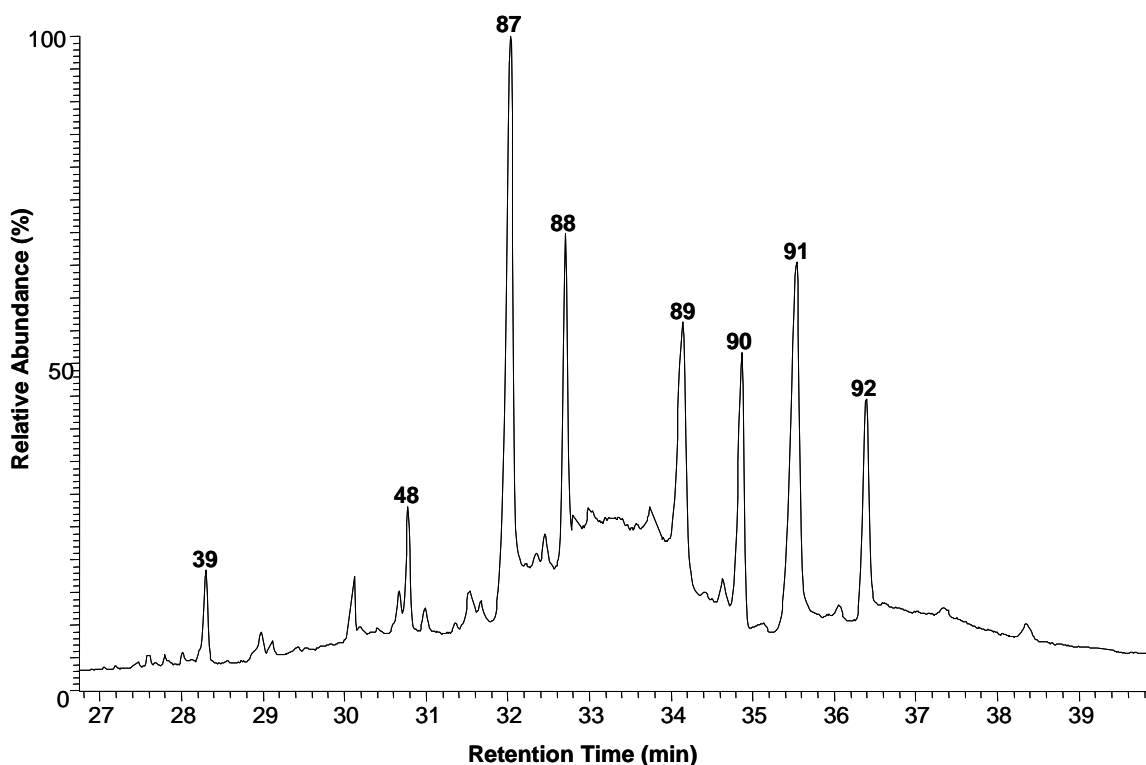
Figure 4.4. Partial TIC of TMS derivatives of *H. chrysophylla* in blooming stage (for the identified compound members see Table 4.1, conditions **GC3**).

The TMS derivatives of identified compounds of *H. chrysophylla* oils are summarized in Table 4.1. The DAGs of diacetoxy fatty acids (C_{20}, C_{22}) and acetyl function are presented as major compounds *ca.* 50−60% and along with TAGs of diacetoxy fatty acids and two acetyl moieties (*ca.* 35%). The position of the acetoxy moieties on the diacetoxy fatty acid chain could not be determined by analysis of the TMS derivatives. However, based on the EI-MS results of the TMS derivatives from the FAME profiling, one could conclude that the acetoxy groups are located at C-3 and C-9 (see Figure 3.12 and Scheme 3.2). So far, we could assign the absolute configuration of this compound of *H. chrysophylla*. However, so far in all cases of floral oil studies, the (*R*)-

configuration was determined. Reis *et al.*, (2007) also reported this type of compound (3,7-diacetoxy fatty acids; named byrsonic acid) from *Byrsonima intermedia* (Malpighiaceae). Mosher experiments indicated (*R*)-configuration at C-3 and C-7 of the fatty acid. Also, based on the biosynthetic consideration, the (*R*)-configured isomer is feasible (Seipold *et al.*, 2004).

Table 4.1. TMS derivatives of identified compounds of *H. chrysophylla* oil in the active stage investigated by GC/EI-MS.

No.	t_R (min)	Compound[a]	Relative composition (%)
39	28.30	2-[(3*R*)-acetoxystearoyl]-1-acetylglycerol	4.0
48	30.78	2-[(3*R*)-acetoxyeicosanoyl]-1-acetylglycerol	5.6
87	34.15	1-acetyl-2-(3,9-diacetoxyeicosanoyl)glycerol	19.8
88	32.03	1-acetyl-3-(3,9-diacetoxyeicosanoyl)glycerol	18.5
89	32.71	1,3-diacetyl-2-(3,9-diacetoxyeicosanoyl)glycerol	15.9
90	36.40	1-acetyl-2-(3,9-diacetoxydocosanoyl)glycerol	10.7
91	34.87	1-acetyl-3-(3,9-diacetoxydocosanoyl)glycerol	13.5
92	35.54	1,3-diacetyl-2-(3,9-diacetoxydocosanoyl)glycerol	12

[a]see Appendix 2 for EI-mass spectral data (Table A 2.6 and A 2.13).

The EI mass spectra of and 1-acetyl-2-(3,9-diacetoxyeicosanoyl)glycerol (**87**) and 1-acetyl-3-(3,9-diacetoxyeicosanoyl)glycerol (**88**) shows no molecular ion, the highest mass peak is from an ion of type **a** ($[M–Me–HOAc]^+$) (Figure 4.5). A **d**-type ion, corresponding to the acylium ion ($[M–R'COOH]^+$) is not be observed in this case. However, ions of the type (**d**–HOAc) and (**d**–2HOAc) are significantly present. The ions of type **g** (*m/z* 189) and **h** (*m/z* 175) appear in both 1,2- and 1,3-DAGs, respectively. However, the TMS derivatives of 1,2-DAGs (**87, 90**) show a base peak of ion type **g** at *m/z* 189. A further key ion of 1,3-DAG (**88, 91**) is ion **h** (*m/z* 175) which is of low abundance in the TMS derivatives of 1,2-DAGs (Scheme 4.1).
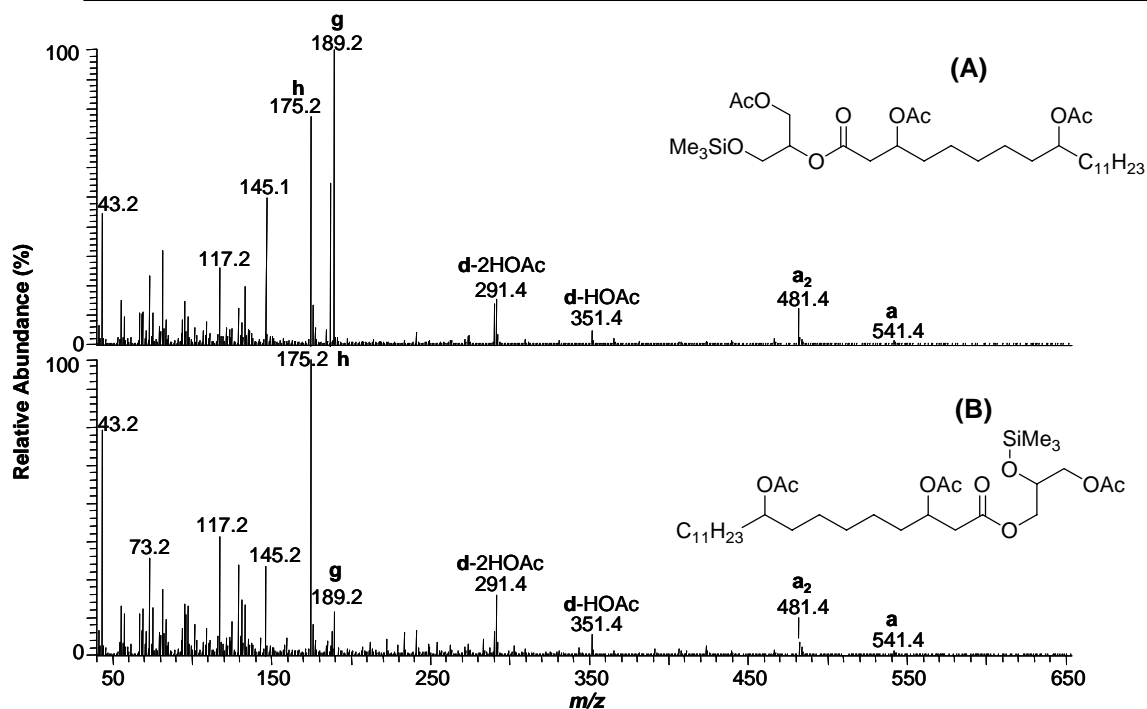
Figure 4.5. 70 eV EI-mass spectra of (A) 1-acetyl-2-(3,9-diacetoxyeicosanoyl)glycerol (**87**) and (B) 1-acetyl-3-(3,9-diacetoxyeicosanoyl)glycerol (**88**) (see Scheme 4.1).
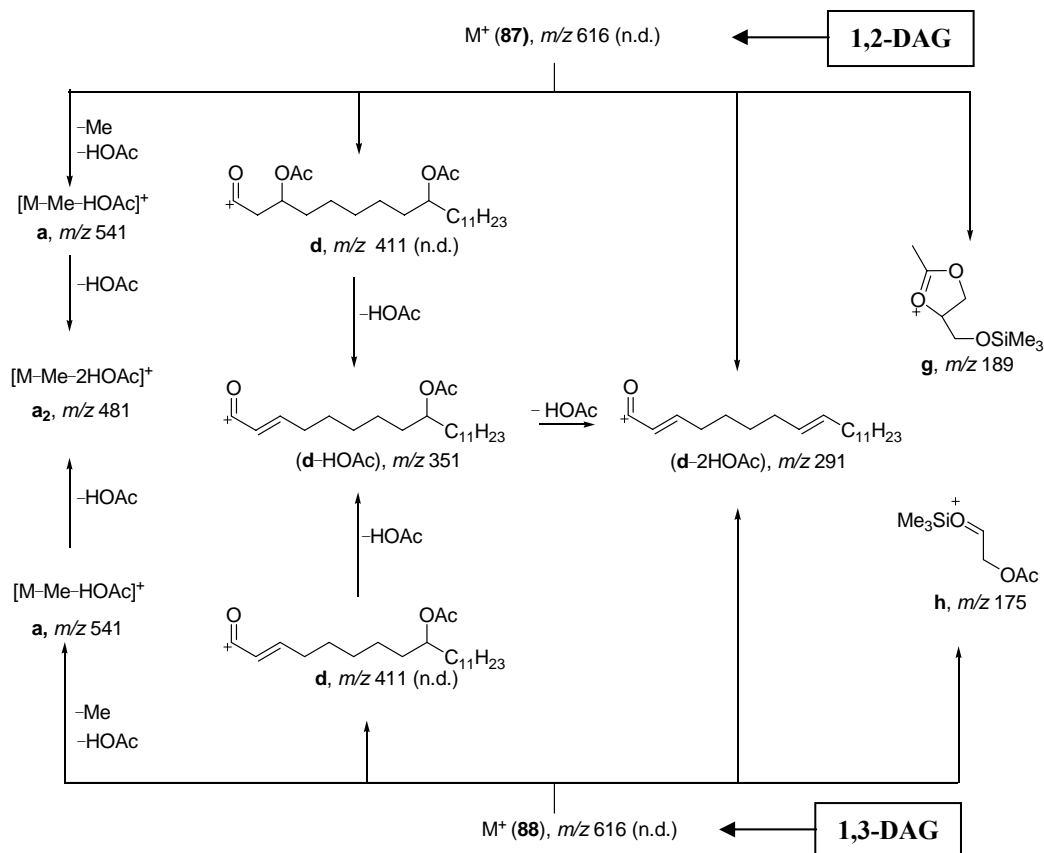
Scheme 4.1. Significant fragments of the diacylglycerols 1-acetyl-2-(3,9-diacetoxyeicosanoylglycerol (**87**) and 1-acetyl-3-(3,9-diacetoxyeicosanoyl)glycerol (**88**) (n.d = not detected).

TAGs in floral oil of *H. chrysophylla* (**89**, **92**) consist of one 3,9-diacetoxy fatty acids (C_{20} and C_{22}) at C-2 and two acetyl moieties at C-1 and C-3 of the glycerol backbone. Figure 4.6 shows and EI mass spectrum of 1,3-diacetyl-2-(3,9-diacetoxyeicosanoyl)glycerol (**89**). While the ion of type $\mathbf{a_1}$ ([M–2HOAc]$^+$) represents the *m/z* value of highest mass, the fragment ion at *m/z* 159 (type $\mathbf{e_2}$) indicates the presence of [M–R´COOH]$^+$ (Scheme 4.2).
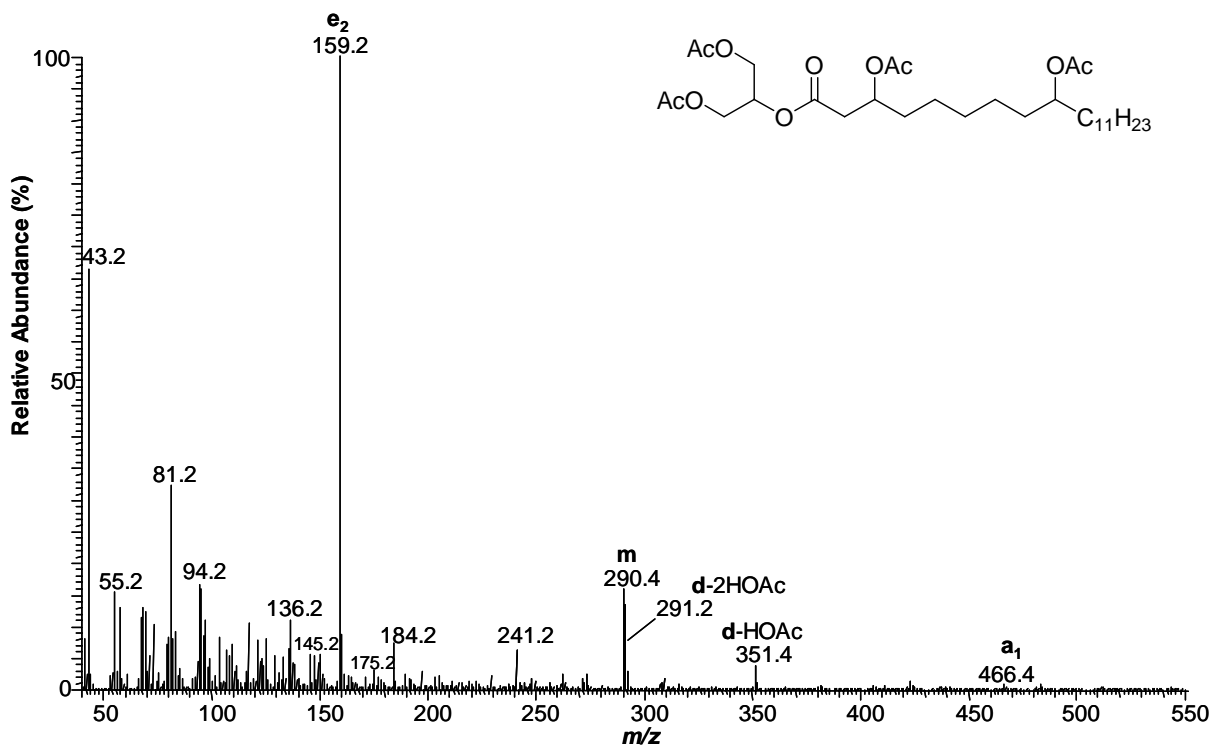
Figure 4.6. 70 eV EI-Mass spectrum of 1,3-diacetyl-2-(3,9-diacetoxyeicosanoyl) glycerol (**89**) (see Scheme 4.2).
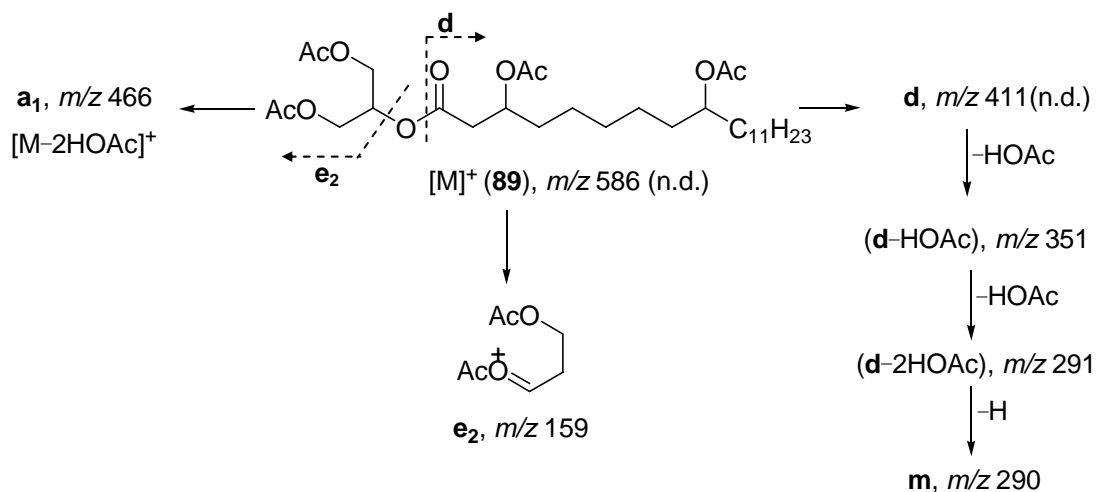
Scheme 4.2. Significant fragments of the triacylglycerol (TAG) 1,3-diacetyl-2-(3,9-diacetoxyeicosanoyl)glycerol (**89**) (n.d. = not detected).

4.2.2. ESI-FTICR-MS analysis

The underivatized oil of *H. chrysophylla* is also investigated by positive ion ESI-FTICR mass spectrometry (Figure 4.7, Table 4.2). The sample exhibited the characteristics of acylglycerols of diacetoxy fatty acids. The ions $[C_{29}H_{52}O_9 Na^+]$ at *m/z* 567.34774 (**87, 88**) and $[C_{31}H_{56}O_9Na^+]$ at *m/z* 595.37869 (**90, 91**) are indicative of DAGs possessing one acetyl and one C_{20} or C_{22} diacetoxy fatty acid moiety, respectively. TAGs of diacetoxy fatty acids (C_{20} and C_{22}) with two acetyl groups attached to the glycerol backbone display an ion $[C_{31}H_{54}O_{10}Na]^+$ at *m/z* 609.35697 (**89**) and $[C_{33}H_{58}O_{10} Na]^+$ at *m/z* 637.38719 (**92**), respectively. The positive ion ESI-FTICR shows the TAG of the diacetoxy fatty acid (C_{22}, **92**) as the highest abundance peak (100%, rel.), while it was detected by GC/EI-MS only *ca.* 20% relative composition. None of DAGs (**39, 48)** was detected by positive ESI-FTICR-MS. It might be relate to the sensitivity of each acylglycerols of diacetoxy fatty acids during ionization process. The ESI-FTICR-MS is a very powerful technique to help structural elucidation. However, the absolute abundance or even relative abundance of peaks in the ESI-FTICR does not certainly reflect the real proportions (Pulfer and Murphy 2003; Han and Gross 2005). Therefore, with respect to the relative intensity, GC/EI-MS data were taken into the tables for an indication of the relative abundance of indicative compounds. Nevertheless, qualitatively all the significant acylglycerols were detected with both methods.
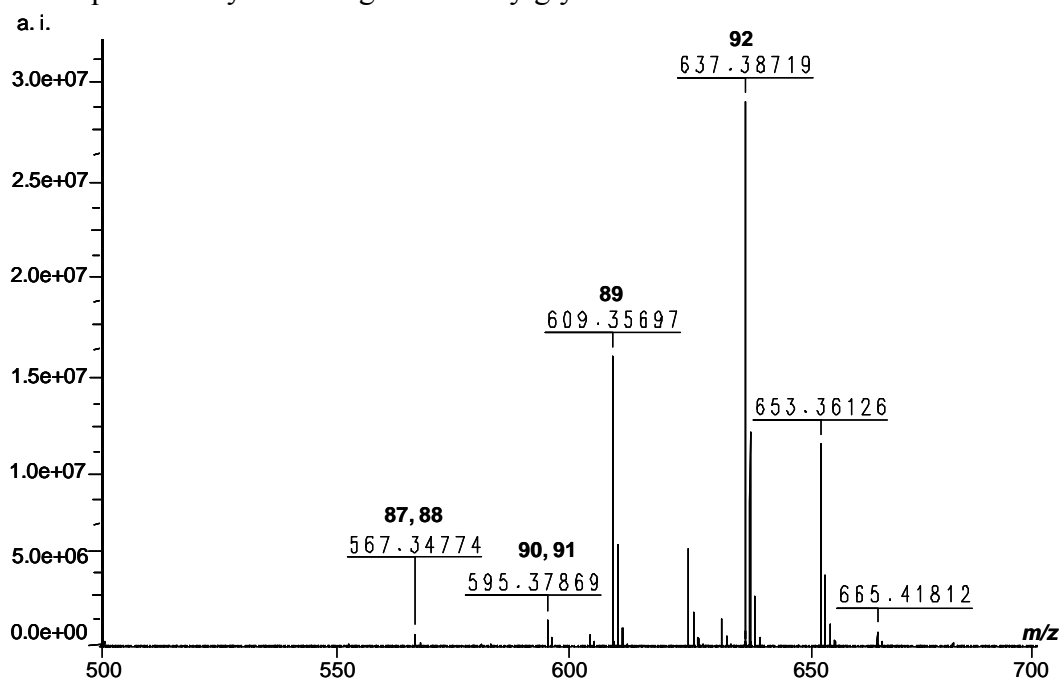
Figure 4.7. Positive ion ESI mass spectrum of *H. chrysophylla* oil. The corresponding compounds present in Table 4.2 (see also Table 4.1).

Table 4.2. Positive ion ESI-FTICR mass spectral data of *H. chrysophylla* floral oil.

No.	Compound type[a]	Elemental composition	*m/z* ([M+Na]$^+$)	Error (ppm)	MW	Relative abundance (%)
87, 88	DAG (diOAc 20:0, OAc)	$C_{29}H_{52}O_9Na^+$	567.34774	+0.5	544	2.3
90, 91	DAG (diOAc 22:0, OAc)	$C_{31}H_{56}O_9Na^+$	595.37869	+0.5	572	4.9
89	TAG (diOAc 20:0, diOAc)	$C_{31}H_{54}O_{10}Na^+$	609.35697	-0.9	586	53.2
92	TAG (diOAc 22:0, diOAc)	$C_{33}H_{58}O_{10}Na^+$	637.38719	-2.0	614	100

[a]see full name of compounds in Table 4.1, MW = molecular weight

4.3. Development of *H. chrysophylla* calyx glands

The acylglycerol content of the calyx glands is significantly related to their morphological development (Figure 4.8., Table 4.1). A time course analysis of the acylglycerol compounds (**39**, **48**, **87−92**) from the initial stage to the active stage of *H. chrysophylla* calyx glands was followed for 21 days. The acylglycerol production during calyx gland development was simply calculated from the percentage of peak area ratio between detected acylglycerols and an internal standard (pentadecanoic acid). Oil production of calyx glands reached the maximum level after 15 days of development (Figure 4.8.). After 9 days, the acylglycerol content were rapidly increased. The lipid content is decreasing during the senescence stage starting after 15 days of development (based on the TEM, Figure 4.3E-F). The abundance of lipid droplets could be observed in the cell structure in active stage of calyx gland (Figure 4.3 C-D).

This study was undertaken to elucidate the structural and ultrastructural features related to the anatomy and chemical secretions of calyx glands in *H. chrysophylla* flowers. The TEM observations show several ultrastructural changes during the secretion. Active secretory cells exhibit a conspicuous nucleus, dense cytoplasm, lipid droplets, numerous vesicles, mitochondria, Golgi bodies and rough endoplasmic reticulum (RER). Ultrastructure characteristics of the calyx glands indicate abundant lipid droplets at the blooming stage of the flower. DAGs and TAGs composed of diacetoxy fatty acid and one or two acetyl moieties are the major lipid constituents. TMS derivatives of calyx gland oil allowed characterizing the fatty acid portions by FAME profiling. In the

developmental growth curve, expectedly the maximum level of lipid compounds could be detected in the active stage or blooming stage of *H. chrysophylla* flowers.
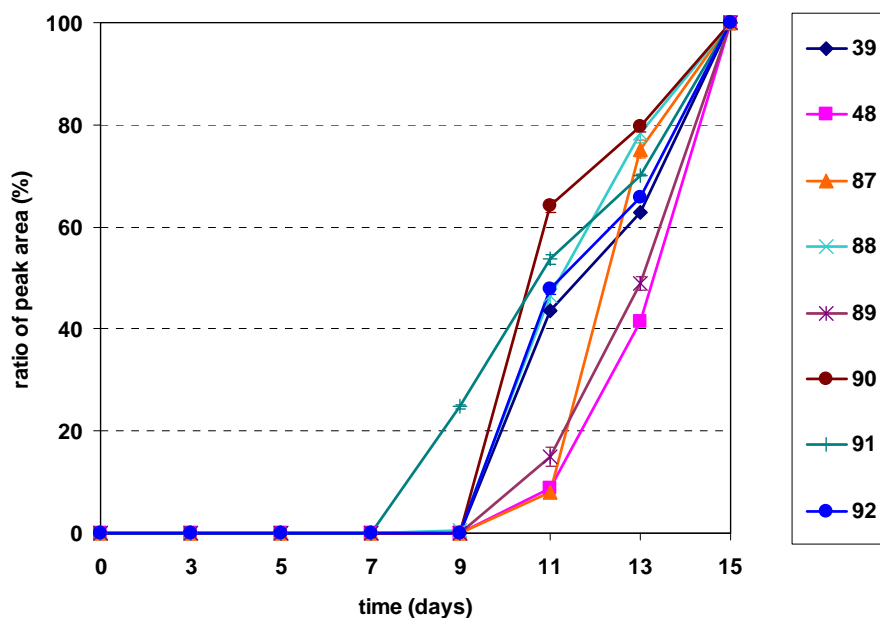
Figure 4.8. Time course acylglycerol formation in *H. chrysophylla* calyx glands from initial stage until the blooming stage. The y−axis shows the percentage of peak area ratio between detected compounds (**39**, **48**, **87−92**) and internal standard (pentadecanoic acid) and x−axis demonstrates the time of *H. chrysophylla* calyx glands development from initial stage (budding) untill active stage (blooming).

CHAPTER 5

From Flowers and Bees:

the Chemical Relation Between *Lysimachia & Macropis*

Summary

Field observations have suggested that females of the solitary oil-collecting bee *Macropis fulvipes* (Melittidae) harvest oil rewards from the oil-producing flower plant *Lysimachia punctata* (Myrsinaceae) and uses it to create a nest cell lining. We present some chemical investigations dealing with the chemical transformation of oil constituents by the bee. The predominant constituents of *L. punctata* oil are diacylglycerols, which contain a long-chain (3*R*)-acetoxy fatty acid and an acetyl moiety, Chemical studies of *M. fulvipes* cell linings reveal the formation of di-[hydroxyfatty acid]-monoacylglycerols as prominent compounds. Interestingly, none of the dominant acetylated acylglycerols from *L. punctata* oil can be detected directly in the bee cell linings. It was hypothesized that female *M. fulvipes* bees are able to convert flower oils chemically e.g. by enzyme excretion, to cell lining compounds. Evidence is presented here for an involvement of the salivary gland or labial gland secretions in this process. *In vitro* experiments of *L. punctata* oil treated with *M. fulvipes* labial gland secretions reveal novel intermediate compounds which structurally link the flower oils to the compounds detected in the cell lining. The results obtained show that the labial gland secretions of *M. fulvipes* play an important role with regard to the construction of cell linings.

Results and Discussion

5.1. Morphology of bee nest cell lining

Macropis oil-collecting bees are closely associated with *Lysimachia* oil flowers (Myrsinaceae) (Cane *et al*., 1983, Vogel 1986). The females of these species collect oil from the elaiphores of the flowers (at the base of the stamen). They present typical morphological adaptations for the collection and transport of oils, such as typical hairs on the legs (Celary 2004) (Figure 5.1A). The genus *Lysimachia* L. consists of *ca.* 180 species mostly occurring in temperate and subtropical areas of the Northern Hemisphere (but also present in the Neotropical region). Most of the European *Lysimachia* species possess oil-producing flowers. The nesting behavior of *Macropis* was first discussed by Vogel (1986, Figure 5.2). *M. fulvipes* belongs to the summer species and has only one generation a year. Males emerge 10–12 days before females. *M. fulvipes* bees show an extreme activity of *ca.*10 days in early July during their nesting period (Figure 5.1B).
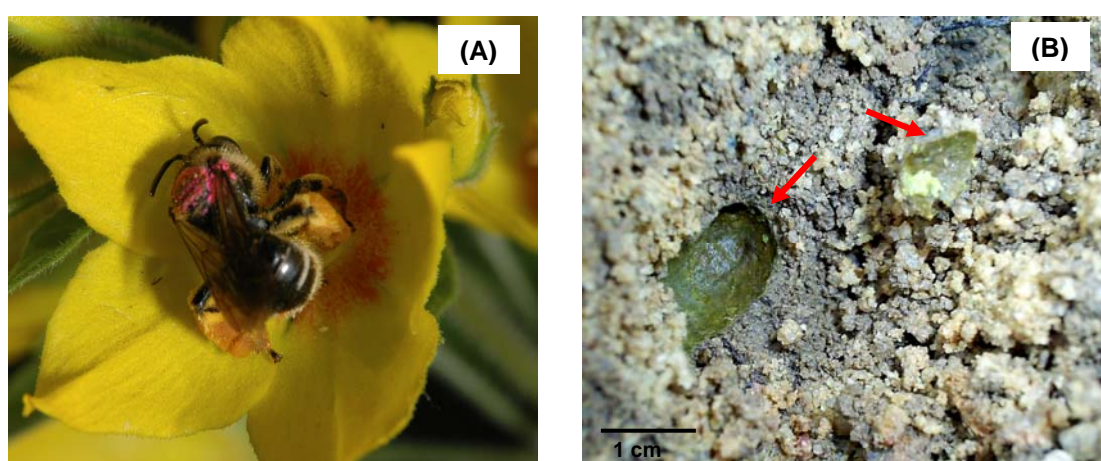
Figure 5.1. (A) A *M. fulvipes* female bee collects oil and pollen from *L. punctata* flowers and (B) a cross-section of the nest cell lining of a *M. fulvipes* bee (arrows) (photos by (A) S. Dötterl and (B) K. Dumri).
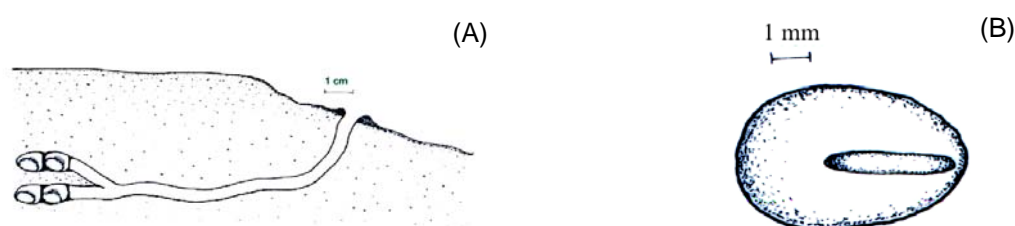
Figure 5.2. (A) Vertical section through the nest of *M. fulvipes* and (B) single nest cell with provision with and an egg of *M. fulvipes* (from Celary 2004).

The *M. fulvipes* nest cell lining is made of uniform larvae cells, and each nest is constructed by a single adult female (Michener 1964; Cane *et al.*, 1983; Vogel 1986; Wcislo and Cane 1996; Celary 2004). The yellowish-brown, waxy, water-proof material is around 1–1.5 cm long and 8.5–10 mm in diameter. The layer of cell lining, which is insoluble in various organic solvents, is difficult to hydrolyze completely even under strongly acidic conditions (Albans *et al.*, 1980).

Previous microscopic examinations of cell linings of oil-collecting *Hylaeus*, *Colletes* and *Ptiloglossa* bees have revealed fiber-like strands of variable size embedded in a solid matrix (Hefetz *et al.*, 1979; Albans *et al.*, 1980; Espelie *et al.*, 1992). In contrast, our observations have shown the *M. fulvipes* cell lining to be non-fibrous and to consist of thin material. The cells of several oil-producing bee species contain pollen deposit which may be accidental or may be used as nutrition for larvae development (Hefetz *et al.*, 1979; Cane *et al.*, 1983; Vogel 1986; Vinson *et al.*, 1996; Vieira de Jesus and Garófalo 2000; Celary 2004). Figure 5.3 illustrates a microscopic examination (A) and a SEM picture of continuous and non-fibrous surface of the cell lining membrane of *Macropis* cells (B). The clusters of pollen grains are found throughout the cell.

The biological habits of *Macropis* bees were first reported by Vogel (1986). It was suggested that female bees harvest oil and pollen from *Lysimachia* for nest construction and to provide food for larvae. The hydrophobic characteristic of the oil and pollen probably explains how these cell linings could resist physical and biological attack under the ground for a year. Furthermore, the humidity of nest cell lining is a significant factor for nest construction (Michener 1964).
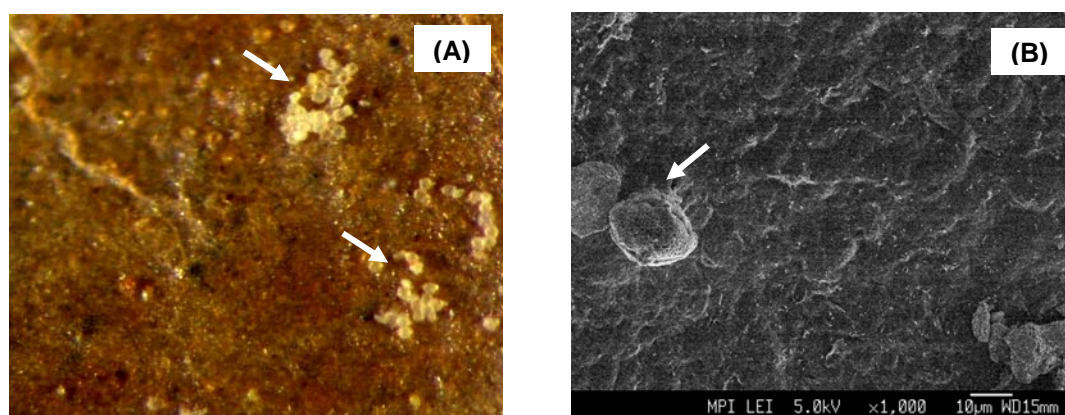
Figure 5.3. The surface of *M. fulvipes* cell lining investigated by stereomicroscopy (A) and by scanning electron microscopy (SEM). (B) Arrows illustrate pollen grains (photos by (A) B. Hause and (B) W. Erfurth).

5.2. Morphology of *M. fulvipes* labial gland

Most morphological investigations of insect salivary glands focus on the honey bee salivary gland. The saliva of honey bees contains several enzymes. The putative functions of secretory products of the thoracic salivary gland from honey bee (*Apis mellifera*) are to dissolve sugar and honey as well as to moisten materials such as pollen, wax, etc. (Schönitzer and Seifert 1990). Most ground-nesting bees use the secretions of Dufour's gland to construct the cell lining. The chemical components of Dufour's gland such as macrocylic lactones, triglycerides, aliphatic hydrocarbons, aliphatic aldehydes, ketones, acids and esters have been reported (Hefetz *et al.* 1979; Albans *et al.* 1980; Norden *et al.*, 1980; Cane 1983; Abdalla and Cruz-Landim 2001). In particular, *Macropis* and *Tetrapedia* bees use oil; secretions from Dufour′s gland are not involved in cell lining construction. It was hypothesized by us that the cell lining is enzymatically processed (polymerized) by secretions from the labial gland as a main source. A previous report about *Anthophora* bees also observed that the liquid triglycerides of their Dufour's gland are converted into solid diglycerides by unknown enzymes of thoracic salivary glands and form transparent insoluble polyester for cell lining construction (Batra and Norden 1996; Norden *et al.*, 1980). The labial gland of *M. fulvipes* female is located in the thorax (Figures 5.4 and 5.5). The structure is paired and each part is situated anterolaterally in the pronotum. Each pair of the gland consists of many grape-shaped acini made up of glandular cells.
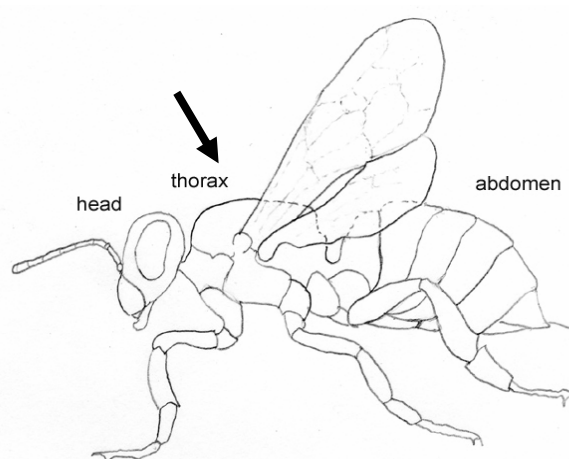
Figure 5.4. Schematic of a *M. fulvipes* female bee. The arrow shows the labial gland position at the anterior part of thorax.

(from: http://www.friendsofthedunes.org/natural_history/BeeFiles/anatomy.html).
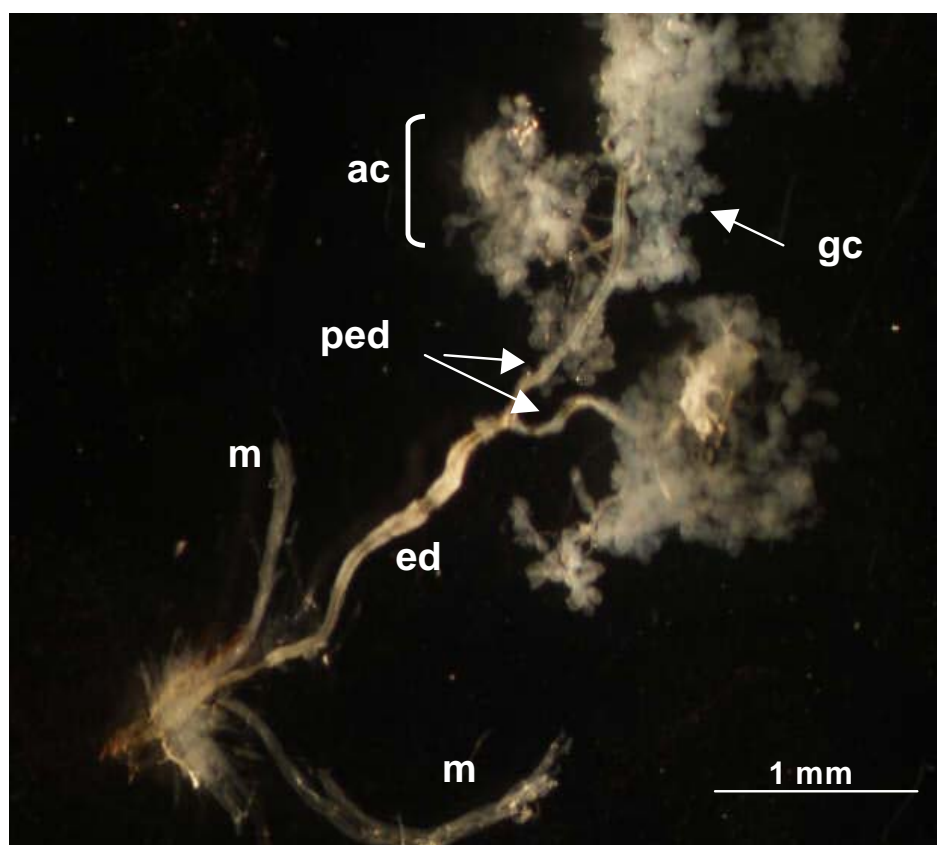
Figure 5.5. Labial gland of *M. fulvipes* female. The grape-shaped acini consist of many globular gland cells. The glandular tissue and the paired efferent duct are located in the anterior part of the thorax (**m** = muscles, **ed** = efferent duct, **ped** = paired efferent duct, **ac** = acini, **gc** = globular gland cells) (photo by K. Dettner).

5.3   GC/EI-MS analysis

GC/EI-MS analyses reveal the lipid pattern of *L. punctata* oil, labial gland and nest cell lining of *M. fulvipes* as well as of *L. punctata* oil treated with labial gland secretions of *M. fulvipes* (Table 5.1). *L. punctata* oil consists of 1-MAGs and 2-MAGs of acetoxy fatty acids (**34–37**) and 1,2-DAGs and 1,3-DAGs possessing acetoxy fatty acid and acetyl moiety (**40–43**) as well as common mono- and diacylglycerol of long-chain fatty acids (**5–9**). 1,2-DAGs of long-chain a (3*R*)-acetoxy fatty acid and acetyl moiety (**40**, **42**) are the main compounds. The characteristic key ions of these compounds are similar to the dominant 1,2-DAG compounds from *Diascia* species (**22**, **30**, **39**; Chapter 2). The molecular mass of 1,2-DAGs is deduced from the appearance of a significant ion of type **a** ([M−Me−HOAc]$^+$). The TMS derivatives of 1,2-DAGs of *Diascia* floral oils (**22**, **30**, **39**) show a significant fragment at *m/z* 188 (type **e**, see Figure 2.6 and Scheme 2.2);

their moderate intensity hint that the (3*R*)-acetoxy fatty acid is attached to the secondary hydroxyl group of the glycerol backbone (Seipold 2004). Whereas the 1,2-DAG compounds of *L. punctata* oil show no significant ion at *m/z* 188 (type **e**). This fact indicates that (3*R*)-acetoxystearic acid is attached to the primary hydroxyl group of the glycerol backbone (Seipold 2004, Figure 5.6). The interpretation of the EI mass spectra of other acylglycerols is discussed in Chapter 2. Characteristic key ions are summarized in Appendix 2 (Table A 2.6).
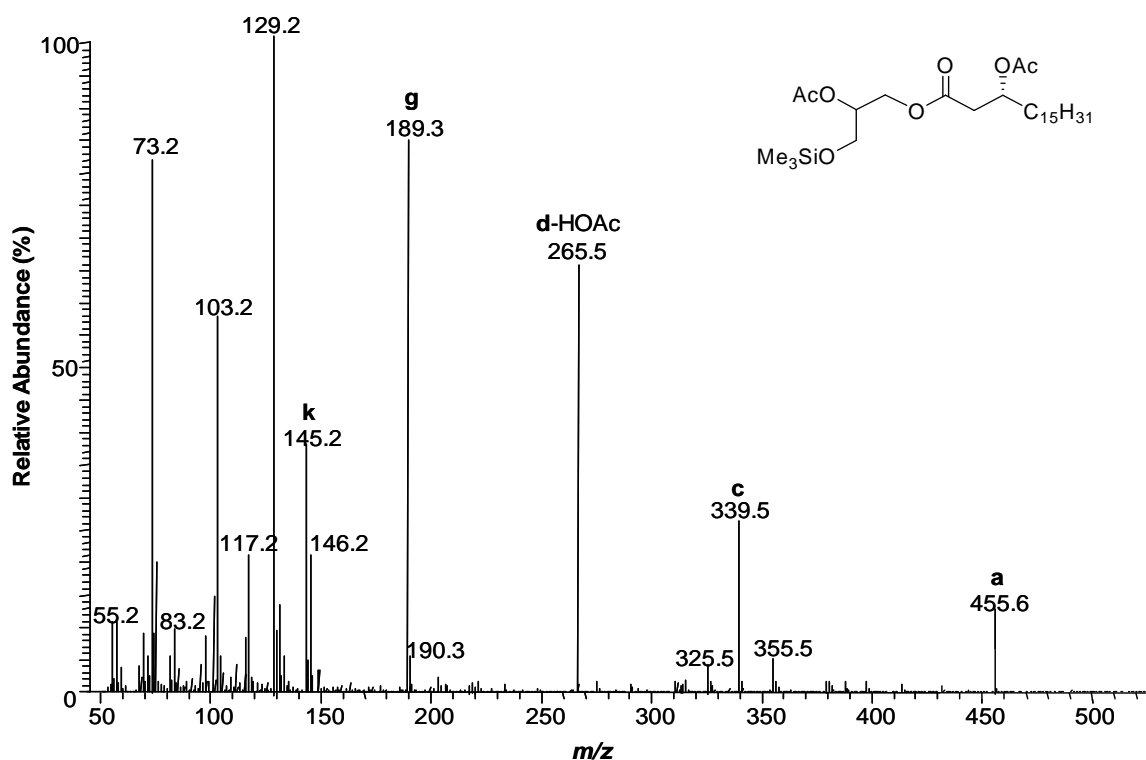
Figure 5.6. 70 eV-EI mass spectrum of TMS derivative of 1-[(3*R*)-acetoxystearoyl]-2-acetylglycerol (**41**, see corresponding ions in Scheme 2.1 and 2.2; Chapter 2).

Table 5.1. Identified compounds of *L. punctata* oil, cell lining and the labial gland of *M. fulvipes* as well as of *L. punctata* oil treated with *M. fulvipes* labial gland secretions investigated by GC/EI-MS analysis (as TMS derivatives).

| No. | Compound[a] | t_R (min) | Relative composition (%) | | | |
			L. punctata oil	*M. fulvipes* cell lining	*M. fulvipes* labial gland	*L. punctata* oil treated with *M. fulvipes* labial gland secretions
15	(3*R*)-hydroxypalmitic acid	17.90[b]	-	3.0	-	-
16	(3*R*)-hydroxyoleic acid	20.43[b]	-	15.1	-	-
17	(3*R*)-hydroxystearic acid	20.73[b]	-	51.0	-	-
19	(3*R*)-hydroxyeicosanoic acid	23.55[b]	-	1.6	-	-
34	2-[(3*R*)-acetoxyoleoyl]glycerol	27.78[c]	5.8	-	-	1.8
35	2-[(3*R*)-acetoxystearoyl]glycerol	28.02[c]	5.0	-	-	5.9
36	1-[(3*R*)-acetoxyoleoyl]glycerol	28.23[c]	12.0	-	-	5.7
37	1-[(3*R*)-acetoxystearoyl]glycerol	28.46[c]	10.9	-	-	1.7
40	1-[(3*R*)-acetoxyoleoyl]-2-acetylglycerol	28.79[c]	20.4	-	-	5.6
41	1-[(3*R*)-acetoxystearoyl]-2-acetylglycerol	29.02[c]	12.3	-	-	5.9
42	1-[(3*R*)-acetoxyoleoyl]-3-acetylglycerol	29.18[c]	3.0	-	-	-
43	1-[(3*R*)-acetoxystearoyl]-3-acetylglycerol	29.29[c]	2.0	-	-	-

Table 5.1. (continued).

No.	Compound	t_R (min)	Relative composition (%)			
			L. punctata oil	*M. fulvipes* cell lining	*M. fulvipes* labial gland	*L. punctata* oil treated with *M. fulvipes* labial gland secretions
71	1-palmitoylglycerol	23.29[c]	3.6	1.7	52.2	4.0
79	1-stearoylglycerol	26.04[c]	2.0	1.3	47.8	2.4
80	1-acetyl-2-linoleoylglycerol	27.07[c]	6.4	-	-	10.1
81	1-acetyl-2-oleoylglycerol	27.29[c]	8.6	-	-	8.9
82	1-acetyl-2-stearoylglycerol	27.56[c]	8.0	-	-	12.7
93	1-[(3R)-hydroxyoleoyl]glycerol	27.45[b]	-	15.0	-	17.8
94	1-[(3R)-hydroxystearoyl]glycerol	27.68[b]	-	10.3	-	-
95	1-[(3R)-hydroxyoleoyl]-2-acetylglycerol	27.85[d]	-	-	-	5.9
96	1-[(3R)-hydroxystearoyl]-2-acetylglycerol	28.06[d]	-	-	-	8.3
97	1-[(3R)-hydroxyoleoyl]-3-acetylglycerol	28.16[d]	-	-	-	1.8
98	1-[(3R)-hydroxystearoyl]-3-acetylglycerol	28.39[d]	-	-	-	1.5

[a]see Appendix 2 for key ions of EI-mass spectral data (Table A 2.4, A 2.5, A 2.6, A 2.11 and A 2.14), [b]obtained from *M. fulvipes* cell lining, [c]obtained from *L. punctata* oil, [d]obtained from *L. punctata* oil treated with *M. fulvipes* labial gland secretions, (-) = not detected, conditions **GC1**

M. fulvipes cell lining consists of hydroxy fatty acids along with common MAGs of long chain fatty acids (**71**, **72**) and hydroxylated monoacylglycerols (**93**, **94**) as new compounds. Evidence for the presence of hydroxy fatty acid moieties in compounds **93** and **94** is also deduced from GC/EI-MS data obtained from samples prepared by alkaline degradation of the *M. fulvipes* cell lining which showed dominant peaks for hydroxy fatty acids (Table 5.2).

Table 5.2. Identified fatty acids after alkaline degradation of *M. fulvipes* nest cell lining[a].

No.	t_R (min)	Compound	Relative composition (%)
3	15.54	palmitic acid	8.9
4	17.94	oleic acid	2.6
5	18.32	stearic acid	4.2
10	17.89	(3*R*)-hydroxypalmitic acid	3.4
11	20.43	(3*R*)-hydroxyoleic acid	18.8
12	20.73	(3*R*)-hydroxystearic acid	60.2
13	20.61	(3*R*)-hydroxyeicosanoic acid	1.8

[a]see Appendix 2 for key ions of EI-mass spectral data (Table A 2.1 and A 2.3), condition **GC1**.

Figure 5.7 illustrates the EI mass spectrum of TMS derivative of 1-[(3*R*)-hydroxystearoyl]glycerol (**94**). The [M−Me]$^+$ ion represents the *m/z* value of highest mass. Significant evidence of the 1-MAGs of (3*R*)-hydroxy fatty acid is obtained from the formation of an ion at *m/z* 379 (**j**) as an unique peak, including the **f**-type ion at *m/z* 205. Most of the 1-MAGs show the key ion of type **b** ([M−103]$^+$) corresponding to the loss of $CH_2OSi(CH_3)_3$ (Johnson and Holman 1966; Curstedt 1974; Myher *et al*., 1974; Wood 1980). While the **d**-type ion at *m/z* 355 represents the acylium ion and the ion at *m/z* 313 (type **q**) originates by an α-cleavage. The fragment ion at *m/z* 143 (type **n**) indicated the presence of a hydroxyl group at C-3 of fatty acid chain (Scheme 5.1).
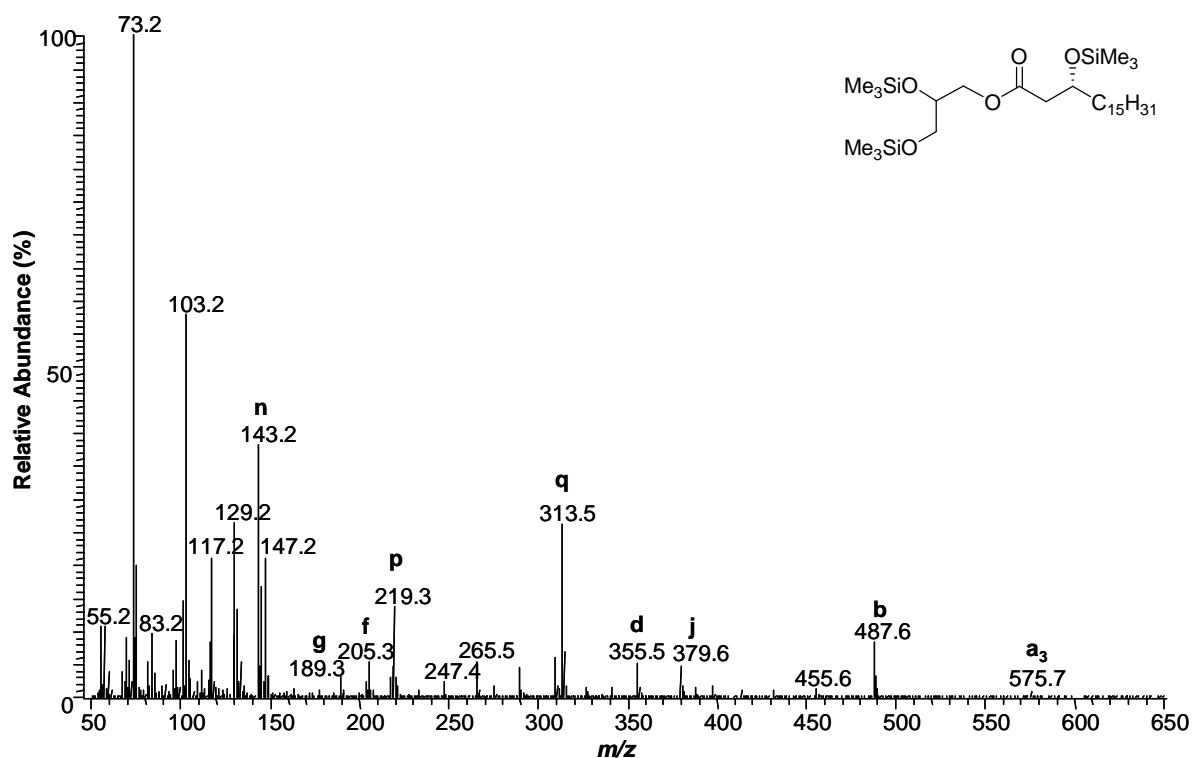
Figure 5.7. 70 eV-EI mass spectra of the TMS derivative of 1-[(3*R*)-hydroxystearoyl]glycerol (**94**, see Scheme 5.1, Appendix 2 in Table A 2.14).
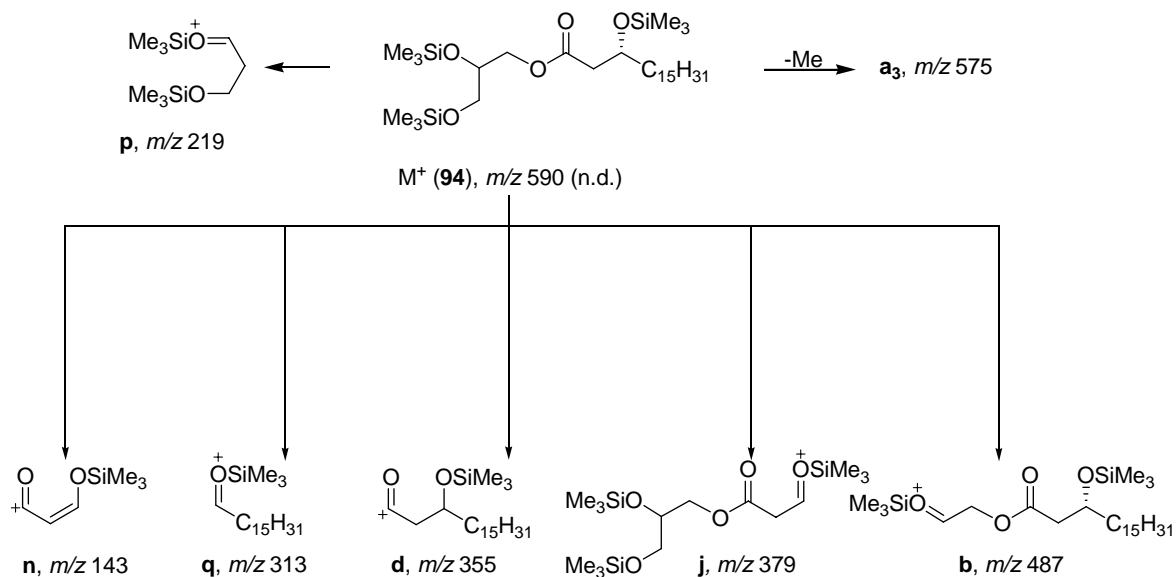
Scheme 5.1. Mass spectral fragmentations of 1-[(3*R*)-hydroxystearoyl]glycerol (**94**) as TMS derivative (n.d. = not detected).

Interestingly, none of the acetylated acylglycerols, the main compounds of *L. punctata* oil were detected in the *M. fulvipes* cell lining, although it has been suggested that *M. fulvipes* bees harvest *L. punctata* oil for their solid nest cell lining. We assumed that bees probably mix the oil with their saliva, and that most likely the labial gland is involved. Therefore, a novel *in vitro* test was designed in that *L. punctata* oil was treated with labial gland secretions. The results show novel compounds of DAGs, possessing (3*R*)-hydroxy fatty acid and acetyl moiety (**95–98**) in addition to traces of the compounds detected in *L. punctata* oil, whereas only acylglycerols of fatty acid were detected in labial gland extracts (control) themselves. Mass spectra of TMS derivatives of the typical compounds 1-[(3*R*)-hydroxystearoyl]-2-acetylglycerol (**96**) and 1-[(3*R*)-hydroxystearoyl]-3-acetylglycerol (**98**) are illustrated in Figure 5.8.
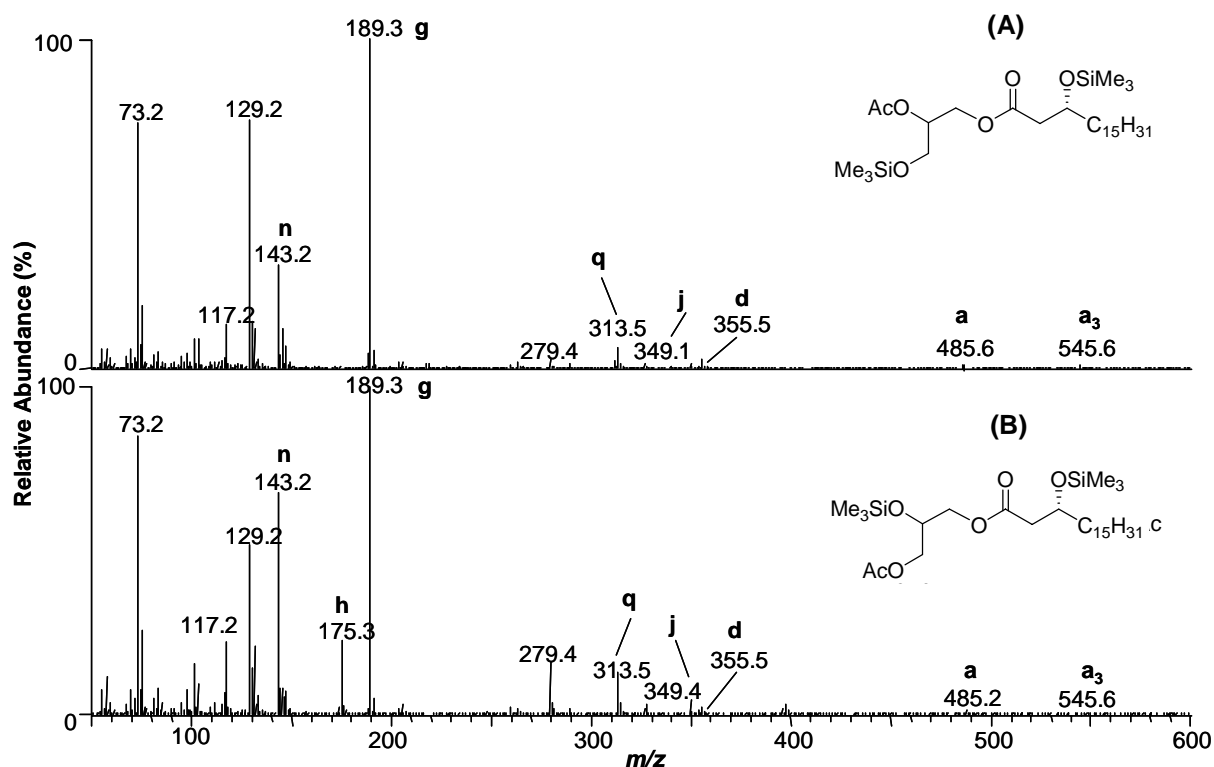
Figure 5.8. Mass spectra of TMS derivatives of (A) 1-[(3*R*)-hydroxystearoyl]-2-acetylglycerol (**96**) and (B) 1-[(3*R*)-hydroxystearoyl]-3-acetylglycerol (**98**, see Schemes 5.1 and 5.2).

M$^+$ (**96**), *m/z* 560 (n.d.)
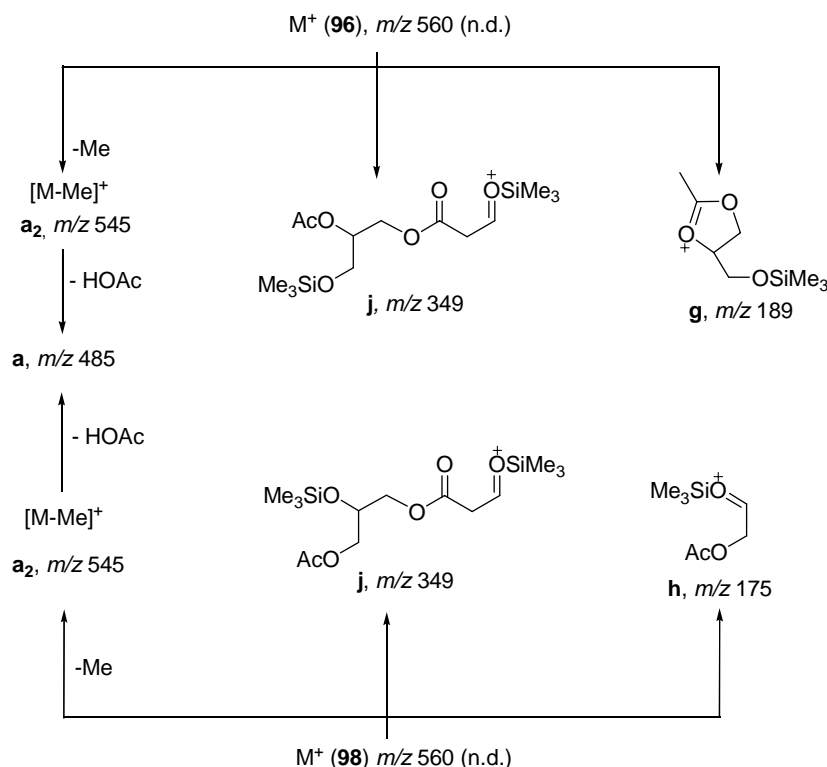
Scheme 5.2. Mass spectral fragmentation of 1-[(3*R*)-hydroxystearoyl]-2-acetylglycerol (**96**) and (B) 1-[(3*R*)-hydroxystearoyl]-3-acetylglycerol (**98**) (n.d. = not detected).

The EI mass spectra of these compounds show an ion at *m/z* [M–Me]$^+$ (**a$_3$**) as a peak of highest mass. An ion at *m/z* 189 (**g**) appearing both in 1,2- and 1,3-DAGs can be explained as a cyclic structure (Curstedt 1974) as shown in Scheme 5.2 and no hint of analogous fragment at *m/z* 188 (type **e**, see Scheme 2.2). Therefore, it could be a hint that the (3*R*)-hydroxy fatty acid is attached to the first hydroxyl group of the glycerol backbone. It should be pointed out that the ions at *m/z* 175 (type **h**) only appears in the mass spectra of 1,3-diacylglycerols (**98**, Scheme 5.2, Seipold 2004). Mass spectral data of these compounds (**93−98**) are presented in Appendix 2 (Table A 2.14). According to GC/EI-MS results, none of the 1,2-DAGs possessing of (3*R*)-acetoxy fatty acid and acetyl moiety of *L. punctata* oil are detected in *M. fulvipes* cell lining but after treating the *L. punctata* oil with labial gland secretions, we could detect the 1,2-DAGs of (3*R*)-hydroxy fatty acid as a long chain and acetyl moiety. We assume that the fatty acid moiety has been deacetylated. Only hydroxylated acylglycerols could be observed in the cell lining. We conclude that the bees relied on the floral liquid oil compounds of *L. punctata* to build their solid nest cell linings using the labial secretions.

5.4 ESI-FTICR-MS analysis

The lipid profiling of underivatized of *L. punctata* oil, cell linings and labial glands of *M. fulvipes* as well as of *L. punctata* oil treated with labial gland secretions of *M. fulvipes* is analyzed using the positive ion ESI-FTICR-MS technique (Table 5.3). The acetylated diacylglycerol ions at *m/z* 479.29818 ([$C_{25}H_{44}O_7Na$]$^+$: **40**, **42**) and at *m/z* 481.31412 ([$C_{25}H_{46}O_7Na$]$^+$: **41**, **43**) are mainly detected from *L. punctata* oil (Figure 5.9A). These results are also confirmed the GC/EI-MS data. However, the ESI-FTICR-MS results of *M. fulvipes* cell lining in particular demonstrate three novel compounds appearing as sodium adduct ions at *m/z* 675.51768 (**99**, [$C_{39}H_{72}O_7Na$]$^+$), 677.53228 (**100**, [$C_{39}H_{74}O_7Na$]$^+$) and 679.54709 (**101**, [$C_{39}H_{76}O_7Na$]$^+$) (Figure 5.9B). The oily lipid compounds of *L. punctata* are not detected in the cell lining. In fact, field studies have shown that *M. fulvipes* bees harvest oil from *L. punctata* for their cell lining architecture. These results provide additional evidence that bees could convert oil compounds in the course of the nest cell lining construction. Based on the elemental compositions of these compounds and LC-ESI-MS/MS investigations (Figure 5.10), the cell lining structures can be assumed to be either a di-[hydroxyfatty acid]-monoacylglycerol form or a diacylglycerol of two hydroxy fatty acids on oligomeric esters thereof.

The positive ESI-CID mass spectra of significant compounds of *M. fulvipes* cell lining show molecular ions [M+H]$^+$ at *m/z* 653 (**99**), 655 (**100**) and 657 (**101**). The loss of long-chain unsaturated and saturated hydroxy fatty acid moieties corresponds to ion at *m/z* 397 and 399, respectively. Also, both of these ions are observed in compound **100** (Figure 5.10B). These results relate to the presence of double bonds in each structure. Further, the appearance of hydroxy fatty acid moieties is obtained after the alkaline degradation of *M. fulvipes* cell lining from GC/EI-MS data (Table 5.2). To confirm the linking of the hydroxy fatty acids on the glycerol backbone, we derivatized the bee nest extract with 3-(dansylamino)phenylboronic acid (DABA) reagent that is used for the derivatization of 1,2-diols (Gamoh *et al.*, 1990). In that case, the positive ion ESI-FTICR mass spectrum displays compounds at *m/z* 989.64408 ([$C_{57}H_{89}O_9N_2SB$]$^+$, [**100**daba+H]$^+$) and *m/z* 991.66238 ([$C_{57}H_{91}O_9N_2SB$]$^+$, [**101**daba+H]$^+$. These compounds are evidence for the 1,2-bridging between the boron atom of DABA and two free oxygen atoms of glycerol backbone. Therefore, the formation of a link between the hydroxy fatty acids in the cell lining acylglycerol as di-[hydroxyfatty acid]-

monoacylglycerol is supported by high-resolution MS data (Figure 5.11-5.12). The DABA derivative of compound **99** could not be observed in the positive ion ESI-FTICR mass spectrum (Figure 5.11). Despite the ESI-FTICR and LC-ESI-MS(MS) results, we were unable fully to determine the structure(s) of di-[hydroxyfatty acid]-monoacylglycerol (**100**). Its structure apparently consists of two chains of both saturated and unsaturated hydroxy fatty acids (C_{18}-chain). However, the order in which the two fatty acids are attached to each other and the primary hydroxyl of the glycerol backbone is not detectable. Some putative structures (**100**) are shown in Figure 5.13.

After treating the labial gland secretions with *L. punctata* oil, we observed the formation of the cell lining compounds (**99–101**). Interestingly, we could detect some novel compounds displaying a higher degree of acetylation as indicated by a corresponding mass shift of 42 and 84 mass units, respectively (Figure 5.9C). These compounds, which appear neither in the oil nor in the cell lining, represent possible intermediates. Their elemental compositions were determined by ESI-FTICR mass spectrometry via the corresponding sodium adduct ions $[M+Na]^+$ (Table 5.3). These compounds were found at *m/z* 717.52865 (**102**, $[C_{41}H_{74}O_8Na]^+$), 719.54325 (**103**, $[C_{41}H_{76}O_8Na]^+$) and 721.55876 (**104**, $[C_{41}H_{78}O_8Na]^+$) as well as at *m/z* 759.53700 (**105**, $[C_{43}H_{76}O_9Na]^+$), *m/z* 761.55359 (**106**, $[C_{43}H_{78}O_9Na]^+$) and *m/z* 763.56817 (**107**, $[C_{43}H_{80}O_9Na]^+$) (Figure 5.9C and Table 5.3). It is noteworthy, that these intermediate compounds appear particularly during the *in vitro* tests of *L. punctata* oil treated with *M. fulvipes* labial gland secretions. These results provided the chemical evidence that *M. fulvipes* female bees can convert the acetylated acylglycerols of the harvested oil into hydroxylated acylglycerols using their special secretions.
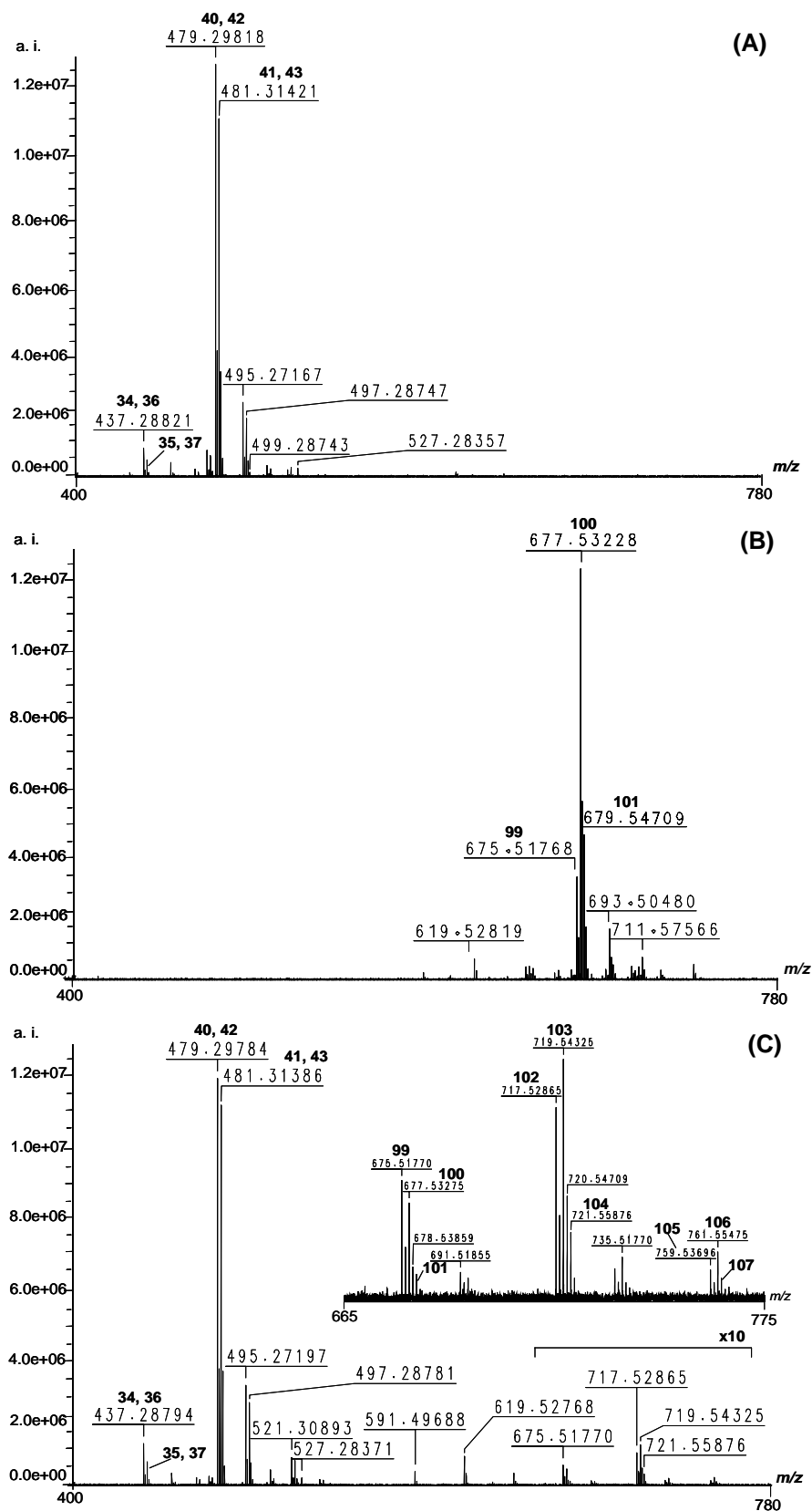
Figure 5.9. Positive ion ESI-FTICR-MS of (A) *L. punctata* oil, (B) *M. fulvipes* cell lining and (C) *in vitro* assay of *L. punctata* oil treated with *M. fulvipes* labial gland secretions (see Table 5.3).
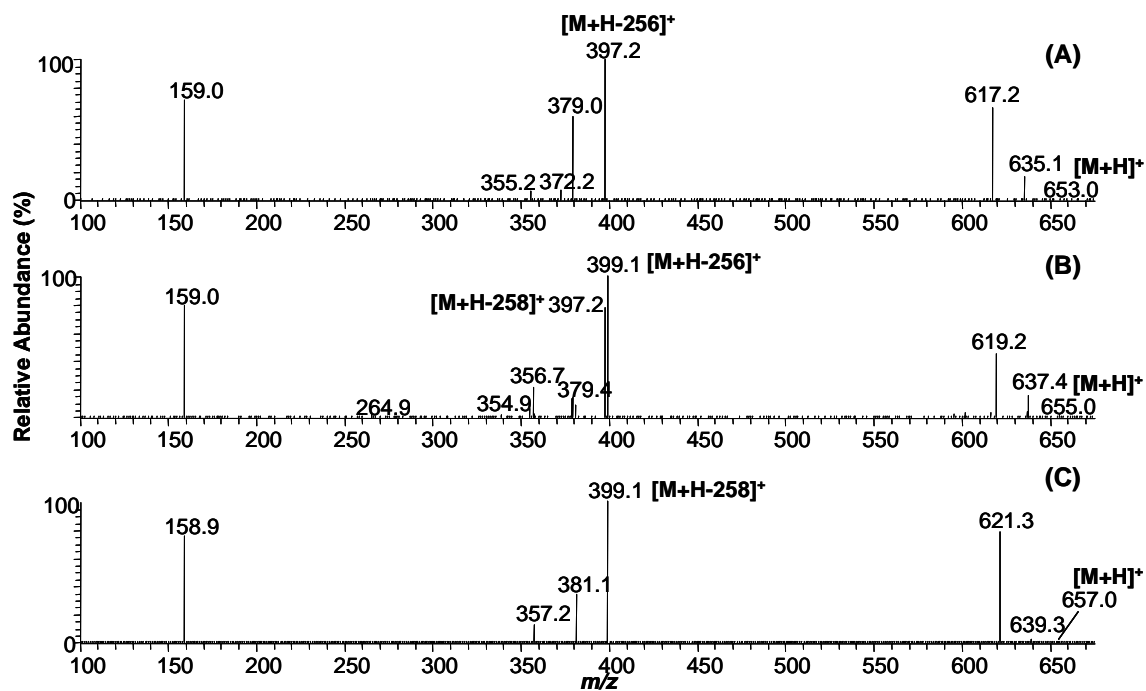
Figure 5.10. 20 eV positive ion ESI-CID mass spectra of the significant *M. fulvipes* cell lining compounds (A) **99**, (B) **100** and (C) **101**.
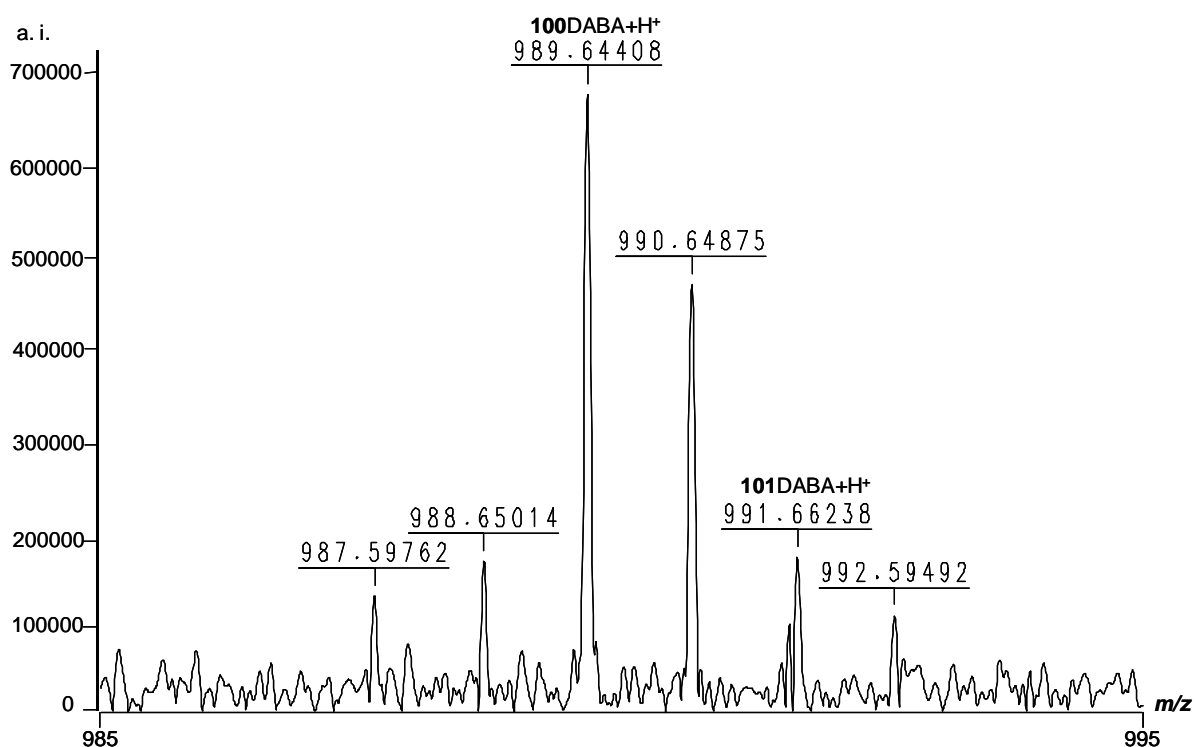
Figure 5.11. Positive ion ESI-FTICR mass spectra of 3-(dansylamino)phenylboronic acid (DABA) derivatives of *M. fuvipes* cell lining (see also Figure 5.12).
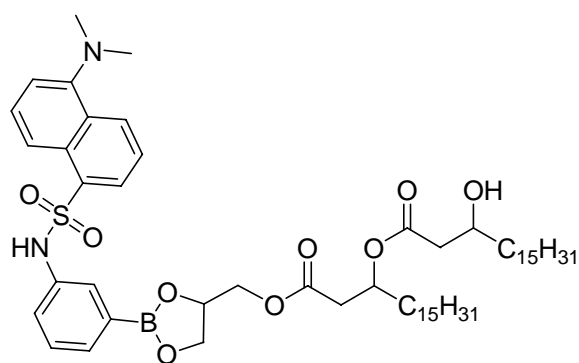
Figure 5.12. DABA derivative of di-[hydroxystearoyl]-monoacylglycerol (**101,** M.W.= 990).
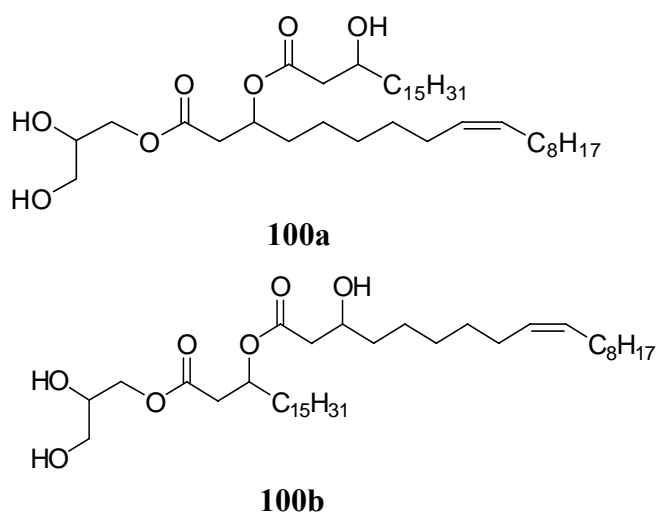
Figure 5.13. Putative structures of intermediate dimer compound (**100**) of *M. fulvipes* cell lining compounds.

The putative pathway of acylglycerol dimerization in the cell lining can be explained by sequential deacetylation processes along with the linking of an acetoxy fatty acid (Figure 5.14). The introduction of a hydroxyl group into their intermediates can probably produce dendrimeric polymers (Bonaventure *et al.,* 2004). This may render nest cell lining material insoluble in various organic solvents. The introduction of a hydroxyl group into cell lining compounds might be necessary to protect the larva and cell linings free from microbial decomposition. However, the nature of the labial gland secretions is still unclear, further biological features of *M. fulvipes* labial gland components (and other salivary glands) need to be elucidated.
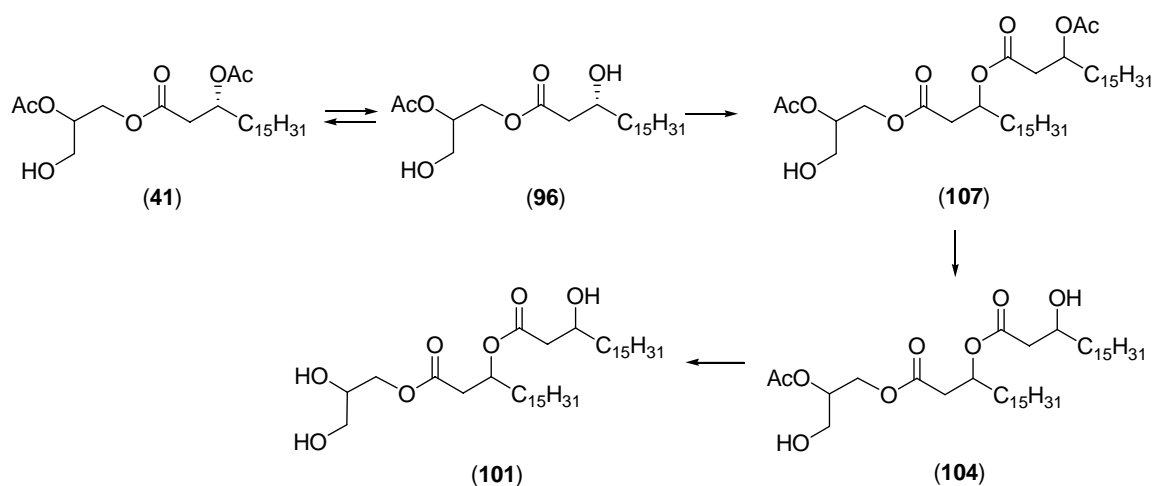
Figure 5.14. Main putative pathway for the transformation of floral acylglycerols to (acyloxy)$_n$-acylglycerols in bees' nest cell lining (as shown by an example of the saturated hydroxy fatty acid, **101**). 1-[(3*R*)-hydroxystearoyl]-2-acetylglycerol (**96**) is detected by GC/EI-MS measurement (identified as TMS derivative) of *L. punctata* oil treated with *M. fulvipes* labial gland secretions.

Table 5.3. Positive ion ESI-FTICR mass spectral data of *L. punctata* oil, cell lining and labial gland of *M. fulvipes* as well as of *L. punctata* oil treated with *M. fulvipes* labial gland secretions.

No.	Elemental composition	*m/z* ([M+Na]$^+$)	MW	Error (ppm)	*L. punctata* oil	*M. fulvipes* cell lining	*M. fulvipes* labial gland	*L. punctata* oil treated with *M. fulvipes* labial gland secretions
34, 36	$C_{23}H_{42}O_6\,Na^+$	437.28821	414	-0.4[a]	+	-	-	+
35, 37	$C_{23}H_{44}O_6\,Na^+$	439.30264	416	-0.8[a]	+	-	-	+
40, 42	$C_{25}H_{44}O_7\,Na^+$	479.29818	456	+0.5[a]	+	-	-	+
41, 43	$C_{25}H_{46}O_7\,Na^+$	481.31421	458	+1.0[a]	+	-	-	+
99	$C_{39}H_{72}O_7\,Na^+$	675.51768	652	+1.0[b]	-	+	-	+
100	$C_{39}H_{74}O_7\,Na^+$	677.53228	654	-0.6[b]	-	+	-	+
101	$C_{39}H_{76}O_7\,Na^+$	679.54709	656	-1.8[b]	-	+	-	+
102	$C_{41}H_{74}O_8\,Na^+$	717.52865	694	+0.8[c]	-	-	-	+
103	$C_{41}H_{76}O_8\,Na^+$	719.54325	696	+1.0[c]	-	-	-	+
104	$C_{41}H_{78}O_8\,Na^+$	721.55876	698	-0.5[c]	-	-	-	+
105	$C_{43}H_{76}O_9\,Na^+$	759.53700	736	+1.4[c]	-	-	-	+
106	$C_{43}H_{78}O_9\,Na^+$	761.55359	738	-0.6[c]	-	-	-	+
107	$C_{43}H_{80}O_9\,Na^+$	763.56817	740	-0.8[c]	-	-	-	+

[a]obtained from *L. punctata* oil, [b]obtained from *M. fulvipes* cell lining, [c]obtained from *L. punctata* oil treated with *M. fulvipes* labial gland secretions, MW = molecular weight, (+) = detected, (-) = not detect.

CHAPTER 6

Materials and Methods

6.1. Chemicals

All chemicals and reagents used in this study were analytical grade.

6.2. Oil-secreting flowers

Different specimens of oil-secreting flowers were cultivated in various locations. They were selectively collected during the blooming stage (Table 6.1).

6.3. Cell lining of *Macropis fulvipes* (Melittidae)

The nest cell linings of *Macropis fulvipes* were collected from a flight cage in the Botanical Garden of University Bayreuth (Germany) from June to July 2006.

6.4. Gathering of floral oils

Fresh flowers were cut and floral oils collected from the elaiophores in the laboratory. Tiny pieces of filter paper were used to carefully adsorb the oil from trichome elaiophores. The amount of non-volatile oil per flower varied from 0.5–2 μL. The floral oils of Malpighiaceae were collected using micro-capillary tubes by disturbing the cuticle of epithelial elaiophores located at the calyx glands. The secretion accumulates directly under the cuticle and forming small blisters. The average volume collected from one flower was 5–10 μL. All samples were transferred into 450 μL mixture of *t*-butylmethylether (MTBE)/methanol (2:1; v/v) and stored under N_2 at -18 °C (Seipold 2004; Seipold *et al*., 2004; Neff and Simpson 2005).

6.5. Calyx glands of *Heteropterys chrysophylla* (Malpighiaceae) collection

The calyx glands of different stages of *H. chrysophylla* were cut by microtome, and rapidly washed to minimize contamination from cell lipids and pigments. The entire glands were stored in a mixture of MTBE/methanol (2:1; v/v) and sealed under N_2 atmosphere (Seipold *et al*., 2004).

Table 6.1. List of oil-secreting flowers.

Location	Family	Species
Greenhouse of Botanical garden Munich	Orchidaceae	*Zygostates lunata*
		Cyrtochilum serratum
		Sigmatostalix putumayensis
		Oncidium cheirophorum
		Oncidium ornithorhynchum
	Iridaceae	*Cypella herbertii*
	Malpighiaceae	*Malpighia urens*
		Bunchosia argentea
		Stigmaphyllon ellipticum
		Byrsonima coriacea
		Janusia guaranitica
	Scrophulariaceae	*Angelonia integerrima*
	Cucurbitaceae	*Thladiantha dubia*
		Momordica anigosantha
		Momordica foetida
	Myrsinaceae	*Lysimachia vulgaris*
Flight cage in the Botanical garden of University Bayreuth	Myrsinaceae	*Lysimachia punctata*
Area surrounding of Drakensberg in Southern Africa (Wietsieshoek and Sani Pass)	Scrophulariaceae	*Diascia purpurea*
		Diascia vigilis
		Diascia cordata
		Diascia megathura
		Diascia integerrima
	Orchidaceae	*Pterygodium magnum*
		Pterygodium hastata
		Corycium dracomontanum
Greenhouse of Leibniz Institute of Plant Biochemistry Halle (Saale)	Malpighiaceae	*Heteropterys chrysophylla*

6.6. *Macropis fulvipes* (Melittidae) cell lining extraction

The cell linings are insoluble in both aqueous and organic solvents. Washing with water and removal of soil contaminants were carried out in a sonicator. 5 mg of cell lining materials was extracted three times with 5 mL of methanol and evaporated under vacuum.

6.7. *Fatty acid methyl ester* (FAME) profiling

The reaction was carried out according to a previously described procedure by Seipold *et al.* (2004). The floral oils underwent trans-esterification, followed by trimethylsilylation. Floral oils (50 µL) in the mixture of MTBE/methanol (2:1; v/v) were dried under N_2 stream, followed by addition of 700 µL of each MTBE and methanol. Borontrifluoride-methanol (BF_3-MeOH, 350 µL) was added and heated at 70 °C for 4 h. The mixture was allowed to come to room temperature and extracted twice with 1 µL of *iso*-octane. The organic phase was collected, washed twice with distilled water and dried over anhydrous Na_2SO_4. The solvent was dried under N_2 stream and dissolved in 200 µL of CH_2Cl_2. Trans-esterified oils were then converted to the trimethylsilyl (TMS) derivatives by using 100 µL of 2,2,2-trifluoro-*N*-methyl-*N*-(trimethylsilyl) acetamide (MSTFA) as silylating reagent.

6.8. Trimethylsilyl (TMS) derivatization

25 µL of crude oils, 50 µL of trans-esterified oils and 25 µL cell lining extract were TMS derivatized by treating each of them with 100 µL of MSTFA. The reaction was completed after 2 h at 100 °C in the heat box and dried under N_2 stream. The TMS derivatives were used for GC/EI-MS analysis as described below (Morrison and Smith 1964; Seipold 2004).

In case of *H. chrysophylla* ontogeny studies (see Chapter 4), 100 mg/ml of pentadecanoic acid was used as internal standard. Pentedecanoic acid (10 µL) was added during the TMS derivative preparation of calyx gland excretion in different developmental stages. The samples were analyzed by GC/EI-MS.

6.9. Acetylation reaction

6.9.1. Acetylation of floral oil samples

Trans-esterified oil samples (50 µL) were dissolved in 50 µL of acetic anhydride in pyridine (5:1; v/v), and kept at room temperature overnight. The reagent was then removed under a stream of N_2. The acetylated oil samples were analyzed by GC/EI-MS (Christie 1989).

6.9.2 [^{2}H]-acetylation of oil samples

The reaction was carried out by similar procedure as mentioned above, by using deuterated pyridine ([D_5]-pyridine) and deuterated acetic acid anhydride ([D_6]-acetic acid anhydride) (Christie 1989).

6.10. Dimethyldisulfide addition

Trans-esterified samples (50 µL) were dissolved in 200 µL of dimethyldisulfide followed by the addition of 1 mL of iodine in diethyl ether (0.6%; w/v). The mixture was stirred for 24 h and sodiumthiosulphate was added until the iodine color disappeared. The product was dried under N_2 stream and dissolved in CH_2Cl_2 for GC/EI-MS analysis (Christie 1989; Seipold 2004).

6.11. Alkaline degradation of cell lining

1.0 mg of cell lining was hydrolysed with 10% KOH in methanol in a microwave oven (Microwave Emrys Optimizer). The reaction was stirred at 80 °C for 60 min, followed by for N_2 venting for 15 min. The hydrolysate of the cell lining was extracted twice with a mixture of *iso*-octane/*n*-hexane (1:2; v/v) (Bonaduce and Colombini 2004). The extract was dried under vacuum and dissolved in CH_2Cl_2. TMS derivative of the samples was prepared for GC/EI-MS analysis.

6.12 DABA derivatization

0.1-1 mg of cell lining extract, obtained as described above, was treated with 300 µl of 0.1% 3-(dansylamino)phenylboronic acid (DABA) (HPLC grade, Fluka, ≥ 98%) (v/v) pyridine in acetonitrile (10 mg of DABA in 1 ml of 0.1% v/v pyridine in acetonitrile). Reaction was heated at 70 °C for 10 min. After cooling, the product was dried under N_2

atmosphere and re-dissolved in acetonitrile for ESI-FTICR-MS analysis (Gamoh *et al.* 1990).

6.13. Synthesis of (3*R*)-hydroxypalmitic acid methyl ester (Scheme 6.1)

In a 50 ml two neck-flask, equipped with a drop funnel with pressure balance and reflux cooler, 1.44 g (10 mmol) calcium chloride were added to 1.38 g Meldrum's acid (17.4 mmol) in 12 ml CH_2Cl_2 and 1.4 ml pyridine at 0 °C, followed by 2.9 ml myristic acid chloride (10.7 mmol) dropwise. The solution was stirred for 1 h at 0 °C and further 4 h at room temperature. The orange solution was washed twice with 2 N HCl and then with 5% aqueous $NaHCO_3$ soln. The upper layer was separated and the solvent evaporated under vacuum. The orange residue was dissolved in 25 ml MeOH and refluxed for 3 h. The crude 3-ketopalmitic acid methyl ester was purified by silica gel chromatography (hexane/EtOAc (6:1, v/v)) to give an overall yield of 61% (1.61 g) (Valcavi *et al.*, 1989; Oikawa *et al.*, 1978; Seipold 2004). ^{1}H NMR (300 MHz, $CDCl_3$): δ 0. 88 (3H, *t*, *J* = 6.8 Hz), 1.23-1.30 (22H, *m*), 1.61 (2H, *m*), 2.53 (2H, *t*, *J* = 7.31 Hz), 3.45 (2H, *s*); 3.74 (3H, *s*) (Seipold 2004).

500 mg of 3-ketopalmitic acid methyl ester (1.76 mmol) in 15 ml of MeOH/CH_2Cl_2 (96:4 v/v) were degassed by triple freezing and thawing under vacuum. Under protector gas (Ar), 10 mg of dichloro[(*R*)(+)2,2'bis(diphenylphosphino)1,1'binaphthyl]-ruthenium(II) [$RuCl_2(C_{44}H_{32}P_2)$]$_x$, (794.67 g/mol, 0.013 mmol, Strem Chemicals, USA) was added. The reduction was carried out in a pressure reactor under a hydrogen atmosphere of 34.5 bar (500 psi) for 24 h at 80 ºC (Heiser *et al.,* 1991). The solvent was evaporated under vacuum. The residue was dissolved in a mixture of benzene/EtOAc (4:1, v/v) and filtered through 2 g silica gel to eliminate the catalyst (Heiser *et al.*, 1991). (3*R*)-hydroxypalmitic acid methyl ester was obtained in a purity > 99% (GC). The optical specific rotation was −14.2° at 24 ºC (λ 589 nm) (Lit. −14.3°, Tulloch and Spencer 1964). The (2*S*)-phenylpropionate derivative of (3*R*)-hydroxypalmitic acid methyl ester was obtained in 93% ee (GC). (3*R*)-Hydroxypalmitic acid methyl ester was obtained in 97% overall yield (m.p. 82 °C, literature: 83−85 °C, Valcavi *et al.,* 1989). ^{1}H NMR (300 MHz, $CDCl_3$): δ 0.88 (3H, *t*, J = 6.9 Hz), 1.23-1.30 (22H, *m*), 1.44 (2H, *m*), 2.41 (1H, *dd*, J_1 = 16.5 Hz, J_2 = 8.8 Hz), 2.52 (1H, *dd*, J_1 = 16.5 Hz, J_2 = 3.3 Hz), 3.71 (3H, *s*), 4.0 (1H, *m*) (Seipold 2004). The purity (%) and ee (%) measurements were

obtained from GC 8000 series (Fisons Instruments) gas chromatograph with MS-detector (DB-5 MS, 20 m × 0.18 mm, i.d., 0.18 μm film thickness (J&W Scientific, Folsom, CA, USA). The column temperature was programmed for 1 min at 60 °C, step increased 15 °C/ min from 60 to 200 °C and 5 °C/ min to 300 °C and completed at 300 °C for 20 min. The column temperature was programmed at 1 min at 60 °C, 15 °C/ min increase from 60 to 200 °C, 5 °C/ min to 300 °C and additional 20 min at 300 °C. The mass spectrometers was operated with an electron impact (EI) 70 eV, ion source temperature 180 °C and mass range 40–800 amu. (3R)-Hydroxypalmitic acid methyl ester was obtained in 97% overall yield (m.p. 82 °C, literature: 83–85 °C, Valcavi et al., 1989). ^{1}H NMR (300 MHz, CDCl$_3$): δ 0.88 (3H, t, J = 6.9 Hz), 1.23-1.30 (22H, m), 1.44 (2H, m), 2.41 (1H, dd, J$_1$ = 16.5 Hz, J$_2$ = 8.8 Hz), 2.52 (1H, dd, J$_1$ = 16.5 Hz, J$_2$ = 3.3 Hz), 3.71 (3H, s), 4.0 (1H, m) (Seipold 2004).
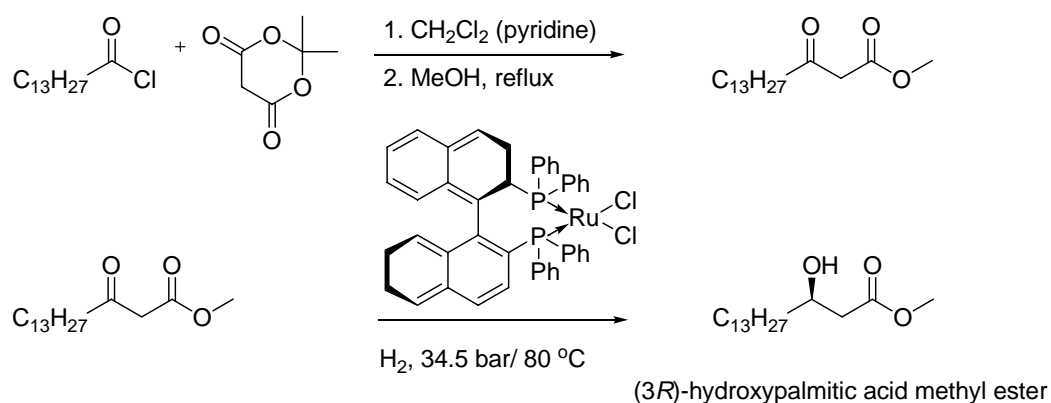
Scheme 6.1. Synthetic route to (3R)-hydroxypalmitic acid methyl ester.

6.14. Determination of the absolute configuration

The procedures were performed using GC/EI-MS techniques. A comparison of retention times between the (2S)-phenylpropionyl derivatives of floral oils and (3R)-hydroxypalmitic methyl ester as chiral standard was carried out (Hammarström 1975; Wollenweber et al., 1985; Gradowska and Larsson 1994). Racemic mixtures were obtained from the floral oils themselves by oxidation with potassium dichromate (K$_2$CrO$_4$) and subsequent reduction with sodium borohydride (NaBH$_4$) (Fabritius et al., 1996). 0.1 mg of oil sample was dissolved in 1 mL of diethylether. 100 μL of 30% (w/v) K$_2$CrO$_4$ was added and followed by 150 μL of conc. H$_2$SO$_4$. The reaction was

stirred for 2 h at room temperature and washed twice with distilled water. The organic phase was taken and dried under N_2 stream. The oxidized product was dissolved in 1 mL methanol and 50 mg of $NaBH_4$ was added at 5 °C. The reaction was stirred for 1 h, and then 1 drop of H_2SO_4 was added to it and washed 3 times with *iso*-octane. The organic phase was separated and dried over anhydrous Na_2SO_4. The racemic mixture was then derivatized by (2*S*)-phenylpropionyl chloride (Hammarström 1975; Seipold 2004).

6.15.   Synthesis of (2*S*)-phenylpropionyl chloride

Thionyl chloride (120 μL) was added at 0 °C to 90 mg (0.55 mmole) of (+)-(2*S*)-phenylpropionic acid. The reaction was stirred at 70 °C for 30 min. After completion of reaction, the solvent was evaporated under vacuum by repeated addition of dried benzene to remove traces of thionyl chloride. The residue was dissolved in 1 mL dry benzene and kept at 4 °C in a sealed flask (Hammarstroem 1975; Seipold 2004).

6.16.   (2*S*)-Phenylpropionyl derivatization

The (2*S*)-phenylpropionyl derivatives gave a complete separation of the *R*- and *S*-hydroalkanoates under the GC/EI-MS conditions (**GC1**) described below for derivatization. Sample (0.1 mg) was stirred with 90 μL of (2*S*)-phenylpropionyl chloride (see above) and 10 μL of pyridine. The reaction mixture was kept for 2 h at room temperature and dissolved in CH_2Cl_2 for GC/EI-MS analysis (Hammarström 1975).

6.17.   GC/EI-MS analysis

The GC-MS measurements were performed using a Finnigan Voyager GC/MS system mounted with a capillary column (DB-5 MS, 30 m × 0.25 mm i.d., 0.25 μm film thickness (J&W Scientific, Folsom, CA, USA). Helium was used as the GC carrier gas at a constant flow of 1 mL/min.

Conditions:

Ionization:	electron ionization (EI)
Electron voltage:	70 eV
Ion source temperature:	200 °C

GC interface temperature: 300 °C

Injection module: splitless

Injection volume: 1 µL

Mass range: 40−800

Temperature program:

GC1:

Temperature program: 60 (1 min)→ (10 °C/ min)→ 200 °C → (5 °C/min)→ 300 °C →
300 °C (20 min)

GC2:

Temperature program: 60 (1 min)→ (10 °C/ min)→ 200 C (5 °C/min)→ 300 °C →
300 °C (30 min) (remaining conditions by analogue to **GC1**)

GC3:

Temperature program: 60 (1 min)→ (15 °C/ min)→ 200 °C → (5 °C/min)→ 300 °C →
300 °C (20 min)

6.18. ESI-FTICR-MS analysis

10 µL of floral oil samples were taken from the stock solutions and dried under a N_2
stream. The sample was dissolved in 300 µL of methanol and centrifuged at 1200 rpm
for 5 min before analysis. The positive ion high resolution ESI mass spectra of oils of
all species were obtained on a Bruker Apex III Fourier transform ion cyclotron
resonance (FTICR) mass spectrometer (Bruker Daltonics, Billerica, USA) equipped
with an Infinity™ cell, a 7.0 Tesla superconducting magnet (Bruker, Karlsruhe,
Germany), an RF-only hexapole ion guide and an APOLLO electrospray ion source
(Agilent, off axis spray, voltages: endplate, −3.700V; capillary, −4.200V; capillary exit,
100 V; skimmer 1, 15.0 V; skimmer 2, 10.0 V). N_2 was used as drying gas at 150 °C.
The sample solutions were introduced continuously via a syringe pump with a flow rate
of 120 µLh^{-1}. All data were acquired with 512 k data points and zero filled to 2048 k by
averaging 32 scans.

6.19. LC/ESI-MS (MS) analysis

The positive ion ESI mass spectra of *M. fulvieps* cell lining compounds (**99**−**101**) were
obtained from a Finnigan MAT TSQ Quantum Ultra AM system equipped with a hot

ESI source (HESI, electrospray voltage 3.0 kV, sheath gas: nitrogen; vaporizer temperature: 50 °C; capillary temperature: 250 °C; The MS system is coupled with a Surveyor Plus micro-HPLC (Thermo Electron), equipped with a Ultrasep ES RP18E-column (5 μm, 1 × 100 mm, SepServ). For the HPLC a gradient system was used starting from H_2O/CH_3CN (80:20, v/v) (each of them containing 0.2% HOAc) to 100 CH_3CN within 15 min and then hold on 100% for further 45 min; flow rate 70 μLmin^{-1}. The collision-induced dissociation (CID) mass spectra of *M. fulvieps* cell lining compounds (**99–101**) were recorded during the HPLC run with a collision energy of −20 eV for the $[M+H]^+$-ions at *m/z* 653 (**99**), 655 (**100**) and 657 (**101)** (collision gas: argon; collision pressure: 1.5 mTorr).

99: RT_{HPLC} = 35.78 min, ESI-CID mass spectrum (*m/z*, rel int. (%)): 653 ($[M+H]^+$, 635 (20), 617 (60), 397 (100), 379 (65), 159 (78)

100: RT_{HPLC} = 49 min, ESI-CID mass spectrum (*m/z*, rel int. (%)): 655 ($[M+H]^+$, 637 (18), 619 (40), 399 (100), 397 (80), 379 (20), 381 (10), 159 (80)

101: RT_{HPLC} = 32.54 min, ESI-CID mass spectrum (*m/z*, rel int. (%)): 657 ($[M+H]^+$, 639 (2), 621 (80), 399 (100), 381 (40), 159 (80)

6.20. Microscopy of the calyx glands of *H. chrysophylla*

6.20.1. Transmission electron microscopy (TEM)

The calyx glands of *H. chrysophylla* were prefixed with 2.5% (v/v) glutaraldehyde/phosphate buffer pH 7.4 for 2 h and post-fixed in 1% (w/v) of osmium tetraoxide (OsO$_4$) in Palade buffer (14.7 g of Veronal-Na and 9.7 g of sodium acetate in 500 mL deionized water) for 1 h. Dehydration was performed in a series of increasing concentrations of acetone and embedded in ERL 4206 (vinyl cyclohexene dioxide) (Table 6.2). Ultra thin sections (50–70 nm) were cut with a diamond knife, stained with lead citrate and viewed using a transmission electron microscope (EM 912 OMEGA LEO Elektronenmikroskopie, Oberkochen Deutschland).

Table 6.2. Procedure of TEM sample preparation.

Process	Chemical	Temperature (°C)	Time
Primary fixation	2.5% (v/v) glutaraldehyde in phosphate buffer pH 7.4		2 h
Wash	phosphate-buffer		15 min
			30 min
			60 min
			60 min
Secondary fixation	1% OsO_4 (w/v) in Palade-buffer		60 min
Wash	distilled water		20 min
			20 min
			20 min
			20 min
Dehydration[a]	20% acetone/ 2% uranylacetate (1:1; v/v)	25 °C	30 min
	30% acetone		10 min
	50% acetone		10 min
	75% acetone		10 min
	90% acetone		10 min
	acetone		20 min
	acetone		20 min
	acetone/ERL (1:1)		20 min
	acetone/ERL (1:2)		20 min
	ERL 4206		60min
	ERL 4206		12 h

[a]prepared in distilled water solution

6.20.2. Light microscopy

The embedded samples of *H. chrysophylla* calyx glands (from 6.19.1) were cut as semi-thin sections (1−2 μm). The sections were stained with Azur II/methylene blue (1% azur II in aqua distilled /1% methylene blue in 1% aqueous borax = 1:1) for light micrographs.

6.21. Physiological structure analysis of *Macropis fulvipes* cell lining

Stereomicroscopy was used to investigate the overview of nest cell lining as a whole. For scanning electron microscopy (SEM), cell lining of *M. fulvipes* was prefixed with 2.5% (v/v) glutaraldehyde/phosphate buffer pH 7.4 (2 h), fixed with 1% (w/v) OsO_4/ Palade buffer (1 h) and dehydrated in series of ethanol washes (Table 6.3). Specimens were dried using the procedure of critical point drying. After dehydration by serial ethanol washes, the samples were transferred into the chamber of a semi-automatic critical point drying apparatus. The dehydrates were displaced with transitional fluid (liquid carbon dioxide). After mounting onto the specimen stubs, they were coated with thin layer of a conductive material by sputtering. SEM studies were done with a JSM-6340F scanning electron microscopy (JEOL Company, Japan).

Table 6.3. Procedure for SEM samples preparation.

Process	Chemical	Temperature (°C)	Time (min)
Primary fixation	2.5% (v/v) glutaraldehyde in phosphate buffer		120
Wash	phosphate-buffer p.H 7.4		15
			30
			60
			60
Secondary fixation	1% (w/v) OsO_4/Palade-buffer	4 °C	60
Wash	distilled water		20
			20
			20
			20
Dehydration[a]	30% ethanol		10
	50% ethanol		10
	70% ethanol	4 °C	10
	90% ethanol		10
	absolute ethanol		20
	absolute ethanol		20
Critical point drying			
Mounting on specimen stubs			
Coating with conductive material by sputtering			

[a]prepared in distilled water solution

References

Abdalla, F. C. & Cruz-Landim, C. (2001) Dufour glands in the hymenopterans (apidae, formicidae, vespidae): a review. *Rev. Brasil. Biol.*, **61**, 95−106.

Albans, K. R., Aplin, R. T., Brehcist, A. J., Moore, J. F. & Otoole, C. (1980) Dufour's gland and its role in secretion of nest cell lining in bees of the genus *Colletes* (Hymenoptera: Colletidae). *J. Chem. Ecol.*, **6**, 549−564.

Alves-dos-santos, I., Melo, G. A. R. & Rozen, J. G. (2002) Biology and immature stages of the bee tribe *Tetrapediini* (Hymenoptera: Apidae). *Am. Mus. Novit.* **3377**, 1−45.

Anderson, W.R. (1979) Floral conservation in Neotropical Malpighiaceae. *Biotropica*, **11**, 219−233.

Attala, N. C. & Machado, S. R. (2003) Anatomy and ultrastructure of *Banisteriopsis variabilis* gates (Malpighiaceae) calyx glands. *Acta Microsc.*, **12**, 635−636.

Batra, S. W. & Norden, B. B. (1996) Fatty food for their brood: how *Anthophora* bees make and provision their cells (Hymenoptera: Apoidea). *Mem. Entomol. Soc. Wash.*, **17**, 36−44.

Bonaventure, G., Beisson, F., Ohlrogge, J. & Pollard, M. (2004) Analysis of the aliphatic monomer composition of polyesters associated with *Arabidopsis* epidermis: occurrence of octadeca-cis-6, cis-9-diene-1,18-dioate as the major component. *Plant J.*, **40**, 920−930.

Browse, J. & Somerville, C. R. (1991) Glycerolipid metabolism, biochemistry and regulation. *Annu. Rev. Plant Physiol. Plant Mol. Biol.*, **42**, 467−506.

Buchmann, S. L. (1987) The ecology of oil flowers and their bees. *Ann. Rev. Ecol. Syst.*, **18**, 343−369.

Byrdwell, W.C & Neff, W. E. (1996) Analysis of genetically modified canola varieties by atmospheric pressure chemical ionization mass spectrometric and flame ionization detection. *J. Liquid Chromatogr. & Related Technol.*, **19**(14), 2203−2225.

Byrdwell, W. C., Emken, E. A., Neff, W. E. & Adlof, R. O. (1996) Quantitative analysis of triglycerides using atmospheric pressure chemical ionization-mass spectrometry. *Lipids*, **31**(9), 919−935.

Byrdwell,W. (2001) Atmospheric pressure chemical ionization mass spectrometry for analysis of lipids. *Lipids*, **36**, 327−346.

Cane, J. H. (1983) Preliminary chemosystematics of the andrenidae and exocrine lipid evolution of the short-tougued bees (Hymenoptera: Apoidea). *Syst. Zool.*, **32**, 417−430.

Cane, J. H., Eickwort, G. C., Wesley, F. B. & Spielholz, J. (1983) Foraging, grooming and mate-seeking behaviors of *Macropis nuda* (Hymenoptera, Melittidae) and use of *Lysimachia ciliata* (Myrsinaceae) oils in larval provisions and cell linings. *Am. Midl. Nat.*, **110**, 257−264.

Castro, M. A., Vega, A. S. & Mulgura, M. E. (2001) Structure and ultrastructure of leaf and calyx glands in *Galphimia brasiliensis* (Malpighiaceae). *Am. J. Bot.*, **88**, 1935−1944.

Celary, W. (2004) A comparative study on the biology of *Macropis fulvipes* (Fabricius, 1804) and *Macropis europaea* (Warncke, 1973) (Hymenoptera: Apoidea. Melittidae). *Folia biologica*, **52**, 81−85.

Christie, W. W. Gas chromatography and lipid; A practice guide, Oily press Ltd., Dundee

Christie, W. W. The lipid Library. availabiel online at www.lipidlibrary.co.uk. 2006.

Comisarow, M. B. & Marshall, A. G. (1974) Fourier transform ion cyclotron resonance spectroscopy. *Chem. Phys. Lett.* **15**, 282−283.

Curstedt, T. (1974) Mass spectra of trimethylsilyl ethers of ^{2}H-labelled mono- and diacylglycerides. *Biochim. Biophys. Acta,* **360**, 12−23.

Dötterl, S. & Schäffler, I. (2007) Flower scent of floral oil-producing *Lysimachia punctata* as attractant for the oil-bee *Macropis fulvipes*. *J. Chem. Ecol.*, **33**, 441−445.

Espelie, K. E., Cane, J. H. & Himmelsbach, D. S. (1992) Nest cell lining of the solitary bee *Hylaeus bisinuatus* (Hymenoptera: Colletidae). *Experientia*, **48**, 414−416.

Fabritius, D., Schäfer, H. J. & Steinbüchel, A. (1996) Identification and production of 3-hydroxy-9-cis-1,18-octadecenedioic acid by mutants of *Candida tropicalis. Appl. Microbiol. Biotech.*, **45**, 342−348.

Fard, A. M., Turner, A. G. & Willett, G. D. (2003) High-resolution electrospray-ionization fourier-transform ion cyclotron resonance and gas chromatography-mass spectrometry of macadamia nut oil. *Aust. J. Chem.*, 56, 499−508.

Feng, X. & Siegel, M. M. (2007) FTICR-MS applications for the structure determination of natural products. *Anal. Bioanal. Chem.*, **389**(5), 1341−1363.

Fenn, J. B., Mann, M., Mend, C. K., Wong, S. F. & Whitehouse, C. M. (1990) Electrospray ionization-principles and practice. *Mass Spectrom. Rev.*, 9, 37−70.

Gamoh, K., Okamoto,N., Takatsuto, S. & Tejima, I. (1990) Determination of traces of natural brassinosteroids as dansylaminophenylboronates by liquid chromatography with fluorimetric detection. *Anal. Chim. Acta*, **228**, 101−105.

Gradowska,W. & Larsson, L. (1994) Determination of absolute configurations of 2- and 3-hydroxy fatty acids in organic dust by gas-chromatography-mass spectrometry. *J. Microbiol. Methods*, **20**, 55−67.

Halket, J. M. & Zaikin, V. G. (2003) Derivatization in mass spectrometry- 1. Silylation. *J. Mass Spectrom.* **9**, 1−21.

Ham, B. M., Jacob, J. T., Keese, M. M. & Cole, R. B. (2004) Identification, quantification and comparison of major non-polar lipids in normal and dry eye tear lipidomes by electrospray tandem mass spectrometry. *J. Mass Spectrom.*, **39**, 1321−1336.

Han, X. & Gross, R. W. (2005) Shotgun lipidomics: Electrospray ionization mass spectrometric analysis and quantitation of cellular lipidomes directly from crude extracts of biological samples. *Mass Spec. Rev.*, **24**, 367−412.

Hammarstroem, S. (1975) Microdetermination of stereoisomers of 2-Hydroxy and 3-Hydroxy Fatty Acids. *Methods Enzymol.*, **35**, 326−334.

Harwood, J. L. (1988) Fatty acid metabolism. *Annu. Rev. Plant Physiol. Plant Mol. Biol.* **39**, 101−183.

Hefetz, A., Fales, H. M. & Batra, S. W. T. (1979) Natural polyesters: Dufour's gland macrocyclic lactones form brood cell lamiesters in Colletes bees. *Science*, **204**, 415−417

Heiser, B., Broger, E. A. & Crameri, Y. (1991) New efficient methods for the synthesis and *in situ* preparation of ruthenium(II) complexes of atropisomeric diphosphines and their application in asymmetric catalytic hydrogenations. *Tetra. Asym.*, **2**, 51−62.

Hendrickson, C. L. & Emmett, M. R. (1999) Electrospray ionization Fourier transform ion cyclotron resonance mass spectrometry. *Annu. Rev. Phys. Chem.,* **50**, 517−536.

Hills, M. J., Dann, R., Lydiate, D. & Sharpe, A. (1994) Molecular cloning of a cDNA from *Brassica napus* L. for a homologue of acyl-CoA-binding protein. *Plant Mol. Biol.*, **25**, 917−920.

Ishida, M., Yamazaki, T., Houjou, T., Imagawa, M., Harada, A., Inoue, K. & Taguchi, R. (2004) High-resolution analysis by nano-electrospray ionization Fourier transform ion cyclotron resonance mass spectrometry for the identification of molecular species of phospholipids and their oxidized metabolites. *Rapid Commun. Mass Spectrom.*, **18**, 2486−2494.

Jaworski, J. G., Clough, R. C. & Barnum, S. R. (1989) A cerulenin insensitive short chain 3-ketoacyl-acyl carrier protein synthase in *Spinacia oleracea* leaves. *Plant Physiol.*, **90**, 41−44.

Johnson, C. B. & Holman, R. T. (1966) Mass spectrometry of lipids. II monoglycerides, their diacetyl derivatives and their trimethylsilyl ethers. *Lipids*, **1**, 371−380.

Kalo, P., Kemppinen, A., Ollilainen, V., Kuksis, A. (2003) Analysis regioisomers of short-chain triacylglycerols by normal phase liquid chromatography-electrospray tandem mass spectrometry. *Inter. J. Mass. Spec.*, 229, 167−180.

Kuksis, A. & Myher, J. J. (1995) Application of tandem mass spectrometry for the analysis of long-chain carboxylic acids. *J. Chromatogr. B*, **671**, 35−70.

Laakso, P. (2002) Mass spectrometry of triacylglycerols. *Eur. J. Lipid Sci. Technol.,* **104**, 43−49.

Lyubachevskaya, G. & Boyle-Roden, E. (2000) Kinetics of 2-monoacylglycerol acyl migration in model *Chylomicra. Lipids*, **35**, 1353−1358.

Machado, I. C., Vogel, S. & Lopes, A. V. (2002) Pollination of *Angelonia cornigera* Hook. (Scrophulariaceae) by long-legged, oil-collecting bees in NE Brazil. *Plant Biol.*, **4**, 352−359.

Marshall, A.G., Hendrickson, C. L. & Jackson, G. S. (1998) Fourier transform ion cyclotron resonance mass spectrometry: a primer. *Mass Spectrom. Rev.,* **17**, 1–35.

Mayberry,W. R. (1980) Hydroxy fatty acids in Bacteroides Species: D-(-)-3-hydroxy-15-methylhexadecanoate and its homologs. *J. Bacteriol.,* **143**, 582–587.

McMaster, M.C. (2005) LC/MS a practical user's guide. John Wiley & Sonc. Inc., New Jersey.

Michener, C. (1964) Evolution of the nests of bees. *Am. Zoologist,* **4**, 227–239.

Michez, D. & Patiny, S. (2005) World revision of the oil-collecting bee genus *Macropis* Panzer 1809 (Hymenoptera: Apidea: Melittidae) with a description of a new species from Laos. *Ann. Soc. Entomol. Fr.,* **41,** 15–28.

Mielniczuk, Z., Alugupalli, S., Mielniczuk, E. & Larson, L. (1992) Gas chromatography-mass spectrometry of lipopolysaccharide 3-hydroxy fatty acids: comparison of pentafluorobenzoyl and trimethylsilyl methyl ester derivatives. *J. Chrom.,* **623**, 115-122.

Mielniczuk, Z., Mielniczuk, E. & Larsson, L. (1993) Gas chromatography-mass spectrometry methods for analysis of 2- and 3-hydroxylated fatty acids: application for endotoxin measurement. *J. Microbiol. Methods,* **17**, 91–102.

Morrison, W. R. & Smith, L. M. (1964) Preparation of fatty acid methyl esters and dimethylacetals from lipids with boron fluoride-methanol. *J. lipid Res.,* **5**, 600–608.

Myher, J. J., Marai, L. & Kuksis, A. (1974) Identification of monoacyl- and monoalkylglycerols by gas-liquid chromatography-mass spectrometry using polar siloxane liquid phases. *J. Lipid Res.,* **15**, 586–592.

Neff, J. L. & Simpson, B. B. (2005) Other rewards: oils, resins, and gums. *Practical Pollination Biology* (Dafni, A., Keven, P. G. and Husband, B. C.), Enviroquest Ltd, Cambridge, 314–328.

Norden, B., Batra, S. W. T., Fales, H. M., Hefetz, A. & Shaw, G. J. (1989) Anthora bees: unusal glyderides from Maternal dufour's glands serves as larval food and cell lining. *Science,* **207**, 1095–1097.

Ohlrogge, J. & Browse, J. (1995) Lipid biosynthesis. *The Plant Cell,* **7**, 957–970.

Ohlrogge J. B., Joworski J. G. & D. Post-Beittenmiller (1993) *De Novo* fatty acid biosynthesis. In lipid metabolism in plants. Edited by T. S. Moore: CRC Press, 3−32.

Pulfer, M. & Murphy, R. C. (2003) Electrospray mass spectrometry of phospholipids. *Mass Spectrom Rev*. **22**, 332−364.

Raith, K., Brenner, C., Farwanah, H., Müller, G., Eder, K. & Neubert, R. H. H. (2005) A new LC/APCI-MS method for the determination of cholesterol oxidation products in food. *J. Chrom.* **1067**, 207−221.

Raman, S. (1989) The trichomes on the corolla of the Scrophulariaceae - II: Tribes Hemimeridae and Calceolarieae. *Beiträge zur Biologie der Pflanzen*, **64**, 141−155.

Rawsthorne, S. (2002) Carbon flux and fatty acid synthesis in plants. *Prog. Lipid Res.*, **41,** 182−196.

Reis, M. G., Faria, A. D., Bittrich, V., Amaral, M. C. E. & Marsaioli, A. J. (2000) The chemistry of flower rewards - *Oncidium* (Orchidaceae). *J. Braz. Chem. Soc.*, **11**, 600−608.

Reis, M. G., Faria, A. D., Bittrich, V., Amaral, M. C. E. & Marsaioli, A. J. (2003) Oncidinol - a novel diacylglycerol from *Ornithophora radicans* Barb. Rodr. (Orchidaceae) floral oil. *Tetrahedron Lett.* **44**, 8519−8523.

Reis, M. G., Faria, A. D., dos Santos, I. A., Amaral, M. C. E., Marsaioli, A. J. (2007) Byrsonic acid−the clue to floral mimicry involving oil-producing flowers and oil-collecting bees. *J. Chem. Ecol.*, **33**, 1421−1429.

Roberts, R. B. & Vallespir, S. R. (1978) Specialization of hairs bearing pollen and oil on the legs of bees (Apoidea: Hymenoptera). *Annals. Ent. Soc. Am.* **71**, 619−627.

Sazima, M. & Sazima, I. (1989) Oil-gathering bees visit flowers of glandular morphs of the oil-producing Malpighiaceae. *Bot. Acta*, **102**, 106−111.

Schiller, J., Zschörnig, O., Petkovi, M., Müller, M., Arnhold, J. & Arnold, K. (2001) Lipid analysis of human HDL and LDL by MALDI-TOF mass spectrometry and ^{31}P-NMR. *J. lipid Res.*, **42**, 1501−1508.

Schiller, J., Süß, R., Arnhold, J., Fuchs, B., Leßig, J., Müller, M., Petkovic, M. Spalteholz, H., Zschörnig, O. & Arnold, K. (2004) Matrix-assisted laser desorption and ionization time-of-flight (MALDI-TOF) mass spectrometry. *Prog. Lipid Res.*, **43**, 449−488.

Schönitzer, K. & Seifert, P. (1990) Anatomy and ultrastucture of the salivary gland in the thorax of the honey worker, *Apis mellifera* (Insecta, Hymenoptera). *Zoomorphology*, **109**, 222.

Seipold, L. (2004) Blütenöle – Chemische Analyse, Biosynthese und Betrachtungen zur Entstehung von Ölblumen. Martin-Luther-Universität Halle-Wittenberg.

Seipold, L., Gerlach, G. & Wessjohann, L. (2004) A new type of floral oil from *Malpighia coccigera* (Malpighiaceae) and chemical considerations on the evolution of oil flowers. *Chem. Biodiv.,* **1**, 1519–1528.

Seigler, D. (1978) Free 3-acetoxyfatty acids in floral glands of *Krameria* species. *Phytochemistry*, **7**, 995–996.

Simpson, B. B., Neff, J. L. & Seigler, D. (1977) Krameria, free fatty acids and oil-collecting bees. *Nature*, **267**, 150–151.

Simpson, B. B. (1979) Lipid from the floral glands of *Krameria. Biochem. Syst. Ecol.*, **7**, 193–194.

Simpson, B. B. & Neff, J. L. (1981) Floral rewards: alternatives to pollen and nectar. *Ann. Mo. Bot. Gard.,* **68**, 301–322.

Simpson, B. B. & Neff, J. L. (1983) Evolution and diversity of floral rewards. New York: Scientific and Academic, 142–157.

Simpson, B. B., Neff, J. L., & Dieringer, G. (1990) The production of floral oils by Monttea (Scrophulariaceae) and the function of tarsal pads in *Centris* bees. *Plant Syst. Evol.,* **173**, 209–222.

Slabas, A. R. & Fawcett, T. (1992) The biochemistry and molecular biology of plant lipid biosynthesis. *Plant Mol. Biol.,* **19**, 169–191.

Steiner, K. E. (1985) Functional dioecism in the Malpighiaceae: the breeding system of *Spachea membranacea* Cuatr. *Am. J. Bot.*, **72**, 1537–1543.

Steiner, K. E. & Whitehead, V. B. (1988) The association between oil-producing flowers and oil-collecting bees in the Drakensberg of Sounthern Africa. *Monogr. Syst. Bot. Missouri Bot. Grad.*, **25**, 259–277.

Steiner, K. E. & Whitehead, V. B. (1990) Pollinator adaptation to oil-secreting flowers *Rediviva* and *Diascia. Evolution*, **44**, 1701–1707.

Steiner, K. E. & Whitehead, V. B. (1991) Oil flowers and oil bees: further evidence for pollinator adaptation. *Evolution*, **45**, 1493–1501.

Steiner, K. E. & Whitehead, V. B. (2002) Oil secretion and the pollination of *Colpias mollis* (Scrophulariaceae). *Pl. Syst. Evol.* **235**, 53−66

Taylor, D. W. & Crepet, W. L. (1987) Fossil floral evidence of Malpighiaceae and early plant-pollinator relationship. *Am .J. Bot.*, **74**, 274−286.

Tulloch, A.P., Spencer, J. F. T. (1964) Extracellular glycolipids of *Rhodotorula* species. *Can. J. Chem.,* **42**, 166−173.

Valcavi, U., Albertoni, C., Brandt, A., Corsi, G. B., Farima, P., Poresta, P. & Pascucci, M. T. (1989) New potential immunoenhancing compounds. Synthesis and pharmalogical evaluation of new long-chain 2-amido-2-deoxy-D-glucose derivatives. *Arzneim.-Forsch./ Drug Res.*, **39**, 1190−1195.

Vieira de Jesus, B. M. & Garófalo, B. M. V. (2000) Nesting behavior of *Centris* (Heterocentris) *analis* (Fabricius) in Southeastern Brazil (Hymenoptera, Apidae, Centridini). *Apidologie*, **31**, 503−515.

Vinson, S. B., Williams, H. J. & Frankie, G. W. (1989) Chemical contents of male mandibular glands of three *Centris* species (Hymenoptera: Anthophoridae) from Costa rica. *Comp. Biochem. Physiol.* **93B**, 73−75.

Vinson, S. B., Frankie, G. W. & William, H. J. (1996) Chemical ecology of bees of the genus *Centris* (Hymenoptera: Apidae). *Fla. Entomol.*, **79**, 109−129.

Vinson, S. B., Williams, H. J., Frankie, G.W. & Shrum, G. (1997) Floral lipid chemistry of *Byrsonima crassifolia* (Malpighiaceae) and a use of floral lipids by *Centris* bees (Hymenoptera: Apidae). *Biotropica*, **29**, 76−83.

Vinson, S. B., Frankie, G. W. & William, H. J. (2006) Nest liquid resources of several cavity nesting bees in the genus *Centris* and the identification of a preservative, levulinic acid. *J. Chem. Ecol.*, **32**, 2013−2021.

Vogel, S. (1969) Flowers offering fatty oil instead of nectar (Abstract No. 229). Seattle, WA, USA.

Vogel, S. (1971) Ölproduzierende Blumen, die durch ölsammelnde Bienen bestäubt werden. *Naturwissenschaften*, **58**. 58−69.

Vogel, S. (1974) Ölblumen und ölsammelnde Bienen. Akademie der Wissenchaften und der Litertur, Mainz.

Vogel, S. (1981) Abdominal oil-mopping- a new type of goraging in bees. *Naturwissenschaften*, **68**, 627−628.

Vogel, S. (1986) Ölblumen und ölsammelnde Bienen. Akademie der Wissenschaften und der Literatur, Mainz.

Vogel, S. (1990a) History of the Malpighiaceae in the light of pollination ecology. *Mem. New York Bot. Gard.,* **55**, 133−142.

Vogel, S. (1990b) Ölblumen und ölsammelnde Bienen. Akademie der Wissenschaften und der Literatur, Mainz

Vogel, S. & Machado, I. C. (1991) Pollination of four sympatric species of *Angelonia* (Scophulariaceae) by oil-collecting bees in NE Brazil. *Plant Syst. Evol.,* **178**, 153−178.

von Poser, G. L., Damtoft, S., Schripsema, J., Henriques, A. T. & Jensen, S.R. (1997) Iridoid glucosides from *Angelonia integerrima. Phytochemistry*, **46**, 371−373.

Wcislo, W. T. & Cane, J. H. (1996) Floral resource utilization by solitary bees (hymenoptera: Apoidea) and exploitation of their stored foods by natural enemies. *Annu. Rev. Entomol.*, **41**, 257−286.

Weil, K., Humpf, H.-U., Schwab, W. & Schreier, P. (2002) Absolute configuration of 3-hydroxy acids formed by *Stenotrophomonas maltophilia*: Application of multidimensional gas chromatography and circular dichroism spectroscopy. *Chirality*, **14**, 51−58.

Wollenweber, H. W., Schramek, S., Moll, H. & Rietschel, E. T. (1985) Nature and linkage type of fatty acids present in lipopolysaccharides of phase I and II *Coxiella burnetii. Arch. Microbiol.*, **142**, 6−11.

Wood: Edited by, G. W. (1980) Complex Lipids. In Biochemical Applications of Mass Spectrometry. John Wiley & Sons.

Wu, Z., Rodgers, R. P. & Marshall, A. G. (2004) Characterization of vegetable oils: detailed compositional fingerprints derived from electrospray ionization fourier transform ion cyclotron resonance mass spectrometry. *J. Agric. Food Chem.*, **52**, 5322−5328.

Zachowski, A., Guerbette, F., Grobois, M., Jolliot-Croquin & A., Kader, J.C. (1998) Characterisation of acyl binding by a plant lipid transfer protein. *Eur. J. Biochem.* **257**, 443−448.

APPENDIX 1

R/*S* absolute configuration

It is possible to determine the enantiomeric composition in limited amounts of samples by GC-MS analysis of diastereoisomeric derivatives in comparison to synthetic pure samples. Instead of diasteromers on achiarl columns, chiral chiral column can be used too. Both require the use of racemate to prove separation of the two isomers, and to determine which of the two methods is more suitable. The absolute configuration of 2- and 3-hydroxy fatty acid methyl esters was determined using the (*S*)-phenylpropionate derivatives (Hammarström, 1975; Gradowska, 1994; Seipold 2004).

In most cases, *fatty acid methyl ester* profiling (FAME) of oil flower samples allowed no detection of intact acylglycerols due to a complete trans-esterification reaction. Thus usually only fatty acids and oxygenated fatty acids could be detected. In general, mass spectra of 3-hydroxy fatty acid methyl esters and 3-acetoxy fatty acid methyl esters as TMS derivatives give analogous patterns. Therefore, (2*S*)-phenylpropionate derivatives of synthesized (3*R*)-hydroxypalmitic acid methyl ester was used as a chiral standard. Racemic mixtures (*R*/*S*) were obtained from the oils through oxidation with potassiumdichromate (K_2CrO_4) and backward reduction with sodiumborohydride ($NaBH_4$) (Fabritius *et a.l*, 1996). (2*S*)-Phenylpropionyl chloride was reacted with the samples using pyridine as base. The (2*S*)-phenylpropionyl derivatives gave complete separation of the *R*- and *S*-derivatives under GC-MS condition (Hammarström, 1975; Seipold 2004). Figure A 1.1 shows the TIC of racemic mixture of (2*S*)-phenylpropionyl derivatives of (3*R*)-hydroxy fatt acid methyl ester and (3*S*)-hydroxy fatt acid methyl ester (A) and (3*R*)-[(2*S*)-phenylpropanoyloxy]-fatty acid methyl ester (B). The results indicate that the hydroxyl group at C-3 has (*R*)-configuration. In most cases of floral oil investigations, (*R*)-configuration was identified. The fact that hydroxy acids usually are of the D-(-)-3-hydroxy family originates in their appearance of intermediates of fatty acid biosynthesis (Mayberry, 1980). Figure A 1.2 illustrates a mass spectrum of (3*R*)-[(2*S*)-phenylpropanoyloxy]-hexadecanoic acid methyl ester. The dominant peak at *m/z* 105 is the characteristic of phenylpropionyl derivative (Hammarström, 1975; Wollenweber *et al.*, 1985; Gradowska and Larsson 1994; Seipold 2004).
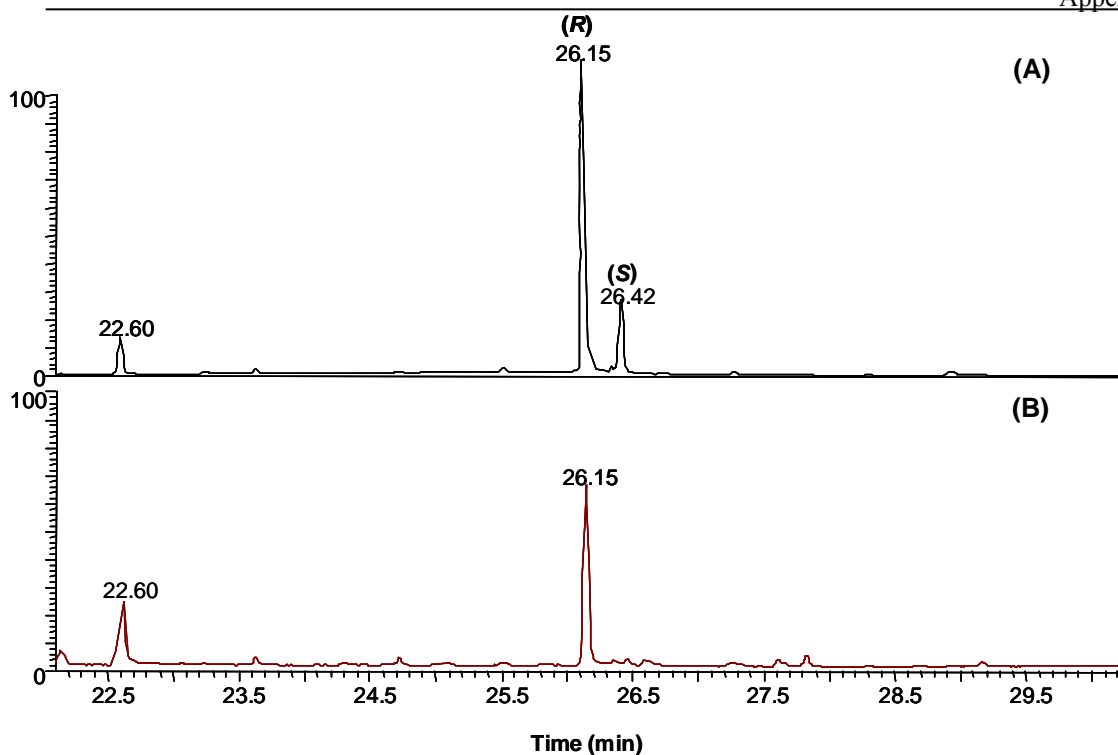
Figure A 1.1. (A) An example of TIC of racemic mixture of (2*S*)-phenylpropionyl derivatives of (3*R*)-hydroxy hexadecanoic acid methyl ester and (3*S*)-hydroxy hexadecanoic acid methyl ester and (B) (3*R*)-[(2*S*)- phenylpropanoyloxy]-hexadecanoic acid methyl ester.
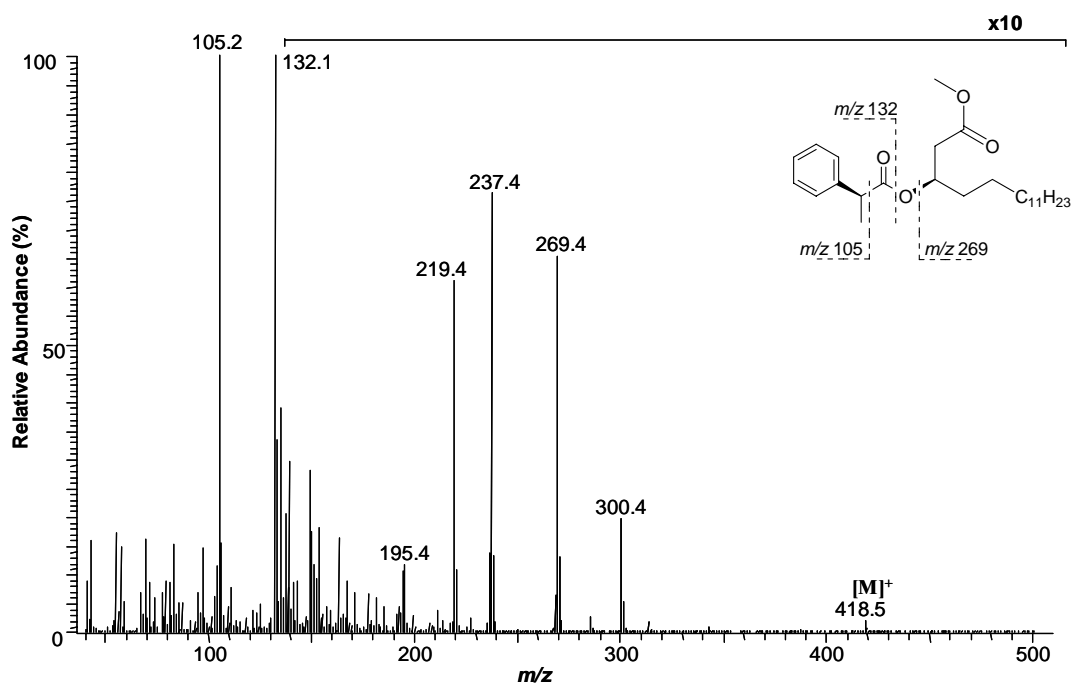
Figure A 1.2. (3*R*)-[(2*S*)- phenylpropanoyloxy]-hexadecanoic acid methyl ester (MW = 418).

APPENDIX 2

Mass spectral data

Tables of Molecular Ions, significant fragments and relative abundances (%) of compounds catagories.

Table A 2.1. Key ions in the EI-mass spectra of TMS derivatives of non-oxygenated free fatty acids (Finigan Voyager GC/MS system).

No.	Compound	Characteristic of EI-mass spectral data [m/z, (rel.int. %)]					
		$[M]^+$	$[M-Me]^+$	$[M-MeO]^+$	$[CH_2CHCHOSiMe_3]^+$	$[OCOSiMe_3]^+$	$[SiMe_3]^+$
1[a]	myristic acid	300 (2)	285 (2)	257 (2)	129 (45)	117 (100)	73 (88)
2[b]	palmitoleic acid	326 (1)	311 (40)	283 (1)	129 (45)	117 (90)	73 (100)
3[a]	palmitic acid	328 (2)	313 (45)	285 (2)	129 (41)	117 (100)	73 (88)
4[b]	oleic acid	354 (1)	339 (18)	311 (-)	129 (51)	117 (80)	73 (100)
5[a]	stearic acid	356 (5)	341 (41)	313 (7)	129 (38)	117 (100)	73 (80)
6[c]	cis-11-eicosenoic acid	382 (1)	367 (10)	339 (-)	129 (20)	117 (80)	73 (100)
7[d]	eicosanoic acid	384 (3)	369 (13)	341 (2)	129 (37)	117 (85)	73 (100)
8[c]	cis-13-docosenoic acid	410 (1)	395 (8)	367 (-)	129 (30)	117 (82)	73 (100)

The data were obtained from [a]*Pterygodium hastata* (Orchidaceae), [b]*Cypella herbertii* (Iridaceae), [c]*Oncidium cheirophorum* (Orchidaceae) and [d]*Macropis fulvipes* (Melittidae), conditions **GC1**.

Table A 2.2. Key ions in the EI-mass spectra of TMS derivatives of (3*R*)-hydroxy fatty acid methyl esters[a] (Finigan Voyager GC/MS system).

No.	Compound	Characteristic of EI-mass spectral data [*m/z*, (rel.int. %)]					
		$[M]^+$	$[M–Me]^+$	$[MeOCOCH_2COSiMe_3]^+$	$[OCOSiMe_3]^+$	$[OSiMe_3]^+$	$[SiMe_3]^+$
9	(3*R*)-hydroxymyristic acid	330 (-)	315 (80)	175 (90)	117 (60)	89 (95)	73 (100)
10	(3*R*)-hydroxypalmitic acid	358 (-)	343 (75)	175 (95)	117 (50)	89 (90)	73 (100)
12	(3*R*)-hydroxystearic acid	386 (-)	371 (72)	175 (94)	117 (68)	89 (92)	73 (100)

[a]The data were obtained from *Diascia vigilis* (Scrophulariaceae) (see corresponding ions in Scheme 3.1, Chapter 3), conditions **GC1**.

Table A 2.3. Key ions in the EI-mass spectra of TMS derivatives of (3*R*)-hydroxy fatty acid[a] (Finigan Voyager GC/MS system).

No.	Compound	Characteristic of EI-mass spectral data [*m/z*, (rel.int. %)]					
		$[M]^+$	$[M–Me]^+$	α_1	$[Me_2SiOSiMe_3]^+$	$[OCOSiMe_3]^+$	$[SiMe_3]^+$
10	(3*R*)-hydroxypalmitic acid	416 (-)	401 (2)	233 (50)	147 (62)	117 (9)	73 (100)
11	(3*R*)-hydroxyoleic acid	442 (-)	427 (1)	233 (10)	147 (42)	117 (8)	73 (100)
12	(3*R*)-hydroxystearic acid	444 (-)	429 (3)	233 (42)	147 (57)	117 (8)	73 (100)
13	(3*R*)-hydroxyeicosanoic acid	472 (-)	457 (4)	233 (48)	147 (58)	117 (10)	73 (100)

[a]The data were obtained from *Macropis fulvipes* (Melittidae) nest cell lining (see corresponding ions in Scheme 3.1, Chapter 3), condition **GC1**.

Table A 2.4. Key ions in the EI-mass spectra of TMS derivatives of (3*R*)-acetoxy fatty acid[a] (Finigan Voyager GC/MS system).

No.	Compound	Characteristic of EI-mass spectral data [*m/z*, (rel.int. %)]						
		$[M]^+$	$[M-Ac]^+$	$[M-HOAc]^+$	**A** $[M-Me-HOAc]^+$	161	$[OCOSiMe_3]^+$	$[SiMe_3]^+$
14	(3*R*)-acetoxymyristic acid	358 (-)	315 (16)	298 (15)	283 (70)	161 (55)	117 (92)	73 (100)
15	(3*R*)-acetoxypalmitic acid	386 (-)	343 (19)	326 (18)	311 (75)	161 (50)	117 (90)	73 (100)
16	(3*R*)-acetoxyoleic acid	412 (-)	369 (16)	352 (12)	337 (65)	161 (35)	117 (85)	73 (100)
17	(3*R*)-acetoxystearic acid	414 (-)	371 (20)	354 (15)	339 (75)	161 (55)	117 (88)	73 (100)
18	(3*R*)-acetoxyeicosenoic acid	440 (-)	397 (18)	380 (13)	365 (70)	161 (35)	117 (80)	73 (100)
19	(3*R*)-acetoxyeicosanoic acid	442 (-)	399 (20)	382 (16)	367 (72)	161 (52)	117 (95)	73 (100)

[a]The data were obtained from *Thladiantha dubia* (Cucurbitaceae) (excepted compound **14** from *Momordica foetida* (Cucurbitaceae) (see corresponding ions in Scheme 2.1, Chapter 2), condition **GC2**.

Table A 2.5. Key ions in the EI-mass spectra of TMS derivatives of monoacylglycerols (MAGs) possessing long chain (3R)-acetoxy fatty acid (Finigan Voyager GC/MS system).

No.	Compound	Characteristic of EI-mass spectral data [m/z, (rel.int. %)]											
		$[M]^+$	a	b	(b−HOAc)	c	d−HOAc	e	e−Me	f	147	129	73
20[a]	2-[(3R)-acetoxymyristoyl]glycerol	504	429	-	-	283	209	218	203	-	147	129	73
		(-)	(15)			(35)	(60)	(85)	(39)		(66)	(100)	(55)
21[a]	1-[(3R)-acetoxymyristoyl]glycerol	504	429	401	341	283	209	-	203	205	147	129	73
		(-)	(10)	(2)	(88)	(5)	(58)		(22)	(15)	(56)	(28)	(100)
27[a]	2-[(3R)-acetoxypalmitoyl]glycerol	532	457	-	-	311	237	218	203	-	147	129	73
		(-)	(5)			(15)	(36)	(60)	(24)		(55)	(100)	(84)
28[a]	1-[(3R)-acetoxypalmitoyl]glycerol	532	457	429	369	311	237	-	203	205	147	129	73
		(-)	(6)	(2)	(92)	(4)	(48)		(24)	(17)	(60)	(32)	(100)
34[b]	2-[(3R)-acetoxyoleoyl]glycerol	558	483	-	-	337	263	218	203	-	147	129	73
		(-)	(3)			(7)	(16)	(30)	(12)		(40)	(75)	(100)
35[a]	2-[(3R)-acetoxystearoyl]glycerol	560	485	-	-	339	265	218	203	-	147	129	73
		(-)	(4)			(13)	(28)	(60)	(23)		(54)	(100)	(85)
36[b]	1-[(3R)-acetoxyoleoyl]glycerol	558	483	455	395	337	263	-	203	205	147	129	73
		(-)	(8)	(1)	(40)	(7)	(16)		(14)	(11)	(51)	(59)	(100)
37[a]	1-[(3R)-acetoxystearoyl]glycerol	560	485	457	397	339	265	-	203	205	147	129	73
		(-)	(5)	(1)	(60)	(5)	(40)		(19)	(15)	(48)	(48)	(100)

Table A 2.5. (continued).

No.	Compound	[M]+	a	b	(b−HOAc)	c	d−HOAc	e	e−Me	f	147	129	73
		Characteristic of EI-mass spectral data [*m/z*, (rel.int. %)]											
45[c]	2-[(3*R*)-acetoxyeicosenoyl]glycerol	586	511	-	-	365	291	218	203	-	147	129	73
		(-),	(4)			(13)	(28)	(60)	(23)		(54)	(100)	(85)
46[d]	2-[(3*R*)-acetoxyeicosanoyl]glycerol	588	513	-	-	367	293	218	203	-	147	129	73
		(-)	(2)			(15)	(29)	(55)	(20)		(50)	(100)	(80)
47[d]	1-[(3*R*)-acetoxyeicosanoyl]glycerol	588	513	485	425	367	293	-	203	205	147	129	73
		(-)	(2)	(2)	(55)	(3)	(35)		(19)	(12)	(50)	(40)	(100)

The data were obtained from [a]*Diascia vigilis* (Scrophulariaceae), [b]*Lysimachia punctata* (Myrsinaceae), [c]*Oncidium ornithorhynchum* (Orchidaceae) and [d]*Sigmatostlaix putumayensis* (Orchidaceae) (see corresponding ions in the Scheme 2.1 and 2.2, Chapter 2). *m/z* 147 [Me$_2$SiOSiMe$_3$]$^+$, *m/z* 129 [CH$_2$CHCHOSiMe$_3$]$^+$, *m/z* 73 [SiMe$_3$]$^+$, condition **GC1**.

Table A 2.6. Key ions in the EI mass spectra of TMS derivatives of diacylglycerols (DAGs) possessing (3*R*)-acetoxyfatty acid and acetyl moiety (Finigan Voyager GC/MS system).

No.	Compound	$[M]^+$	a	b–HOAc	c	d–HOAc	e	e₁	e₁–CH₂CO	g	h	k	43
						Characteristic of EI-mass spectral data [*m/z*, (rel.int. %)]							
22[a]	2-[(3*R*)-acetoxymyristoyl]-1-acetylglycerol	474 (-)	399 (12)	-	283 (48)	209 (95)	188 (23)	-	146 (10)	189 (50)	-	145 (72)	43 (100)
23[a]	1-[(3*R*)-acetoxymyristoyl]-3-acetylglycerol	474 (-)	399 (14)	341 (7)	283 (5)	209 (44)	-	188 (3)	146 (12)	189 (30)	175 (100)	-	-
29[b]	2-[(3*R*)-acetoxypalmitoleoyl]-1-acetylglycerol	500 (-)	425 (6)	-	309 (35)	235 (75)	188 (22)	-	146 (9)	189 (60)	-	145 (70)	43 (100)
30[a]	2-[(3*R*)-acetoxypalmitoyl]-1-acetylglycerol	502 (-)	427 (10)	-	311 (43)	237 (83)	188 (26)	-	146 (9)	189 (66)	-	145 (74)	43 (100)
31[a]	1-[(3*R*)-acetoxypalmitoyl]-3-acetylglycerol	502 (-)	427 (12)	369 (22)	311 (5)	237 (33)	-	188 (2)	146 (11)	189 (40)	175 (100)	-	-
38[c]	2-[(3*R*)-acetoxyoleoyl]-1-acetylglycerol	528 (-)	453 (5)	337 (30)	-	263 (55)	188 (15)	-	146 (2)	189 (50)	-	145 (55)	43 (100)
39[a]	2-[(3*R*)-acetoxystearoyl]-1-acetylglycerol	530 (-)	455 (8)	339 (34)	-	265 (60)	188 (25)	-	146 (9)	189 (67)	-	145 (70)	43 (100)

Table A 2.6. (continued).

No.	Compound	Characteristic of EI-mass spectral data [*m/z*, (rel.int. %)]											
		$[M]^+$	a	b–HOAc	c	d–HOAc	e	e_1	e_1–CH$_2$CO	g	h	k	43
40	1-[(3R)-acetoxyoleoyl]-2-acetylglycerol	528 (-)	453 (12)	-	337 (22)	263 (65)	-	-	-	189 (80)	-	145 (35)	-
41	1-[(3R)-acetoxystearoyl]-2-acetylglycerol	528 (-)	453 (14)	-	339 (25)	265 (70)	-	-	-	189 (88)	-	145 (38)	-
42[c]	1-[(3R)-acetoxyoleoyl]-3-acetylglycerol	528 (-)	453 (2)	395 (12)	337 (1)	263 (17)	-	188 (1)	146 (12)	189 (29)	175 (100)	-	-
43[a]	1-[(3R)-acetoxystearoyl]-3-acetylglycerol	530 (-)	455 (7)	397 (17)	339 (2)	265 (21)	-	188 (2)	146 (15)	189 (28)	175 (100)	-	-
48[d]	2-[(3R)-acetoxyeicosanoyl]-1-acetylglycerol	558 (-)	483 (2)	425 (2)	-	293 (18)	188 (2)	-	-	189 (20)	-	-	43 (100)

The data were obtained from [a]*Diascia vigilis* (Scrophulariaceae), [b]*Cypella herbertii* (Iridaceae), [c]*Lysimachia punctata* (Myrsinaceae) and [d]*Sigmatostalix putumayensis* (Orchidaceae) (see corresponding ions in Scheme 2.1 and 2.2, Chapter 2), condition **GC1**.

Table A 2.7. Key ions in the EI mass spectra of TMS derivatives of triacylglycerols (TAGs) possessing (3*R*)-acetoxy fatty acid and two acetyl moieties (Finigan Voyager GC/MS system).

No.	Compound	Characteristic of EI-mass spectral data [*m/z*, (rel.int. %)]						
		$[M]^+$	a_1	d	d–HOAc	e_2	$[OCOSiMe_3]^+$	43
24[a]	2-[(3*R*)-acetoxymyristoyl]-1,3-diacetylglycerol	444 (-)	324 (2)	269 (5)	209 (48)	159 (88)	117 (11)	43 (100)
32[a]	2-[(3*R*)-acetoxypalmitoyl]-1,3-diacetylglycerol	472 (-)	352 (1)	297 (4)	237 (37)	159 (96)	117 (10)	43 (100)
44[a]	2-[(3*R*)-acetoxystearoyl]-1,3-diacetylglycerol	500 (-)	380 (-)	325 (4)	265 (27)	159 (88)	117 (20)	43 (100)
49[b]	2-[(3*R*)-acetoxyeicosanoyl]-1,3-diacetylglycerol	528 (-)	408 (1)	353 (5)	293 (25)	159 (90)	117 (20)	43 (100)
51[b]	2-[(3*R*)-acetoxydocosanoyl]-1,3-diacetylglycerol	556 (-)	436 (1)	381 (5)	321 (20)	159 (80)	117 (15)	43 (100)

The data obtained from [a]*Diascia vigilis* (Scrophulariaceae) and [b] *Sigmatostalix putumayensis* (Orchidaceae). The ion type a_1, $[M-2HOAc]^+$ represents for the highest molecular peak (see corresponding ions in Scheme 2.1 and Figure 2.6, Chapter 2), condition **GC1**.

Table A 2.8. Key ions in the EI mass spectra of TMS derivatives of partially acetylated dihydroxyfatty acids (Finigan Voyager GC/MS system).

No.	Compound	Characteristic of EI-mass spectral data [m/z, (rel.int. %)]								
		$[M]^+$	a	a–CH_2CO	a–$HOSiMe_3$	α_1	α_2–HOAc	α_3–CH_2CO	α_3–CH_2CO–$HOSiMe_3$	$[SiMe_3]^+$
55[a]	7-acetoxy-3-hydroxyeicosanoic acid	530	455	413	365	233	339	305	215	73
		(-)	(10)	(1)	(1)	(30)	(1)	(2)	(28)	(100)
56[a]	9-acetoxy-3-hydroxyeicosanoic acid	530	455	413	365	233	339	333	243	73
		(-)	(2)	(1)	(2)	(24)	(1)	(5)	(30)	(100)
59[b]	7-acetoxy-3-hydroxydocosanoic acid	558	483	441	393	233	367	305	215	73
		(-)	(8)	(1)	(2)	(30)	(1)	(2)	(25)	(100)
60[b]	9-acetoxy-3-hydroxydocosanoic acid	558	483	441	393	233	367	333	243	73
		(-)	(3)	(2)	(2)	(28)	(1)	(3)	(29)	(100)
63[b]	9-acetoxy-3-hydroxytetracosanoic acid	586	511	509	421	233	395	333	243	73
		(-)	(2)	(2)	(2)	(25)	(1)	(2)	(35)	(100)
65[c]	7-acetoxy-3-hydroxyhexacosanoic acid	614	539	497	449	233	423	305	215	73
		(-)	(3)	(1)	(3)	(30)	(2)	(1)	(20)	(100)
66[c]	9-acetoxy-3-hydroxyhexacosanoic acid	614	539	497	449	233	423	333	243	73
		(-)	(1)	(1)	(3)	(30)	(2)	(5)	(35)	(100)

The data were obtained from [a]*Byrsonima coriacea*, [b]*Stigmaphyllon ellipticum* and [c]*Malpighia urens* (Malpighiaceae) (see corresponding ions in Scheme 3.1, Chapter 3), condition **GC1**.

Table A 2.9. Key ions in the EI mass spectra of TMS derivatives of diacetoxyfatty acids (Finigan Voyager GC/MS system).

No.	Compound	Characteristic of EI-mass spectral data [m/z, (rel.int. %)]							
		$[M]^+$	a	a_1	a_1–Me	a_1–HOSiMe$_3$	a_1–HOSiMe$_3$–CO	α_3–CH$_2$CO	α_3–CH$_2$CO–HOAc
52[a]	3,7-diacetoxystearic acid	472 (-)	397 (-)	352 (3)	337 (20)	262 (12)	234 (5)	275 (12)	215 (28)
53[b]	3,7-diacetoxyeicosanoic acid	500 (-)	425 (2)	380 (3)	365 (20)	290 (12	262 (5)	275 (11)	215 (28)
54[c]	3,9-diacetoxyeicosanoic acid	500 (-)	425 (-)	380 (3)	365 (20)	290 (12)	262 (5)	303 (10)	243 (22)
57[d]	3,7-diacetoxydocosanoic acid	528 (-)	453 (1)	408 (2)	393 (20)	318 (12)	290 (4)	275 (15)	215 (30)
58[d]	3,9-diacetoxydocosanoic acid	528 (-)	453 (1)	408 (2)	393 (22)	318 (14)	290 (5)	303 (12)	243 (30)
61[d]	3,7-diacetoxytetracosanoic acid	556 (-)	481 (1)	436 (2)	421 (23)	346 (10)	318 (4)	275 (14)	215 (25)
62[d]	3,9-diacetoxytetracosanoic acid	556 (-)	481 (1)	436 (2)	421 (23)	346 (10)	318 (4)	303 (8)	243 (25)
64[e]	3,9-diacetoxyhexacosanoic acid	584 (-)	508 (-)	464 (1)	449 (20)	374 (12)	346 (5)	303 (10)	243 (28)

The data were obtained from [a]*Oncidium cheirophorum* (Orchidaceae), [b]*Byrsonima coriacea* (Malpighiaceae), [c]*Bunchosia argentea* (Malpighiaceae), [d]*Stigmaphyllon ellipticum* (Malpighiaceae) and [e]*Malpighia urens* (Malpighiaceae) (see corresponding ions in Scheme 3.2, Chapter 3), condition **GC1**.

Table A 2.10. Key ions in the EI mass spectra of TMS derivatives of monoacylglycerols of fatty acid (Finigan Voyager GC/MS system).

No.	Compound	Characteristic of EI-mass spectral data [m/z, (rel.int. %)]											
		$[M]^+$	a_3	b	c	d	e	e–Me	f	147	129	103	73
70[a]	2-pamitoylglycerol	474	459	-	313	-	218	203	-	147	129	103	73
		(-)	(2)		(10)		(60)	(20)		(45)	(100)	(65)	(80)
71[b]	1-pamitoylglycerol	474	459	371	313	239	218	203	205	147	129	103	73
		(-)	(4)	(56)	(2)	(23)	(5)	(22)	(17)	(58)	(75)	(28)	(100)
76[c]	2-linoleoylglycerol	498	483	337	-	-	218	203	-	147	129	103	73
		(-)	(1)	(4)			(20)	(10)		(35)	(72)	(100)	(80)
77[c]	2-oleoylglycerol	500	485	-	339	-	218	203	-	147	129	103	73
		(-)	(1)		(8)		(30)	(11)		(40)	(90)	(100)	(78)
78[c]	2-stearoylglycerol	502	487	-	341	-	218	203	-	147	129	103	73
		(-)	(2)		(10)		(60)	(20)		(45)	(100)	(28)	(65)
79[c]	1-stearoylglycerol	502	487	399	341	267	218	203	205	147	129	103	73
		(-)	(3)	(48)	(4)	(13)	(5)	(25)	(20)	(58)	(75)	(28)	(100)
85[a]	2-eicosenoylglycerol	528	513	367	-	-	218	203	-	147	129	103	73
		(-)	(-)	(8)			(30)	(11)		(40)	(90)	(100)	(78)

The data were obtained from [a]*Pterygodium magnum* (Orchidaceae), [b]*Lysimachia punctata* (Myrsinaceae) and [c]*Cyrtochilum serratum* (Orchidaceae) (see corresponding ions in Scheme 2.1 and 2.2, Chapter 2).m/z 147 $[Me_2SiOSiMe_3]^+$, m/z 129 $[CH_2CHCHOSiMe_3]^+$, m/z 103 $[CH_2OSiMe_3]^+$, m/z 73 $[SiMe_3]^+$, condition **GC1**.

Table A 2.11. Key ions in the EI mass spectra of TMS derivatives of diacylglycerol of long chain fatty acid and acetyl moiety[a] (Finigan Voyager GC/MS system).

No.	Compound	Characteristic of EI-mass spectral data [m/z, (rel.int. %)]									
		$[M]^+$	a_3	b	c	d	g	h	k	129	117
67	1-acetyl-2-myristoylglycerol	416	401	-	285	211	189	-	145	129	117
		(-)	(10)		(60)	(42)	(40)		(80)	(82)	(100)
68	1-acetyl-3-myristoylglycerol	416	401	343	285	211	189	175	-	129	117
		(-)	(10)	(20)	(10)	(40)	(10)	(100)		(30)	(50)
72	1-acetyl-2-palmitoylglycerol	444	429	-	313	239	189	-	145	129	117
		(-)	(10)		(50)	(35)	(50)		(80)	(95)	(100)
73	1-acetyl-3-palmitoylglycerol	444	429	371	313	239	189	175	-	129	117
		(-)	(10)	(20)	(10)	(35),	(20)	(100)		(30)	(50)
80	1-acetyl-2-linoleoylglycerol	468	453	-	337	263	189	-	145	129	117
		(-)	(5)		(40)	(38)	(40)		(70)	(90)	(100)
81	1-acetyl-2-oleoylglycerol	470	455	-	339	265	189	-	145	129	117
		(-)	(6)		(35)	(35)	(45)		(75)	(92)	(100)
82	1-acetyl-2-stearoylglycerol	472	457	-	341	267	189	-	145	129	117
		(-)	(8)		(52)	(40)	(55)		(88)	(98)	(100)

[a]The data were obtained from *Pterygodium hastata* (Orchidaceae) (see corresponding ions in Scheme 2.1 and 2.2, Chapter 2). m/z 129 $[CH_2CHCHOSiMe_3]^+$, m/z 117 $[OCOSiMe_3]^+$, condition **GC1**.

Table A 2.12. Key ions in the EI mass spectra of TMS derivatives of triacylglycerols of long chain fatty acid and two acetyl moieties (Finigan Voyager GC/MS system).

No.	Compound	Characteristic of EI-mass spectral data [*m/z*, (rel.int. %)]			
		$[M]^+$	**d**	**e$_2$**	43
69[a]	1,3-diacetyl-2-myristoylglycerol	386 (-)	211 (70)	159 (80)	43 (100)
74[a]	1,3-diacetyl-2-palmitoleoylglycerol	412 (-)	237 (50)	159 (54)	43 (100)
75[a]	1,3-diacetyl-2-palmitoylglycerol	414 (-)	239 (50)	159 (85)	43 (100)
83[a]	1,3-diacetyl-2-oleoylglycerol	440 (-)	265 (50)	159 (55)	43 (100)
84[b]	1,3-diacetyl-2-stearoylglycerol	442 (-)	267 (55)	159 (80)	43 (100)
86[c]	1,3-diacetyl-2-eicosanoylglycerol	470 (-)	295 (55)	159 (85)	43 (100)

The data were obtained from [a]*Pterygodium hastata*, [b]*Corycium dracomontanum* and [c]*Oncidium ornithorhynchum* (Orchidaceae) (see corresponding ions in Scheme 2.1 and Figure 2.6, Chapter 2), condition **GC1**.

Table A 2.13. Key ions in the EI mass spectra of TMS derivatives of acylglycerols of long chain diacetoxy fatty acid[a] (Finigan Voyager GC/MS system).

No.	Compound	Characteristic of EI-mass spectral data (m/z, (rel.int. %))									
		$[M]^+$	a	a$_1$	a$_2$	d−HOAc	d−2HOAc	e$_2$	g	h	m
87	1-acetyl-2-(3,9-diacetoxyeicosanoyl)glycerol	616	541	-	481	351	291	-	189	175	-
		(-)	(1)		(10)	(6)	(20)		(100)	(80)	
88	1-acetyl-3-(3,9-diacetoxyeicosanoyl)glycerol	616	541	-	481	351	291	-	189	175	-
		(-)	(1)		(5)	(3)	(15)		(10)	(100)	
89	1,3-diacetyl-2-(3,9-diacetoxyeicosanoyl)glycerol	586	-	466	-	351	291	159	-	-	290
		(-)		(2)		(5)	(12)	(100)			(15)
90	1-acetyl-2-(3,9-diacetoxydocosanoyl)glycerol	644	569	-	509	379	319	-	189	175	-
		(-)	(2)		(12)	(5)	(18)		(100)	(80)	
91	1-acetyl-3-(3,9-diacetoxydocosanoyl)glycerol	644	569	-	509	379	319	-	189	175	-
		(-)	(2)		(7)	(3)	(20)		(15)	(100)	
92	1,3-diacetyl-2-(3,9-diacetoxydocosanoyl)glycerol	614	-	494	-	379	319	159	-	-	318
		(-)		(3)		(5)	(15)	(100)			(12)

[a]The data were obtained from *Heteropterys chrysophylla* (Malpighiaceae) (see corresponding ions in Scheme 4.1 and 4.2, Chapter 4), condition **GC3**.

Table A 2.14. Key ions in the EI mass spectra of TMS derivatives of acylglycerols of long chain hydroxy fatty acid (Finigan Voyager GC/MS system).

No.	Compound	Characteristic of EI-mass spectral data (m/z, (rel.int. %))												
		$[M]^+$	a_2	a	b	d	d$-$CH$_2$CO	f	g	h	j	n	p	73
93[a]	1-[(3R)-hydroxyoleoyl]glycerol	588	573	-	485	352	311	205	189	-	379	143	219	73
		(-)	(1)		(8)	(2)	(11)	(5)	(2)		(5)	(25)	(12)	(100)
94[a]	1-[(3R)-hydroxystearoyl]glycerol	590	575	-	487	355	313	205	189	-	379	143	219	73
		(-)	(1)		(10)	(5)	(28)	(4)	(3)		(6)	(28)	(15)	(100)
95[b]	1-[(3R)-hydroxyoleoyl]-2-acetylglycerol	558	543	483	466	352	311	-	189	-	347	143	-	73
		(-)	(-)	(1)	(2)	(1)	(1)		(100)		(5)	(25)		(75)
96[b]	1-[(3R)-hydroxystearoyl]-2-acetylglycerol	560	545	485	-	355	313	-	189	-	349	143	-	73
		(-)	(1)	(1)		(1)	(4)		(100)		(6)	(30)		(85)
97[b]	1-[(3R)-hydroxyoleoyl]-3-acetylglycerol	558	543	483	-	352	311	-	189	175	347	143	-	73
		(-)	(-)	(-)		(1)	(3)		(100)	(20)	(5)	(75)		(80)
98[b]	1-[(3R)-hydroxystearoyl]-3-acetylglycerol	560	545	485	-	355	313	-	189	175	349	143	-	73
		(-)	(1)	(1)		(1)	(8)		(100)	(25)	(6)	(80)		(90)

[a]The data were obtained from *Macropis fulvipes* cell lining and [b]*Lysimachia punctata* oil treated with *Macropis fulvipes* labial gland secretions. m/z 73 [SiMe$_3$]$^+$, condition **GC1**.

Table A 2.15. Key ions in the EI mass spectra of TMS derivatives of unidentified compounds[a] from *Diascia* spp. (Chapter 2) (Finigan Voyager GC/MS system).

No.	Compound	Characteristic of EI-mass spectral data (*m/z*, (rel.int. %))
25	unknown	502 (M[+], -), 427 (6), 311 (56), 237 (72), 189 (7), 188 (31), 146 (12), 145 (100), 129 (55), 117 (72), 73 (77), 43 (68)
26	unknown	502 (M[+], -), 427 (5), 369 (10), 311 (2), 237 (24), 189 (2), 188 (2), 175 (100), 146 (12), 117 (20)
33	unknown	530 (M[+],-), 455 (5), 397 (9), 339 (1), 265 (13), 189 (2), 188 (1), 175 (100), 146 (10), 117 (14)

[a]The data were obtained from *Diascia vigilis* (Scrophulariaceae), condition **GC1**.
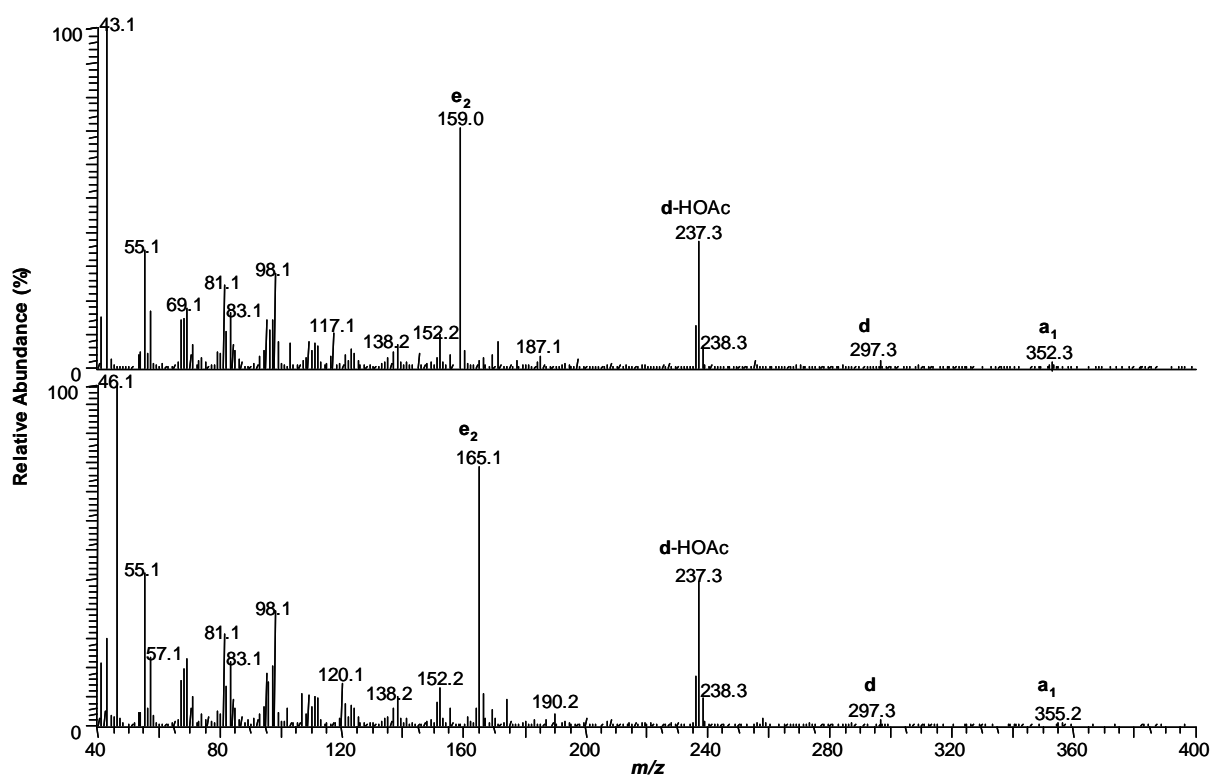
APPENDIX 3

[^{2}H]-labelled mass spectra

Figure A 3.1. Mass spectra of acetylated derivatives of TAGs: (A) 2-[(3*R*)-acetoxypalmitoyl]-1,3-diacylglycerols (**32**) and (B) [^{2}H]-labelled acetylated derivative of **32**. The fragment ions are described in Scheme 2.1 and 2.2, Chapter 2.

CURICULUM VITAE

Personal Information

Name: KANCHANA DUMRI

Date of birth: October 15, 1976

Place of birth: Chiang Mai, Thailand

Nationality: Thai

Education

1991–1993 Suanboonyopathum Lamphun School, Lamphun, Thailand

1994–1997 Department of Chemistry, Faculty of Science,
Chiang Mai University, Thailand

1998–2001 Department of Biotechnology, Faculty of Science,
Mahidol University, Thailand

2004 Leibniz Institute of Plant Biochemistry (Halle), Germany

Academic Qualifications

1993 High School Certificate

1997 B.Sc. (Chemistry) Hon 1st class

2001 M.Sc. (International Program Biotechnology)

Professional Position

Academic 2002 Lecturer in Biochemistry, Faculty of Science, Chiang Mai
University, Thailand

Academic 2004 PhD student of Leibniz Institute of Plant Biochemistry Halle,
Germany

Halle (Saale),

DECLARATION

I hereby declare that I have carried out the analyses and written the thesis myself and that I did not use any devices or received relevant help from any persons other than those mentioned in the text. This dissertation has not been submitted before.

Halle (Saale),   Kanchana Dumri